THE THEORY AND APPLICATION OF A NOVEL SCALED BOUNDARY FINITE ELEMENT METHOD IN COMPUTATIONAL ELECTROMAGNETICS

A THESIS
SUBMITTED TO THE
UNIVERSITY OF HYDERABAD

FOR THE DEGREE OF
DOCTOR OF PHILOSOPHY

BY

V.S.PRASANNA RAJAN

SCHOOL OF PHYSICS
UNIVERSITY OF HYDERABAD
HYDERABAD- 500046, INDIA.

DECEMBER 2002.

DECLARATION

I hereby declare that the work embodied in this thesis has been carried out by me under the supervision of Dr.K.C.James Raju, in the School of Physics, and the same has not been submitted at any other University.

Place: HYDERABAD

Date: 30.12.2002

(V.S.Prasanna Rajan)

CERTIFICATE

Certified that, the work embodied in this thesis entitled **THE THEORY AND APPLICATION OF A NOVEL SCALED BOUNDARY FINITE ELEMENT METHOD IN COMPUATIONAL ELECTROMAGNETICS** has been carried out by **Mr.V.S.Prasanna Rajan** for the full period under Ph.D Ordinances of the University, under my supervision and the same has not been submitted for the award of research degree of any other University.
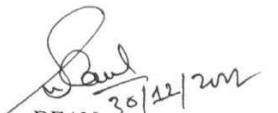
(K. C. James Raju)

PLACE: HYDERABAD   SUPERVISOR

DATE: 30.12.2002   (Dr.K.C. James Raju)

DEAN 30/12/2002
School of Physics,
University of Hyderabad.

ACKNOWLEDGEMENTS

I thank my parents, whose constant support and encouragement during my difficult times in life, is my source of strength.

CONTENTS

PREFACE

This thesis deals with the development and application of a novel method called **"The Scaled Boundary Finite Element Method"** in Computational Electromagnetics. The method is basically a semi-analytical method, which is much similar to the conventional Finite element method, but differs from it in the following aspect. This novel method involves finite element discretization only on the boundary of the structure along the tangential direction and an analytical approach in the radial direction from the scaling center. This is in contrast from the conventional finite element method, where the field solutions are entirely numerical.

The thesis is divided into 6 chapters. The first chapter deals with a brief introduction of the conventional finite element method and the key steps involved in it during the practical implementation of the method. The second chapter deals with the basic theory of the scaled boundary transformation and the physical basis underlying the transformation . The third Chapter deals with the application of the novel method for metallic cavities, and it is illustrated with a numerical example for a spherical metallic cavity. In the fourth chapter, the scaled boundary transformation is applied for multi-layered and multi conductor microstrip transmission line structures and the micro-strip line like Very Large Scale Integrated circuit (VLSI) interconnects encountered in multi-layered mother boards. A shielded coupled planar microstrip transmission line and an open microstrip like structure as a typical VLSI interconnect are studied as an illustration.

In the fifth chapter, the case of periodic structures with transverse confinement of the electromagnetic wave, and which are not invariant in the direction of wave-propagation,

is taken up and the scaled boundary finite element equation is developed for such structures. It is then illustrated by a numerical example.

The sixth chapter deals with the summary of the entire research work and the scope for further development of this novel method.

CHAPTER -1

AN INTRODUCTION TO THE FINITE ELEMENT METHOD

CHAPTER –I

AN INTRODUCTION TO THE FINITE ELEMENT METHOD

A. Introduction: Finite Element Method is a numerical approximation method for solving field problems that possesses the following characteristics: [1]

a) The geometric domain of the problem is subdivided into a set of sub-domains or elements, which cover the entire domain but do not overlap.

b) The quantity to be approximated has a uniquely defined value everywhere within each element.

c) The approximate solution is correct (ie., has minimal error) in a global sense that takes into account the solution values at all points.

d) Only some continuity requirements of the physical problem are strictly enforced at element interfaces: the remainder are implicit in the element formulation.

The term "finite element" is viewed as referring not to finite geometric size but to finiteness of the fundamental quantities involved: like energy or power, reaction, Lagrangians or Hamiltonians of the field. The finite element method has the flexibility of handling the problems which are formulated as a boundary value problem of differential equations or as any mixture of integro-differential operator equations. There is no requirement that the approximation must be locally polynomial. The essential requirement of the approximation functions is the existence of a uniquely defined approximation every where in the problem space. This requirement enables the finite element method to provide approximate solution values at every point in the domain.

In short, the finite element method can be defined as a numerical method, which is a piecewise application of a variational or weighted residual method.

B. Variational Formulation: The term "variational formulation" is used to mean the weak **formulation**[2] in which a differential equation is recast in an equivalent integral form by trading the differentiation between a test function and the dependent variable. The weak formulation is defined as the variational process by which the continuity requirement of the solution is weakened when compared to the original problem. For most linear problems, the weak formulation is equivalent to the minimization of a quadratic functional. The necessary condition for the minimum of a quadratic functional is that, its first derivative (or first variation) with respect to the dependent variable be zero. From calculus of variations, it is known that the minimizing **function** is the true solution of the original differential equation. The following three important steps are involved in the variational formulation of any given differential equation with the specified boundary conditions.

1) The first step involves multiplying the differential equation (with all of the terms on one side of the equality) with an arbitrary test function v and integrating the product over the domain of the problem. The test function v can be thought of as a variation in the dependent variable say u , satisfying the homogenous boundary condition of the problem.

2) In the second step, the order of differentiation is transferred from the dependent variable u to the test function v, and the type of boundary conditions that can be admitted by the variational form is identified.

The purpose of the transfer of differentiation from u to v is to equalize the continuity requirements on u and v. This results in weaker continuity requirements on the solution u in the variational problem than in the original equation. In the process of transferring the differentiation, the boundary terms, which determine the nature of the boundary conditions in the solution is obtained.

3) The third and last step in the formulation consists of simplifying the boundary terms with the aid of the specified boundary conditions, and the identification of the associated quadratic functional, if it exists. Denoting the bilinear (linear in both u and v) form in the weak formulation by $B(u,v)$ and the associated linear form by $L(u,v)$, and if the bilinear form is symmetric, $B(u,v)=B(v,u)$, and $L(v)$ is linear, then the associated quadratic functional is given by [3]

$$I(u) = \frac{1}{2}B(u,v) - L(u) \qquad (1.1)$$

C. Classification of the boundary conditions: From the point of view of the variational formulation, the boundary conditions are classified into two types as Essential and Natural boundary conditions.

Natural Boundary Condition: The specification of the coefficients of the test function *(v)* and its derivatives in the boundary integral constitute the natural boundary condition.

Essential Boundary Condition: The specification of the dependent variable in the same form as the arbitrary function (v) in the boundary integral constitutes the essential boundary condition.

The variables involved in the essential boundary conditions of the problem are called as the primary variables and those in the natural boundary conditions are called as secondary variables of the formulation.

Among the various classical variational methods, the Ritz method, the method of weighted residuals and the Galerkin method are discussed below in detail.

D. The Ritz Method:

Consider the variational problem[4] of finding the solution u such that

$$B(u,v) = L(v) \tag{1.2}$$

for all sufficiently differentiable v that satisfy the homogenous form of essential boundary conditions on $u.$ When the functional B is bilinear and symmetric and L is linear, then the equation (1.2) is equivalent to minimizing the quadratic functional (1.1). The Ritz method seeks an approximate solution to (1.2) in the form of a finite series

$$\mathbf{u}_N = \sum_{j=1}^{N} \mathbf{c}_j \phi_j + \phi_o \tag{1.3}$$

where the constants $\mathbf{c_j}$ are called the Ritz coefficients, chosen such that (1.2) holds for

$v = \varphi_i$ $(\mathbf{i=1,2,\ldots\ldots N})$:

$$B\left(\phi_i, \sum_{j=1}^{N} \mathbf{c}_j \phi_j + \phi_o \right) = L(\phi_i) \quad i = 1,2,\ldots N \tag{1.4}$$

If B is bilinear,

$$\sum_{j=1}^{N} B(\phi_i, \phi_j) \, \mathbf{c}_j = L(\phi_i) - B(\phi_i, \phi_0) \tag{1.5}$$

which represents a system of N linear algebraic equations in N constants c_j. The columns and rows of matrix coefficients Bjj=B (φ_i, φ_j) must be linearly independent in order that the coefficient matrix in the Eq.(1.5) can be inverted. For symmetric bilinear forms, the Ritz method can be viewed as one seeks solution of the form in Eq.(1.3) in which the parameters are determined my minimizing the quadratic functional corresponding to the symmetric bilinear form, that is, functional $I(u)$ in Eq.(1.1). After substituting u_N from Eq.(1.3) for u into Eq.(1.1) and integrating, the functional I(//) becomes an ordinary (quadratic) function of the parameters $c_1, c_2, \ldots$ Then the necessary condition for the minimum of $I(c_1, c_2, \ldots, c_N)$ is that its partial derivatives with respect to each of the parameters be zero :

$$\frac{\partial I(c_j)}{\partial c_1} = 0, \frac{\partial I(c_j)}{\partial c_2} = 0, \ldots, \frac{\partial I(c_j)}{\partial c_n} = 0 \qquad (1.6)$$

Thus there are N linear algebraic equations in N unknowns, c_j (j=1,2,...,N). These equations are same as those in Eq.(1.5) for linear symmetric bilinear forms. The quadratic functional exists only when $B(u,v)$ is symmetric. Also, Eq.(1.5) is more general than Eq.(1.6), and they are the same when $B(u,v)$ is bilinear and symmetric.

The approximation functions fa (i=1,2,...,N) and ϕ_0 should satisfy the following properties :

1. The function ty_0 is selected to satisfy the specified essential boundary conditions of the problem. If the specified essential boundary conditions are all homogenous, then $\phi_0=0$.

2. Since ϕ_0 satisfies the specified essential boundary conditions, it is required that fa (i=1,2,...N) also satisfy the homogenous form of the essential boundary conditions so

that $u_N = \phi_0$ at the points at which the essential boundary conditions are specified.

Since ϕ_i satisfy the homogenous essential boundary conditions, the choice $v = \phi_i$

is consistent with the requirements of a test function.

3. *fa* should be such that $B(\phi_i, \phi_j)$ is well defined and non-zero i.e., sufficiently

differentiable as required by the bilinear form $B(\phi_i, \phi_j)$.

4. For any N, the set *{fa }*i=1 to n along with the columns and rows of B(*fa, fa)* are

linearly independent.

5. *{fa}* is complete.

The above requirements on the approximation functions guarantee, for linear

problems, convergence of the Ritz solution to the exact solution as the value of N is

increased. The convergence is understood to be in the following sense:

$$I(u_N) \ge I(u_M) \quad \text{for} N < M \tag{1.7}$$

For any value of N , the previously computed elements of the matrix coefficients b_{ij} and

the column vector $F_j = L(\phi_i)$ - B(*fa, ϕ_0)* remain unchanged, and the newly computed rows

and columns must be added to the existing rows and columns.

E. The Method of Weighted Residuals: It is always possible to write the integral form

of a differential equation, whether the equation is linear or nonlinear (in the dependent

variables) [5]. However, it is not always possible to construct a symmetric variational form

and the associated functional when the equation under consideration is nonlinear. While

the Ritz method can also be applied to nonlinear problems, it restricts the choice of test

functions to those used for the approximation. The weighted residual method is a

generalization of the Ritz method in which the test functions can be chosen from an

independent set of functions. Further, when it is not possible to construct a weak form,

the method of weighted residuals can be used to approximate the integral form of the equation. Since the integral form does not include the natural boundary conditions of the problem, the approximating functions should be selected such that the approximated solution satisfies the boundary conditions of the problem. However, the test functions can be selected independent of the approximation functions. This flexibility is advantageous in certain nonlinear problems.

Consider the operator equation

$$\mathbf{A}u = \mathbf{f} \text{ in } \Omega \tag{1.8}$$

Where A is an operator (linear or non linear), acting on the unknown dependent variable u, and $\mathbf{f}$ is a known function of position. The function u (i.e., solution) is not only required to satisfy the operator equation (1.8), it is also required to satisfy the boundary conditions associated with the operator.

In the weighted residual method, the solution u is approximated, in much the same way as in the Ritz method, by expressions of the form given in Eq.(1.3) where ϕ_0 must satisfy all the specified boundary conditions of the problem, and ϕ_j must satisfy the homogenous form of the specified boundary conditions, as well as the conditions specified for the approximation functions for the Ritz method. However, the continuity requirement imposed on ϕ_j is the same as that required by Eq.(1.8).

Substituting the approximation given in Eq.(1.3) into the operator equation (1.8) results in a residual (i.e., an error in the equation)

$$E = A(u_N) - f \neq 0 \tag{1.9}$$

Once ϕ_o and *fa* are selected, E is merely a function of the independent variables and the parameters c_j . In the weighted residual method, the parameters are determined by setting the integral over the domain of a weighted residual of the approximation to zero :

where ψ_i are weight functions which, in general, are not the same as the approximation

$$\int_\Omega \psi_i(x,y) \, E(x,y,c_j) \, dx \, dy = 0 \quad \text{for } i = 1,2,...N \tag{1.10}$$

functions *fa* . Also, $\{\psi_i\}$ must be linearly independent set, otherwise the equations provided by (1.10) will not be linearly independent and hence not solvable.

Hence, it can be stated that the weighted-residual method employs a weighted integral form of the equation to be solved. If the operator permits, the differentiation from the solution can be transferred to the weight functions and thereby the continuity requirements on the approximation functions can be relaxed.

When the operator A is linear, Eq.(1.1O) can be simplified to the form

$$\sum_{j=1}^{N} \left(\int_\Omega \psi_i A(\phi_j) \, dx \, dy \right) c_j = \int_\Omega \psi_i \left[f - A(\phi_o) \right] dx \, dy \tag{1.11}$$

or

$$\sum_{j=1}^{N} A_{ij} c_j = f_i \tag{1.12}$$

The coefficient matrix [A] is not symmetric,

$$A_{ij} = \int_\Omega \psi_i A(\phi_j) \, dx \, dy \neq A_{ji} \tag{1.13}$$

11

F. The Galerkin method: For $\psi_i = \phi_i$,the weighted-residual method is known as the Galerkin method. When the operator is a linear differential operator of even order, the Galerkin method reduces to the Ritz method. The reason being, half of the differentiation can be transferred to the weight functions, the resulting coefficient matrix will be symmetric.

G. The need for finite element method: The traditional variational methods i.e., Ritz and Galerkin method described above, cease to be an effective computational method due to a serious shortcoming, namely, the difficulty in choosing the approximation functions. The approximation functions, apart from satisfying the continuity, linear independence, completeness, and essential boundary conditions, are arbitrary; and the selection becomes even more difficult when the given domain is geometrically complex. Moreover, the quality of the approximation is directly affected by the choice of the approximation functions. But there exists no systematic procedure to construct them. Due to this shortcoming, despite the simplicity in obtaining approximate solutions, the variational methods of approximation are never regarded as competitive computationally when compared with traditional finite-difference method.

The finite-element method overcomes the shortcoming of the traditional methods, and it is also endowed with the features of an effective computational technique. An effective computational technique should posses the following features: [6]

1. The method should have a sound mathematical as well as physical basis.

2. The method should not have limitations with regard to the geometry and the physical composition of the domain.

3. The formulation should be independent **of the** shape of the domain and the boundary conditions.

4. The method should be flexible enough to allow choosing a desired degree of approximation without reformulating the entire problem.

5. The method should involve a systematic procedure that can be automated for programming on digital computers.

H. General Methodology of finite-element analysis: The finite-element method consists of representing a given domain, however complex it may be, by geometrically simple shapes over which the approximation functions can be systematically derived. Then the Ritz-Galerkin type approximation of the governing equations are developed over each element. Finally, the equations over all elements of the collection are connected by the continuity of the primary variable or variables, the boundary conditions of the problem are imposed, and then the connected set of equations is solved.

The key steps involved in the finite-element analysis of a given problem can be summarized as follows: [7]

1. Discretization (or representation) of the given domain into a collection of pre-selected finite elements. This step can be further divided into three stages.

   a. Construction of the finite-element mesh of pre-selected elements.

   b. Numbering the nodes and elements.

   c. Generation of the geometric properties (e.g., coordinates, cross-sectional areas, etc.) needed for the problem.

2. Derivation of element equations for all typical elements in the mesh.

   a. Construction of the variational / weighted-residual formulation of the given differential equation over the typical element.

   b. The typical form assumed for the dependent variable $\boldsymbol{u}$ is given by

   $$\boldsymbol{u} = \sum_{i=1} u_i \psi_i \qquad (1.14)$$

   c. The form given above for u is substituted in the step (2a) to obtain element equations in the form

   $$\left[\mathbf{K}^{(e)}\right]\{\boldsymbol{u}^{(e)}\} = \{\mathbf{F}^{(e)}\} \qquad (1.15)$$

   d. The element interpolation functions ψ_i is derived or selected,(if already available in the literature) and the element matrices are computed.

3. The element equations are assembled to obtain the equations of the whole problem. This process is achieved in three stages.

   a. The inter element continuity conditions among the primary variables (relationship between the local degrees of freedom and the global degrees of freedom -connectivity of elements] is identified by relating element nodes to global nodes.

   b. The "equilibrium" conditions among the secondary variables (relationship between the local source and the globally specified source components) are identified.

   c. Using the steps (3a) and (3b), and the superposition property, *[the quadratic -functional (or the variational formulation) associated with the problem is*

equal to the sum of the quadratic functionate of all elements] element equations are **assembled** .

4. The boundary conditions are imposed by identifying the specified global primary and secondary degrees of freedom.

5. The assembled equations are solved numerically.

6. The results obtained by the numerical solution is post processed . This stage involves the process like the computation of the gradient of the solution or other desired quantities from the primary degrees of freedom.

7. The results obtained are represented in a tabular and/or graphic form.

I. Discretization of the Domain into Elements: The domain Ω of the problem under consideration is divided into a set of **pre-selected** element types. The element types may be line elements for problems involving discretization along a line or along a curve , triangular / quadrilateral elements in two-dimensions for problems involving discretization in a two dimensional surface. In the case of three dimensions, the element types may be tetrahedral or hexahedral. These elements may be either planar or curvilinear depending upon whether the surface under consideration is a planar surface or a curvilinear surface. Depending on the nature of the problem, it is possible to mix the element types while performing the discretization of a domain.

The intersection of any two elements constitutes the inter-element boundary. The intersection points, and possibly some intermediate points, are called global nodes. The important aspect, which follows after the discretization of the domain, is the numbering of nodes and the elements. The numbering of nodes and the elements assumes significance in the wake of the implementation of the inter-element continuity conditions.

The numbering of nodes involves both local and global numbering. The local numbering of the nodes of an element corresponds to the sequential numbering of the nodes pertaining only to that element and gets initialized for the successive element. In contrast with the local numbering, the global numbering of the nodes, is the sequential numbering of nodes of all the elements in the finite element mesh of the domain under consideration, starting from the node(s) of the first element and then proceeding sequentially for all the nodes for all the elements without being initialized for every successive element. The correspondence between the local element nodal values and the global nodal values are called the inter-element continuity conditions.

J. Choice of the Interpolation functions: The variational formulation of a given differential equation helps to identify the primary and secondary variables and the type and the minimum degree of interpolation functions that are admissible [8]. The finite-element interpolation functions are constructed such that the finite-element approximation over an element satisfies the end conditions on the primary variables (i.e., it satisfies the essential boundary conditions of the problem). The interpolation functions include element-wise constant states of the primary variables as well as of the secondary variables. The later requirement ensures completeness of the set of finite-element interpolation functions and hence the convergence.

The choice of the interpolation functions assumes a very crucial role in the finite element analysis of a problem. The interpolation functions perform two important tasks for a given problem. The first task is the accurate modeling of the geometry of the problem and the second task is the interpolation of the dependent variable at the nodes of the element. Accordingly, the interpolation functions fall into two broad categories.

The first category of interpolation functions are called shape **functions** which imply that those interpolation functions determine the shape of the element. The second category of interpolation functions, for the interpolation of the dependent variable, has a bearing on the fundamental accuracy of the solution of the problem. In general, these two categories of interpolation functions are different.

Depending on the relationship between degree of the interpolation functions used for shape functions and for the interpolation of the dependent variable, the elements are classified into three categories as sub-parametric elements, **iso-parametric** elements, and super-parametric elements. In the sub-parametric elements, the degree of the interpolation function for describing the shape of the element is lesser than those for the interpolation of the dependent variable. In the case of iso-parametric elements, the degree of the shape functions are equal to the degree of the interpolation function of the dependent variable. In super-parametric elements, the degree of the shape functions is greater than the degree of the interpolation function of the dependent variable. The interpolation functions for the finite element analysis of a problem should have the following characteristics:

1. A necessary criterion is that the element interpolation functions must be capable of modeling any constant values of the dependent variable or its derivatives, to the order present in the defining integral statement, in the limit as the element size decreases. [9]

2. A sufficient criterion is that the element shape functions should be chosen so that at element interfaces, the dependent variable and its derivatives, of one order less than those occurring in the defining integral statement, are continuous.' [1]

3. The interpolation functions for a particular element vanishes outside that element.

4. The interpolation function for a particular **node** assumes the value of unity at that **node** and assumes the value of zero at other nodes, reflecting the property of interpolation.

5. The sum of all interpolation functions of an element over all the nodes of that element equals unity.

6. An interpolation polynomial forms a complete polynomial family of degree N.

The important feature of the interpolation functions is that, they do not depend on the problem but depend on the type of element (geometry, number of nodes, and the number of primary unknowns per node). Also there is a relationship between the order of the approximation used for the dependent variable and the number of nodes in the element. The number of unknown constants in the interpolation functions is equal to the number of nodes of the element. Also the order of the interpolation function is one less than the number of nodes of the element. In other words, a quadratic approximation with three unknown constants requires identification of three nodes.

K. Computation of the element coefficients and the solution of matrix equations:
Once the form of representation of the dependent variable and the interpolation functions are chosen, they are substituted in the functional to get the element equations. The process of forming the element equations involve differentiation and integration operations, which are performed numerically. This process is repeated for all the elements. Then the resulting equations are assembled element by element by enforcing the inter-element continuity conditions. This process leads to a set of matrix equations with the coefficient matrix being sparse and symmetric. The symmetry of the coefficient matrix is a property transferred from variational formulation of the equation being

modeled. The sparseness of the matrix is a result of the finite-element interpolation function, which have nonzero values over a small portion of the domain.

The process of constructing the finite element equation for a differential equation with a single independent variable is illustrated. [11]

Consider the differential equation given by [12]

$$-\frac{d}{dx}\left(a\frac{du}{dx}\right) - f = 0 \qquad 0 < x < L \qquad (1.16)$$

with the associated boundary conditions being given by

$$u(0) = 0 \qquad \left(a\frac{du}{dx}\right)_{x=L} = P \qquad (1.17)$$

Following the procedures outlined for the construction of the variational expression, the variational form for the differential equation in (1.16) is given by

$$\int_{x_A}^{x_B}\left(a\frac{dv}{dx}\frac{du}{dx} - vf\right)dx + \left[v\left(-a\frac{du}{dx}\right)\right]_{x_A}^{x_B} = 0 \qquad (1.18)$$

where v denotes an arbitrary test function (or weight function).

From the boundary expression, it can be noted that the specification of u at $x=x_A$ and X=XB constitute the essential boundary conditions, and the specification of $(-a\, du/dx)$ at at $x=x_A$ and $x=x_B$ constitute the natural boundary conditions for the element. Thus the basic unknowns at the element nodes are the primary variable u and the secondary variable $(a\, du/dx)$.

Let

$$u(x_A) \equiv u_1^{(e)} \qquad u(x_B) \equiv u_2^{(e)} \tag{1.19a}$$

$$\left(-a\frac{du}{dx}\right)_{x_A} \equiv P_1^{(e)} \qquad \left(a\frac{du}{dx}\right)_{x_B} \equiv P_2^{(e)}$$

With the notations given above, the associated quadratic form for a single element given by Eq.(1.1) is

$$I_e(u) = \int_{x_A}^{x_B}\left[\frac{a}{2}\left(\frac{du}{dx}\right)^2 - uf\right]dx - P_1^{(e)}u(x_A) - P_2^{(e)}u(x_B) \tag{1.20}$$

Let the Ritz approximation of u on the element be given by

$$u_e(x) = \sum_{j=1}^{n}\alpha_j^{(e)}\psi_j^{(e)}(x) \tag{1.21}$$

Where α_j are the parameters to be determined, and $\psi_j(x)$ are the approximation functions. Substituting Eq.(1.21) in Eq.(1.20), the following equation is obtained :

$$\left[K^{(e)}\right]\{\alpha^{(e)}\} = \{F^{(e)}\} \quad \text{for } i = 1,2,...,n \tag{1.22}$$

where

$$K_{ij}^{(e)} = \int_{x_A}^{x_B}a\frac{d\psi_i}{dx}\frac{d\psi_j}{dx}dx \tag{1.24}$$

$$F_i^{(e)} = \int_{x_A}^{x_B}\psi_i f dx + P_1^{(e)}\psi_i(x_A) + P_2^{(e)}\psi_i(x_B) \tag{1.25}$$

L. Derivation of the interpolation functions: The properties of the approximation functions for the Ritz method is used to construct the interpolation functions for the differential equation under consideration.

To satisfy the 3rd condition specified in the Ritz method for the approximation functions, Eq.(1.21) should be differentiable at least once with respect to x and satisfies the essential boundary conditions (1.19a). The 5th and 6th conditions for the approximation functions in the Ritz method require $\{\psi_i\}$ to be linearly independent and complete. The $4^{th}, 5^{th},$ and 6th conditions are met if the approximation is of the form

$$u(x) = c_1 + c_2 x = c_1 \phi_1 + c_2 \phi_2 \qquad (1.26)$$

The continuity is satisfied, and $\phi_1 = 1$ and $\phi_2 = x$ are linearly independent and the set $\{1, x\}$ is complete. To satisfy the remaining requirement, namely the 4th condition, u is required to satisfy the essential boundary conditions of the element, which is the Eq.(1.19a) :

$$u(x_e) \quad \equiv u_1^{(e)} = c_1 + c_2 x_e \qquad \textbf{(1.27a)}$$
$$u(x_e + 1) \equiv u_2^{(e)} = c_1 + c_2 x_{e+1} \qquad \textbf{(1.27b)}$$

Solving for c_1 and c_2 in terms of $u_1^{(e)}$ and $u_2^{(e)}$,

$$u(x) = \sum_{i=1}^{2} u_i^{(e)} \psi_i^{(e)} \qquad \textbf{where} \qquad \textbf{(1.28a)}$$

$$\psi_1^{(e)} = \left(\frac{x_{e+1} - x}{x_{e+1} - x_e} \right) \quad \psi_2^{(e)} = \left(\frac{x - x_e}{x_{e+1} - x_e} \right) \qquad \textbf{(1.28b)}$$

$$x_e \leq x \leq x_{e+1}$$

Eq.(1.28a) satisfies the essential boundary conditions of the element, and $\{\psi_i\}$ are continuous, linearly independent, and complete over the element. Since the approximation functions are derived from Eq.(1.26) in such a way that $u(x) = u_1(e)$ at **node 1** ($x_A = x_e$)and $u(x) = u_2(e)$ at **node 2** ($x_B = x_{e+1}$), which signifies interpolation. Hence, they are also called *Lagrange family of interpolation functions.*

Substituting Eq.(1.28a) and Eq.(1.28b) in Eq.(1.22), the expressions for the matrix elements in the finite-element model over an element is given by

$$\left[K^{(e)}\right]\{u^{(e)}\} = \{F^{(e)}\} \tag{1.29}$$

$$K_{ij}^{(e)} = \int_{x_e}^{x_{e+1}} a \frac{d\psi_i}{dx} \frac{d\psi_j}{dx} dx \tag{1.30}$$

$$F_i^{(e)} = \int_{x_A}^{x_B} \psi_i f dx + P_i^{(e)} \tag{\textbf{1.31}}$$

where, for the linear element $(x_A = x_e \text{ and } x_B = x_{e+1})$.

The equations (1.29), (1.30) and (1.31) represent the finite element model of the differential equation (1.16) over an element.

The higher order approximations like quadratic, cubic can also be chosen by adding various powers of x and not leaving out any lower order terms *{to satisfy the completeness condition),* apart from the linear approximation which is chosen for the purpose of illustration. The procedure remains the same. An nth order element requires the inversion of **(n+1)** x **(n+1)** matrix. For higher order elements, Eq.(1.26) requires identification of additional nodes in the element. In other words, a quadratic approximation which has three constants c_1, c_2, c_3 requires identification of three nodes, the third one, say, at the center of the element. Thus, there is a relationship between the order of the approximation used for the dependent variable u and the number of nodes in the element.

The following page shows 'the pictorial representation of the finite element discretization of the one dimensional differential equation.

Finite Element Discretization of the one-dimensional second order differential equation:
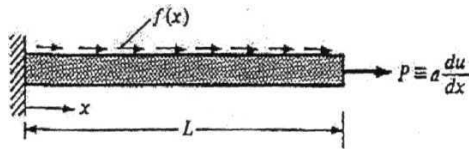
Fig.l(a). Physical Problem.
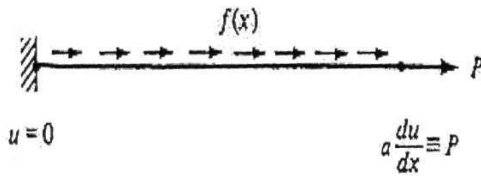
Fig.l(b). Mathematical Idealization.
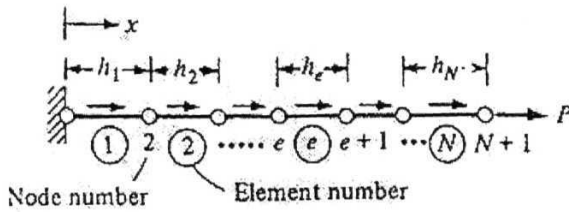
Fig.l(c). Finite Element Discretization.
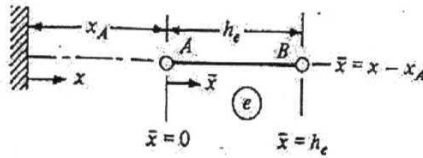
Fig.l(d). A typical finite element from the finite-element mesh shown

in Fig.(1c), where x is the global coordinate and $\bar{x}$ is the local coordinate.
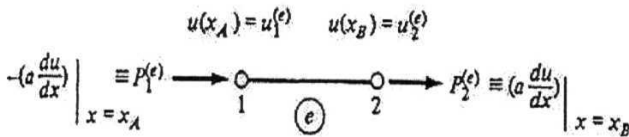
Fig.l(e). A typical element with the definition of the primary variable u and

secondary variable $\left(a\dfrac{du}{dx} \right)$ at the nodes.

In the diagrammatic representation of the process of solving the second order

differential equation in one-variable by the Finite-Element method, the Fig.l(a)

represents the actual problem under consideration. In Fig.l(b), the mathematical

idealization of the problem under consideration is presented. The specification of the

boundary conditions are represented in the figure as corresponding to two end points

denoted by u and P respectively. In Fig.1(c), the finite-element discretization of the

domain [0,L] is represented as being divided into N elements with the number in the

circle representing the element number and the numbers without the circle representing the nodes corresponding to each element. In Fig.l(d), a typical element is illustrated with the global and local co-ordinates and in Fig.1(e), the typical element is represented indicating the nodal definition of the primary variable and the secondary variable involving the derivative of the primary variable.

 Local and Global interpolation functions for the two-node linear element ($x_A=x_e$, $x_B=x_{e+1}$):
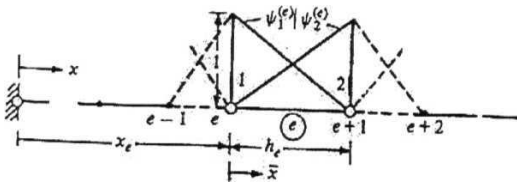
$$\psi_1^{(e)} = 1 - \bar{x}/h_e$$
$$\psi_2^{(e)} = \bar{x}/h_e$$

Fig.l(f) **Local Interpolation functions for a linear element.**
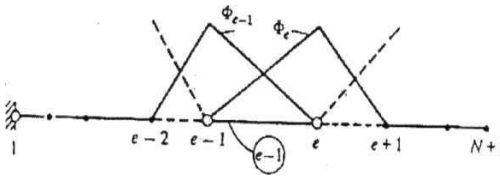
$$\Phi_e = \begin{cases} \psi_2^{(e-1)} & x_{e-1} \leq x \leq x_e \\ \psi_1^{(e)} & x_e \leq x \leq x_{e+1} \end{cases}$$

Fig.l(g) Global Interpolation functions for the two-node element mesh.

Fig.l(f) and Fig.l(g) represent the local and global interpolation functions derived by following the procedures described in section (L) on the derivation of the interpolation functions. In Fig.l(f), the local interpolation functions are represented in terms of the local coordinates. In Fig.l(g), the global interpolation functions are represented in terms of the global coordinates.

M. **Assembly (connectivity)** of **Element equations:** Since Eq.(1.29) is derived for an arbitrarily typical element, it holds for any element from the finite element mesh. For illustrative purpose,- it is supposed that the domain of the problem, $\Omega=(0,L)$, is divided into 3 elements of possibly unequal lengths. Since these elements are connected at nodes 2 and 3 and u is continuous, u_2 of element Ω^e should be the same as u_1 of element Ω^{e+1} for $e=l,2$. Expressing this correspondence mathematically, if the values of u at the global nodes are given the label as U_i (i=l,2,....N) where N is the total number of global nodes, then the following correspondence are obtained between the local (element) nodal values and the global nodal values.

$$u_1^{(1)} = U_1 \qquad\qquad\qquad (1.32a)$$
$$u_2^{(1)} = U_2 = u_1^{(2)} \qquad\qquad (1.32b)$$
$$u_2^{(2)} = U_3 = u_1^{(3)} \qquad\qquad (1.32c)$$
$$u_2^{(3)} = U_4 \qquad\qquad\qquad (1.32d)$$

The above equations are clarified in terms of figures that follow.

Correspondence of local and global nodal values and representation of the finite-element solution by global interpolation functions for the model problem:
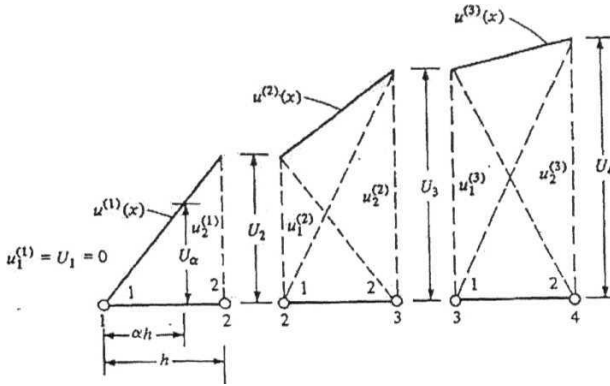
Fig.l(h) Correspondence of element and global nodal values.
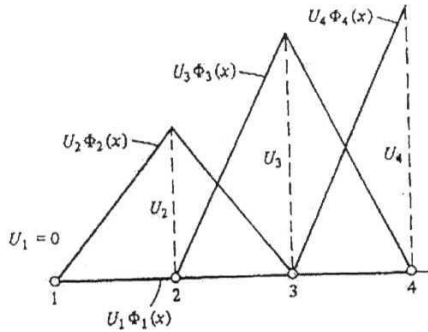
Fig.l(c) Representation of the solution by global interpolation functions.

The conditions expressed in Eq.(1.32) are called inter-element **continuity** conditions.

The assembly of the element equations can be done based on the idea that the quadratic functional (or the variational formulation) associated with the problem is equal to the sum of the quadratic functionals of all elements.

If I denotes the quadratic functional of the problem, and $\mathbf{I_e}$ is the quadratic functional for the element, then the above statement can be expressed as,

$$I(U_i) = \sum_{e=1}^{N} I_e(u_i^e) \qquad (1.33)$$

or, in matrix form,

$$[\delta I(U_i)]\{\delta U_i\} = \sum_{i=1}^{N}[\delta I_e(u_i^e)]\{\delta u_i^e\} = 0 \qquad \textbf{(1.34)}$$

where δu_i^e canbe viewed as the test function values v_i^e,

$$I_e(u_i^e) = \frac{1}{2}\{u^{(e)}\}^T[K^{(e)}]\{u^{(e)}\} - \{u^{(e)}\}^T\{F^{(e)}\} \qquad (1.35)$$

N denotes the number of elements in mesh and δ the variational operator.

Carrying out the necessary algebra in Eq.(1.34) , and using Eq.(1.32), collecting the coefficients of δU_i , (I=1,2,...,N+1), where N+1 is the total number of global nodes, and imposing the requirement that the coefficients of each δU_i should be equal to zero separately, we obtain in matrix form,

$$\begin{bmatrix} K_{11}^{(1)} & K_{12}^{(1)} & 0 & 0 \\ K_{21}^{(1)} & K_{22}^{(1)} + K_{11}^{(2)} & K_{12}^{(2)} & 0 \\ 0 & K_{21}^{(2)} & K_{22}^{(2)} + K_{11}^{(3)} & K_{12}^{(3)} \\ 0 & 0 & K_{21}^{(3)} & K_{22}^{(3)} \end{bmatrix} \begin{bmatrix} U_1 \\ U_2 \\ U_3 \\ U_4 \end{bmatrix} = \begin{bmatrix} F_1^{(1)} \\ F_2^{(1)} + F_1^{(2)} \\ F_2^{(2)} + F_1^{(3)} \\ F_2^{(3)} \end{bmatrix}$$

$$\text{.... (1.36)}$$

N. Imposition of Boundary Conditions: The Eq.(1.28) is valid for any problem described by Eq.(1.16) irrespective of the boundary conditions. The coefficient matrix represented in Eq.(1.28) is singular prior to the imposition of the essential boundary conditions on the primary variables. Upon the imposition of suitable boundary conditions of the problem, a non-singular invertible matrix is obtained.

The natural boundary conditions are included in the column vector $\{F^{(e)}\}$ through $P_j^{(e)}$. At all global nodes between the boundary nodes, the sum of the contributions of the natural boundary condition from **node** 2 of element e and **node 1** of element **e+1** should equal the specified value of the secondary variable (a **du** / dx). This is expressed as:

$$P_2^{(e)} + P_1^{(e+1)} = \textbf{specified value of}\left(a\,\frac{du}{dx} \right)_{x=x_{e+1}} \tag{1.37}$$

For the problem under consideration, (a du / dx) at $x=h_1$ and x= h_1+h_2 are specified to be zero. Since u is not specified at global nodes 2 and 3, it is understood that the secondary variable (a **du** / dx) is specified to be zero at these nodes. Hence,

$$P_2^{(1)} + P_1^{(2)} = 0 \qquad P_2^{(2)} + P_1^{(3)} = 0 \tag{1.38}$$

Regarding the imposition of the essential boundary condition, the only known essential boundary condition is

$$U_1 = u_1^{(1)} = 0 \tag{1.39}$$

The modified columns of the unknowns and $P_i^{(e)}$'s are given by

$$\{\Delta\} = \begin{bmatrix} 0 \\ U_2 \\ U_3 \\ U_4 \end{bmatrix} \qquad \{P\} = \begin{bmatrix} \left(-a\,\dfrac{du}{dx} \right)_{x=0} \equiv P_1^{(1)} \\ 0 \\ 0 \\ P \end{bmatrix} \tag{1.40}$$

O. Solution of Equations: The global finite element equation (1.36) can be partitioned conveniently into the following form:

$$\begin{bmatrix} \begin{bmatrix} K^{11} \end{bmatrix} & \begin{bmatrix} K^{12} \end{bmatrix} \\ \begin{bmatrix} K^{21} \end{bmatrix} & \begin{bmatrix} K^{22} \end{bmatrix} \end{bmatrix} \begin{bmatrix} \begin{bmatrix} \Delta^1 \end{bmatrix} \\ \begin{bmatrix} \Delta^2 \end{bmatrix} \end{bmatrix} = \begin{bmatrix} \begin{bmatrix} F^1 \end{bmatrix} \\ \begin{bmatrix} F^2 \end{bmatrix} \end{bmatrix} \qquad (1.40a)$$

Writing the above equation as two matrix equations,

$$\begin{bmatrix} K^{11} \end{bmatrix} \begin{bmatrix} \Delta^1 \end{bmatrix} + \begin{bmatrix} K^{12} \end{bmatrix} \begin{bmatrix} \Delta^2 \end{bmatrix} = \begin{bmatrix} F^1 \end{bmatrix} \qquad (1.40b)$$

$$\begin{bmatrix} K^{21} \end{bmatrix} \begin{bmatrix} \Delta^1 \end{bmatrix} + \begin{bmatrix} K^{22} \end{bmatrix} \begin{bmatrix} \Delta^2 \end{bmatrix} = \begin{bmatrix} F^2 \end{bmatrix} \qquad (1.40c)$$

From Eq.(1.40c),

$$\begin{bmatrix} \Delta^2 \end{bmatrix} = \begin{bmatrix} K^{22} \end{bmatrix}^{-1} \left[\begin{bmatrix} F^2 \end{bmatrix} - \begin{bmatrix} K^{21} \end{bmatrix} \begin{bmatrix} \Delta^1 \end{bmatrix} \right] \qquad \textbf{(1.40d)}$$

Once $\begin{bmatrix} \Delta^2 \end{bmatrix}$ is known, $\begin{bmatrix} F^1 \end{bmatrix}$ can be computed from Eq.(1.40b). In the present case,

$$\begin{bmatrix} K^{11} \end{bmatrix} = K_{11}^{(1)}$$

$$\begin{bmatrix} K^{12} \end{bmatrix} = \begin{bmatrix} K_{12}^{(1)} & 0 & 0 \end{bmatrix}$$

$$\begin{bmatrix} K^{21} \end{bmatrix} = \begin{bmatrix} K_{21}^{(1)} \\ 0 \\ 0 \end{bmatrix}$$

$$\begin{bmatrix} K^{22} \end{bmatrix} = \begin{bmatrix} K_{22}^{(1)} + K_{11}^{(2)} & K_{12}^{(2)} & 0 \\ K_{21}^{(2)} & K_{22}^{(2)} + K_{11}^{(3)} & K_{12}^{(3)} \\ 0 & K_{21}^{(3)} & K_{22}^{(3)} \end{bmatrix} \qquad (1.41)$$

$$\begin{bmatrix} F^1 \end{bmatrix} = F_1^{(1)} \qquad \begin{bmatrix} F^2 \end{bmatrix} = \begin{bmatrix} F_2^{(1)} + F_1^{(2)} \\ F_2^{(2)} + F_1^{(3)} \\ F_2^{(3)} \end{bmatrix}$$

For a = constant, $h_1=h_2=h_3=L/3$, f= **constant ,** we obtain

$$\left[K^{22}\right]^{-1} = \frac{L}{3a}\begin{bmatrix} 1 & 1 & 1 \\ 1 & 2 & 2 \\ 1 & 2 & 3 \end{bmatrix}$$

(1.42a)

$$\left[\Delta^2\right] = \begin{bmatrix} U_2 \\ U_3 \\ U_4 \end{bmatrix} = \frac{f L^2}{18a}\begin{bmatrix} 5 \\ 8 \\ 9 \end{bmatrix} + \frac{PL}{3a}\begin{bmatrix} 1 \\ 2 \\ 3 \end{bmatrix}$$

(1.42b)

and the unknown natural boundary condition at x=0 is given as

$$P_1^{(1)} \equiv \left(-a\frac{du}{dx}\right)_{x=0} = -(fL+P)$$

(1.43)

Since $\psi_i^{(e)}$ (e =1,2,3) is zero in any element Ω^f for e not equal to f , the global finite element solution for the entire domain is given by

$$u(x) = \sum_{e=1}^{3}\left(\sum_{i=1}^{2}u_i^{(e)}\psi_i^{(e)}\right) \equiv \sum_{I=1}^{4}U_I\Phi_I(x)$$

(1.44)

where $\Phi_I(x)$, I=1,2,...,N+1, are piecewise continuous global interpolation functions,

$$\Phi_1(x) = \begin{cases} \psi_2^{(I-1)}(x) & x_{I-1} \le x \le x_I \\ \psi_1^{(1)}(x) & x_1 \le x \le x_{I+1} \end{cases}$$

(1.45)

Using the above expressions, the procedure for assembling elements leads to a system of linear equations which is solved numerically.

The exact analytical solution of the differential equation given in Eq.(1.16) is given by[12]

$$u_{\text{exact}} = \frac{f}{2a}\left(2xL - x^2\right) + \frac{P}{a}x$$

(1.46)

The accuracy of the finite element solution with the exact analytical solution is depicted below in the graph.
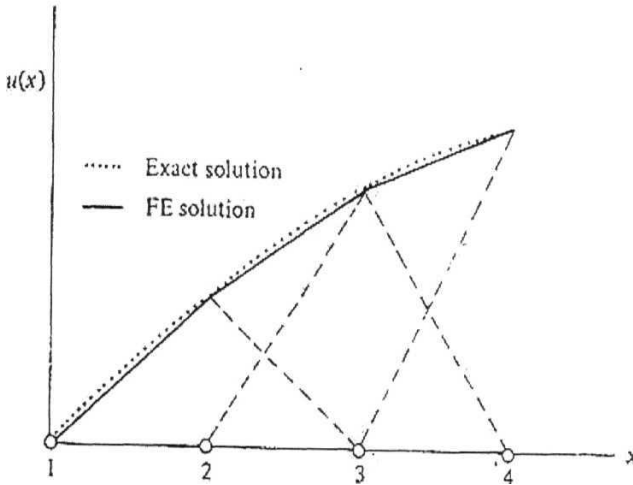
Fig.l(f) Graphical representation of the exact analytical solution and the Finite Element Solution.

P. Errors in the Finite-Element Method:

Approximation errors in the finite-element method: The errors introduced into the finite-element solution of a given differential equation can be attributed to three basic sources: [13]

1. Boundary error: Error due to the approximation of the domain.

2. Quadrature and finite arithmetic errors: Errors due to the numerical evaluation of integrals and the numerical computation on a computer.

3. Approximation error: Error due to the approximation of the solution.

In one-dimensional problems when the domains considered are straight lines, no approximation of the domain is necessary. In two-dimensional problems posed on nonrectangular domains, domain (or boundary) approximation errors are introduced into the finite element problems. In general, these errors can be interpreted as errors in the specification of the data of the problem, since the given differential equation is solved on a modified domain. As the mesh is refined, the domain is more accurately represented, and therefore, the boundary approximation errors are expected to approach zero. When curved elements (i.e., elements with non-straight sides) are involved, the error estimate also depends on the Jacobian of the transformation between the variables in the original coordinate system and the variables in the transformed coordinate .

When finite-element computations are performed on a computer, round-off errors and errors due to the numerical evaluation of integrals are introduced into the solution. In most linear problems with a reasonably small number of total degrees of freedom in the system, these errors are small compared to approximation errors.

The error introduced into the finite-element solution u_h because of the approximation of the dependent variable u is inherent to any problem.

$$u \approx u_h = \sum_{e=1}^{N} \sum_{i=1}^{n} u_i^{(e)} \psi_i^{(e)} = \sum_{i=1}^{M} U_I \Phi_I \qquad \textbf{(1.47)}$$

Where N is the number of elements in the mesh, M is the total number of global nodes, and n is the number of nodes in an element. Then the error E can be defined as

$$\mathbf{E} = u - u_h \qquad (1.48)$$

Q. Various measures of errors: There are several ways to measure the difference or distance between any two functions u and u_h. The *point-wise* error is the difference of u and u_h at each point of the domain.

Assuming that the dependent variable u depends only on $\mathbf{x}$, the difference of u and u_h can also be defined to be the maximum of all absolute values of the differences of u and u_h in the domain $\Omega = (a,b)$:

$$\| u - u_h \|_\infty \equiv \max_{a \leq x \leq b} | u(\mathbf{x}) - u_h(\mathbf{x}) | \tag{1.49}$$

This measure of difference is called **supmetric**. It is important to note that *supmetric* is a real number, whereas the *point-wise error* is a function, and does not qualify for a distance or *norm* in a strict mathematical sense. More generally used measures (or norms) of the difference of two functions are the L_2 norm and the energy norm. For any square-integrable functions u and u_h defined on the domain $\Omega = (a,b)$, the norms are defined by

L₂norm :
$$\| u - u_h \|_0 = \left(\int_a^b | u - u_h |^2 dx \right)^{1/2} \tag{1.50}$$

 Energy **norm :**
$$\| u - u_h \|_m = \left(\int_a^b \sum_{i=0}^m \left| \frac{d^i u}{dx^i} - \frac{d^i u_h}{dx^i} \right|^2 dx \right)^{1/2} \tag{1.51}$$

where 2 m is the order of the differential equation being solved. The word "**energy** norm" is used to indicate that it contains the same order derivatives as the quadratic functional (which denotes energy in solid mechanics) associated with the equation. The above definitions can be easily modified for two or higher dimensions.

The finite element solution u_h is said to *converge in the energy norm* to the true solution u if

$$\| u - u_h \|_m \leq ch^p \text{ for p > 0} \tag{1.52}$$

where c is a constant independent of u and u_h and h is the characteristic length of an element. The constant p is called the rate of convergence.

If the finite element interpolation functions Φ_I ($I=1,2,\ldots,M$) are completely polynomials of degree k, then the error in the energy norm can be shown to satisfy the inequality

$$\|e\|_m \equiv \|u - u_h\|_{k+1} \leq ch^p \qquad p = k + 1 - m > 0 \tag{1.53}$$

where c is a constant. This estimate implies that the error goes to zero at the rate of p as h is decreased (or, the number of elements is increased). In other words, the logarithm of the error in the energy norm versus the logarithm of h is a straight line whose slope is k+1-m. The greater the degree of the interpolation functions, the faster the rate of convergence. The error in the energy norm goes to zero at the rate of k+l-m; the error in the L_2 norm is even faster, namely k+1. In other words, derivatives converge slower than the solution itself. The above error estimates are very useful in the sense that it gives the idea of the accuracy of the approximate solution, whether the true solution is known or not. The estimate also gives an idea of how rapidly the finite-element solution converges to the true solution. It however, does not tell when to stop refining the mesh. The process of termination of mesh refinement rests with the level of the tolerance of the approximate solution for a given problem.

The following sections deals with the application of the Finite Element method in Electromagnetics.

R. Finite Element method in Electromagnetics: The application of the Finite element method in electrical engineering began about 1968-1969 [14]. A paper by Arlett, Bahrani, and Zienkiewicz (1968) addressed waveguides and cavities [15]. A paper giving the finite element formulation of the classical hollow wave guide problem was published in 1969 by Silvester [16]. There followed a rapid succession of papers on magnetostatics, dielectric loaded waveguides (Csendes and Silvester 1971), and other well known boundary value problems of electromagnetics [17]. The method was quickly applied to integral operators as well, both in microwave devices (Benedek and Silvester1972) [18] and wire antenna problems (Silvester and Chan 1972) [19]. Since then, there is an explosive growth in the application of the finite element method in electromagnetics. As per the INSPEC bibliographic database over the 1968-1993 period, a conservative estimate shows that roughly 600 articles are added each year. [20]

The earlier stages of the development of the finite element method in electromagnetics was based on variational principles. Much of the concepts were borrowed from the finite element analysis used in structural mechanics problems. This structural mechanics approach continued to be used in the finite element analysis of vector fields in electromagnetics till 1980s. [21]

The structural mechanics approach, as applied directly to electromagnetic field analysis, had a short coming. The reason being that the fields that occur in structural mechanics and those encountered in electromagnetics are fundamentally different.

The electromagnetic field vectors **not only obey the Maxwell curl equations,** but they are also constrained by the divergence equations

$$\nabla.\mathbf{B} = 0 \qquad\qquad \textbf{(1.54)}$$

$$\mathbf{V}.\mathbf{D} = -\frac{\rho}{\varepsilon} \qquad\qquad (1.55)$$

Solenoidality is required, practically for **all** fields in electromagnetics, but is required only in a limited range in fields belonging to structural mechanics or fluids. If the scalar finite element functions are used, and no particular care is taken to enforce solenoidality, solutions are obtained that satisfy the Maxwell curl equations but not the divergence equations (1.23) and (1.24). Also there are non-physical modes called spurious modes which occur in the finite element analysis using a vector working variable approximated by nodal finite elements. They arise through inadequate finite element modelling of the curl of the magnetic field strength H when the functional is formulated purely in terms of the vector variable H [22]. These spurious solutions are characterized by a substantially high divergence of the magnetic field [23]. Also, in deterministic problems where the Electric field intensity is used as the working variable, the inadequate modeling of the irrotational solutions corresponding to the zero eigen value in the vector helmholtz equation, leads to the appearance of the spurious modes, along with the non-zero eigen values [24].

Among the several approaches suggested **to avoid the spurious mode solutions,** one of the approach is to employ **tangentially continuous vector finite elements,** which implies that only tangential continuity between elements are enforced and not normal continuity. [25]

The logical step towards the implementation of the tangentially continuous vector finite elements to successfully deal with the electromagnetic fields, which are basically vector fields, is to formulate a stationary functional expressed entirely in terms of vector quantities. In this connection, such a functional is developed for a homogenous vector helmholtz equation given by[26],

$$\nabla \times p\nabla \times u - k^2 qu = 0 \qquad (1.56)$$
$$\nabla \times p\nabla \times u - k^2 qu = 0$$

where p and q are scalars and u is the dependent vector variable.

Let

$$F(U) = \frac{1}{2}\int_{\Omega}\left(\nabla \times U \cdot p\nabla \times U - k^2 qU \cdot U\right)d\Omega \qquad (1.57)$$

where p and q represent scalar local material properties. Let U be an approximation to the desired vector quantity, u its exact value. Then the approximate vector may be written as

$$U = u + \theta\, h \qquad (1.58)$$

where h is a vector valued error function, 6 is a scalar parameter. With this substitution, Eq.(1.57) becomes,

$$F(U) = F(u) + \theta\, \delta\, F(u) + \frac{\theta^2}{2}\delta^2\, F(u) \qquad (1.59)$$

where the second variation has a value that characterizes the function h , given by

$$\delta^2 F(u) = F(h) \qquad (1.60)$$

$$\delta\, F(u) = \int_{\Omega}\left(\nabla \times u \cdot p\nabla \times h - k^2 qu \cdot h\right)d\Omega \qquad (1.61)$$

F(U) is stationary if the term in θ vanishes. To this effect, Eq.(1.61) is rewritten using the vector differentiation rule

$$\nabla \cdot \left(a \times h\right) = \left(\nabla \times a\right) \cdot h - a \cdot \left(\nabla \times h\right) \qquad (1.62)$$

Setting a = V x $\boldsymbol{u}$ and integrating over region Ω,

$$\int_{\Omega}(\nabla\times u)\cdot p(\nabla\times h)\,d\Omega = \int_{\Omega}h\cdot\nabla\times(p\nabla\times u)\,d\Omega - \oint_{\partial\Omega}p\nabla\times u\times h \tag{1.63}$$

With this substitution, the first variation $5\,F(\boldsymbol{u})$ becomes,

$$\delta\,F(u) = \int_{\Omega}(\nabla\times p\nabla\times u - k^2 qu)\cdot h\,d\Omega - \oint_{\partial\Omega}p(\nabla\times u)\times h\,dS \tag{1.64}$$

The integral over Ω vanishes identically because the field u satisfies the homogenous vector helmholtz equation (1.56).

Considering the boundary integral term, and rearranging the vector triple product as

$$(\nabla\times u)\times h\cdot dS = (\nabla\times u)\times h\cdot 1_n\,dS = h\times 1_n\cdot\nabla\times u\,dS \tag{1.65}$$

and using the definition of U in Eq.(1.58),

$$\theta\oint_{\partial\Omega}p\nabla\times u\times h\cdot dS = \oint_{\partial\Omega}(U-u)\times 1_n\cdot(p\nabla\times u)\,dS \tag{1.66}$$

Rearranging the triple product on the right cyclically,

$$\theta\oint_{\partial\Omega}p\nabla\times u\times h\cdot dS = \theta\oint_{\partial\Omega}1_n\times(p\nabla\times u)\cdot(U-u)\,dS \tag{1.67}$$

The integral on the boundary term vanishes if either of two conditions holds. These are termed as *natural* and *essential* boundary conditions respectively. The first boundary condition arises when the curl of the correct solution u is purely normal to the boundary,

$$1_n\cdot\nabla\times u = 0$$

This is the condition that comes naturally if no boundary conditions of any sort are imposed on the finite element solution.

The essential boundary condition is,

$$U \times 1_n = u \times 1_n \tag{1.69}$$

This must be imposed by appropriately constraining the vector fields.

Both the boundary conditions refer to the selected vector components and not to all components.

Hence, it can be summarized that the solution of a homogenous vector helmholtz equation of the form (1.56) is fully determinate if the tangential vector field of the form given in Eq.(1.69) is prescribed, and the normal components take care of themselves. Also the boundary value problem (1.56) along with the boundary condition given by

$$u \times 1_n = u_t \tag{1.70}$$

is solved by stationary point of the functional given in Eq.(1.57) over all U which must be differentiable once, satisfying the essential boundary condition.

S. Electric and Magnetic walls: The situations of particular importance in microwave engineering arise when $u = E$ and $u = H$ giving rise to E and H formulations respectively. The natural boundary conditions in these two formulations are discussed.

E formulation: If the field problem is formulated in terms of the electric field vector E, the natural boundary condition is,

$$1_n \times \nabla \times E = 0 \tag{1.71}$$

This condition can be written using Maxwell's electric curl equation as.

$$1_n \cdot \frac{\partial B}{\partial t} = \frac{\partial}{\partial t}(1_n \cdot B) = 0 \tag{1.72}$$

Time - varying fields meet this requirement in such a way that the magnetic flux density vector B must lie parallel to the bounding surface. Such boundaries correspond to perfect conductors and are referred to as *electric walls.* They are surfaces through which no magnetic flux can penetrate, which is satisfied by a perfect electric conductor. [26]

H formulation: If the field problem is formulated in terms of the magnetic field vector H, the natural boundary condition becomes,

$$1_n \cdot \nabla \times H = 0 \tag{1.73}$$

Using Maxwell's magnetic curl equation,

$$1_n \cdot \frac{\partial}{\partial t}\left(J + \frac{\partial D}{\partial t}\right) = 0 \tag{1.74}$$

Inside a wave-guide, cavity, or any other dielectric medium, there cannot exist any conduction current density J. Hence,

$$\frac{\partial^2}{\partial t^2}\left(1_n \cdot D\right) = 0 \tag{1.75}$$

The electric flux density vector D, and also the electric field vector E, must lie parallel to the bounding surface. There cannot be any component of D normal to the boundary. Such boundaries are referred to as *magnetic walls.* No electric flux can penetrate them, and that would be the case were the material perfectly permeable magnetically. [26] They arise frequently as the consequence of geometric symmetry.

T. Implementation of tangentially continuous vector finite element method: Having formulated the stationary functional expressed in terms of the vector field variables, the next step is the representation of the field variable in terms of vector interpolation functions suitable for the finite element implementation.

Under this situation, the variable for which the finite element solution is sought is expanded using vector interpolation functions T, as

$$U(r) = \sum_{m=1}^{M} U_m \tau_m(r) \qquad (1.76)$$

where τ_m, the vector interpolation function, exhibits tangential continuity but not normal continuity between elements.

The mathematical properties of the tangentially continuous vector finite elements of the form given in the expansion given in Eq.(1.56) was done by Nedelec in 1980 [27]. Based on the work of Nedelec, Bossavit in 1982 [28] introduced the first tetrahedral vector finite elements.

An appropriate hexahedral vector element was first introduced in a rudimentary low-order form with straight sides, by Van Welij in 1985 [29]. Subsequently, Crowley, Silvester and Hurwitz in 1988 [30], generalized the hexahedral form with their mixed order covariant projection **elements**[31], which could be of high order and have curved sides. The details of the covariant projection elements are given in the subsequent paragraphs.

For the purpose of illustration, a 27-node curved brick[32] defined by the nodal cartesian coordinates (x_i, y_i, z_i) i=1 to 27 mapped from a reference cube occupying the (u, v, w) space,

$-1 \leq u \leq 1, -1 < v < 1, -1 < w < 1$ is shown below.
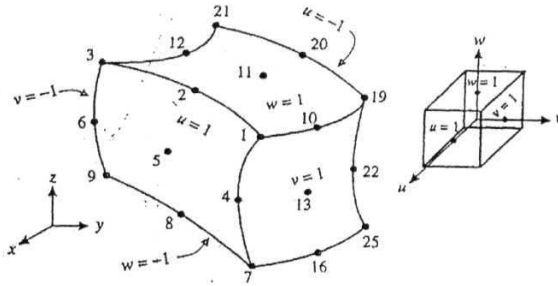
Fig.1(g): A 27-node curvilinear hexahedron in (x,y,z) space and the reference cube in **(u,v,w)** space.

Vectors referred to the rectangular *(x, y, z)* axes are not convenient for such a curvilinear element, because the continuity rules for the vector variables, namely the electric field intensity or the magnetic field intensity E or H, at material interfaces will be expressed in a cumbersome manner. Material interfaces, and finite element boundaries will ordinarily be arranged to coincide; and hence a means of referring vectors to axes related to the element boundary is sought. Then in accordance with the variational rules, tangential vector continuity at material interfaces can be easily enforced and the discontinuous normal components will be allowed to adjust naturally.

U. General mixed-order covariant projection elements: The mapping from $\mathbf{r} = (x, y, z)$ to $\mathbf{p} = (u, v, w)$ for each element with M modes is very conveniently done using scalar nodal interpolation functions $\alpha_m(u, v, w)$ of polynomial form,

$$x = \sum_{m=1}^{M} x_m \alpha_m(u, v, w) \tag{1.77}$$

$$y = \sum_{m=1}^{M} y_m \alpha_m(u, v, w) \tag{1.78}$$

$$z = \sum_{m=1}^{M} z_m \alpha_m(u, v, w) \tag{1.79}$$

The Kronecker delta relation, for α_m is given by

$$\alpha_m(u_n, v_n, w_n) = \delta_{mn} \tag{1.80}$$

The polynomial order of $\alpha_m(u_n, v_n, w_n)$ chosen for this transformation between the real finite element in $\mathbf{r}$ space and the reference cube in $\mathbf{p}$ space is determined by the geometrical boundaries which it is wished to be modeled.

For the case of the 27 node brick shown in Fig.l(g), the equations given in the next page, shows the selection of the 27 nodes ρ_m in (u, v, w) space alongside interpolation functions $\alpha_m(u, v, w)$ having the required behavior $\alpha_m(\rho_m) = \delta_{mn}$.

$$\rho_1 = (1,1,1), \quad \alpha_1 = \frac{u(1+u)v(1+v)w(1+w)}{8} \tag{1.81a}$$

$$\cdot$$

$$\cdot$$

$$\rho_4 = (1,1,0), \quad \alpha_4 = \frac{u(1+u)v(1+v)w(1-w)}{4} \tag{1.81b}$$

$$\rho_5 = (1,0,0), \quad \alpha_5 = \frac{u(1+u)v(1+v)(1-v)(w+1)(1-w)}{2} \tag{1.81c}$$

$$\cdot$$

$$\cdot$$

$$\rho_{14} = (0,0,0), \quad \alpha_{14} = (1+u)(1-u)(1+v)(1-v)(w+1)(1-w) \tag{1.81d}$$

Appropriate sign changes made in the coefficients of u, v, w yield the rest of the 27 interpolation functions. Existence of a single valued inverse of the relations Eqs. (1.77)-(1.79), is assumed to exist for r and p within their respective domains.

V. Unitary Vectors: Consider the point P in r-space designated by its mapped point (u, v, w) in or on the boundary of the reference cube. The equations (1.77)-(1.79) can be compactly written as

$$r = \mathbf{r}(u, v, w) \tag{1.82}$$

The infinitesimal perturbation about P represented by the reference cube perturbation (du, dv, dw) is given by

$$d\mathbf{r} = \frac{\partial \mathbf{r}}{\partial u} du + \frac{\partial \mathbf{r}}{\partial v} dv + \frac{\partial \mathbf{r}}{\partial w} dw \tag{1.83}$$

Keeping v and w constant gives

$$d\mathbf{r} = \frac{\partial \mathbf{r}}{\partial u} du \tag{1.84}$$

Defining a vector

$$\mathbf{a}_u = \frac{\partial \mathbf{r}}{\partial u}$$ (1.85)

The above equation can be evaluated using Eqs.(1.77)-(1.79). Given the curved brick coordinates, and some corresponding set of interpolation functions, the vectors $\mathbf{a}_v$ and $\mathbf{a}_w$ may be similarly constructed. These vectors $\mathbf{a}_u$, $\mathbf{a}_v$, $\mathbf{a}_w$ are called **unitary vectors.**

W. Geometrical Interpretation: The unitary vectors have an important geometrical interpretation. Keeping v and w constant, the parameter u defines a curve in **r-space** to which $\mathbf{a}_u$ is a tangent. Thus the vectors $\mathbf{a}_v$ and $\mathbf{a}_w$ are both tangential to any curved surface u = constant, in particular they are tangential to the faces $u=+1$ and $u= -1$ of a brick element. Tangents to the other curved faces arise similarly. This is shown in Fig.(1h) in the following figure.
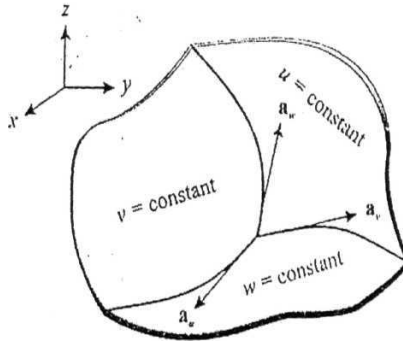
Fig.(lh). Unitary vectors for curvilinear hexahedra.

It is important to note that since the r-space finite element is defined by an arbitrary set of nodal co-ordinates, in general the unitary vectors a are neither of unit length nor are they mutually perpendicular.

X. Covariant projection: If some polynomial trial function representation of the electric field vector, say $\mathbf{E}'(u,v,w)$ related back to r-space of the form

$$\rho = \rho(\mathbf{r}) \qquad (1.86)$$

is constructed for the curvilinear brick element e, then the components of $\mathbf{E}'$ tangential to the curved face $u = -1$ will be represented by their covariant projections

$$E_v^e = \mathbf{E}'.\mathbf{a}_v \qquad (1.87a)$$
$$E_w^e = \mathbf{E}'.\mathbf{a}_w \qquad (1.87b)$$

Hence the covariant projection is defined as the projection of a vector on the unitary set of basis vectors.

Y. Implementation of the inter-element tangential continuity condition:

Extending the polynomial representation of the vector $\mathbf{E}$ in a piecewise fashion to a collection of elements e, using E_u^e, E_v^e, E_w^e corresponding to the various hexahedral faces, it is required to arrange that inter - element tangential components of $\mathbf{E}$ remain continuous while the normal components are left unconstrained. This can be done by ensuring that the appropriate covariant projections E^e are the same for the neighbouring elements.

The subsequent reconstruction of $\mathbf{E}'$ from E_u^e, E_v^e, E_w^e necessary in order to set up the finite element matrix equations is done as follows.

Consider the element vector trial function

$$\mathbf{E}' = E_u^e(u,v,w)\frac{\mathbf{a}_v \times \mathbf{a}_w}{V} + E_v^e(u,v,w)\frac{\mathbf{a}_w \times \mathbf{a}_u}{V} + E_w^e(u,v,w)\frac{\mathbf{a}_v \times \mathbf{a}_u}{V}$$

$$.(1.88)$$

where, the parameter V is given by

$$V = \mathbf{a}_u.\mathbf{a}_v \times \mathbf{a}_w = \mathbf{a}_v.\mathbf{a}_u \times \mathbf{a}_u = \mathbf{a}_w.\mathbf{a}_u \times \mathbf{a}_v \qquad (1.89)$$

The $E^e_{..}$'s and so forth may be considered to be arbitrary polynomial expansions in u, v, w so that Eq.(1.88) represents a vector expansion for **E**. Taking the scalar product of Eq.(1.88) and applying the rules of vector algebra, it can be shown that

$$E' . a_u = E^e_u \qquad (1.90)$$

Similarly for the other two covariant projections. The notation for the reciprocal unitary vectors given in Eq.(1.88) is given as,

$$a^u = \frac{a_v \times a_w}{V} , a^v = \frac{a_w \times a_u}{V} , a^w = \frac{a_u \times a_v}{V} \qquad (1.91)$$

$$E^e_u = \sum_{i=0}^{m} \sum_{j=0}^{n} \sum_{k=0}^{n} E^e_{uijk} h_i(u) h_j(v) h_k(w) \qquad (1.92a)$$

$$E^e_v = \sum_{i=0}^{n} \sum_{j=0}^{m} \sum_{k=0}^{n} E^e_{vijk} h_i(u) h_j(v) h_k(w) \qquad (1.92b)$$

$$E^e_w = \sum_{i=0}^{n} \sum_{j=0}^{n} \sum_{k=0}^{m} E^e_{wijk} h_i(u) h_j(v) h_k(w) \qquad (1.92c)$$

Here E^e_{uijk}, E^e_{vijk}, E^e_{wijk} are unknown coefficients, $m > 0$, $n > 0$ and

$$h_o(\zeta) = 1 - \zeta, h_1(\zeta) = 1 + \zeta, h_i(\zeta) = (1 - \zeta^2)\zeta^{i-2}, i \geq 2 \qquad (1.93)$$

and h_i is a polynomial of order i. The possibility of $m \neq n$ is allowed for. The order of the polynomial approximations in u assigned to the u - covariant projection E^e_u may be different from that assigned in v and w and the polynomial order of v in E^e_v and w in E^e_w may differ from that of the remaining two reference cube variables.

The vector polynomial orders m and n are unconnected with the order of the scalar (x,y,z) to (u,v,w) mapping. The former polynomial orders have a fundamental bearing upon the accuracy of the final solution approximation whereas the latter only affect the accuracy of modeling the problem boundaries. If the boundaries were polygonal, it would suffice to use an eight-node tri-linear transformation between p and r.

Z. Significance of the mixed polynomial order: Consider the trial expansion Eq.(1.88) resulting from using the covariant projection polynomial expansions, along with Eq.(1.92), for some possible pair m,n (neither m=0 nor n=0 is allowed). The tangential continuity between the vectors in the common faces of adjacent hexahedra while leaving free the other components, is explained in the following discussion.

Two of the curved faces of the tetrahedral element are represented by $u = \pm 1, (-1 < v < 1, 1 \leq w \leq 1)$, similarly the other four faces. Confining the attention to $\mathbf{E}$ derived from the covariant projections, represented by Eqs.(1.92-1.93), putting $u = -1$, all of the $h(u)$'s vanish at the curvilinear face $u = -1$ apart from $h_0 = 2$ giving the covariant projections as

$$E_u^e(-1, v, w) = \sum_{j=0} \sum_{k=0} E_{u0\,jk}^e 2h_j(v)h_k(w) \tag{1.94a}$$

$$E_v^e(-1, v, w) = \sum_{j=0}^{m} \sum_{k=0}^{n} E_{v0\,jk}^e 2h_j(v)h_k(w) \tag{1.94b}$$

$$E_w^e(-1, v, w) = \sum_{j=0}^{n} \sum_{k=0}^{m} E_{w0\,jk}^e 2h_j(v)h_k(w) \tag{1.94c}$$

The coefficients $E_{v0\,jk}^e$, $E_{w0\,jk}^e$ define the tangential field at $u = -1$. At the face $u = +1$ it is $h_1 = 2$ which alone survives, and in the same way, the coefficients E_{v1jk}^e, E_{w1jk}^e give the tangential fields there. Similar arguments apply to the coefficients associated with the surfaces $v = \pm 1$ and $w = \pm 1$. Having already satisfied the requirement for tangential continuity of $\mathbf{E}$ at the face $u = -1$, the remaining $i = 0$ coefficient $E_{u0\,jk}^e$ may be left free and unmatched. Similarly E_{u1jk}^e, belonging to the face $u = +1$ and the corresponding coefficients associated with v and w are left on their own. The components of $\mathbf{E}'$ on $u = \pm 1$ relating to all E_{uijk}^e, $i > 1$, $v = \pm 1$ and $w = \pm 1$ vanish, and hence the corresponding coefficients are also left unconstrained.

In a vector finite element finite assembly procedure it becomes necessary to identify those tangential field coefficients relating to any given element face and match them up with the corresponding ones on the neighboring element face connecting to it.

As a whole, the elements are examine face by face, identifying the coefficients E^e in neighboring elements which have to be matched and leaving others unpaired.

In general, for the mixed-order case, the lower-order interpolation functions $h(\zeta)$ are subsets of the higher-order ones. Thus, if desired, different order vector hexahedra can be employed in the same mesh in a similar fashion to the hierarchal scheme described for tetrahedral elements.

AA. Covariant projection elements of mixed order $m=1, n=2$:

The figure below shows the covariant projection element of mixed order $m=1$ and $n=2$.
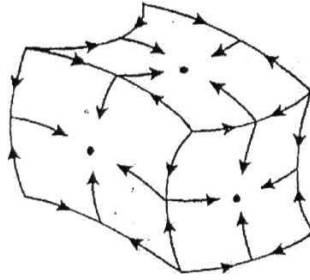
Fig.l(i): Covariant projection element of mixed order m=l and **n=2.**

The covariant projection element of mixed order shown above was first introduced by Crowley, Silvester, and Hurwitz in 1988, representing a practical embodiment of the general hexahedral case.

If the 27-node p to r transformation is employed , then the unitary vectors are

$$a_u = \sum_{i=1}^{27} r_i \frac{\partial \alpha_i}{\partial u} \,, \quad a_v = \sum_{i=1}^{27} r_i \frac{\partial \alpha_i}{\partial v} \,, \quad a_w = \sum_{i=1}^{27} r_i \frac{\partial \alpha_i}{\partial w} \qquad \text{-} \qquad (1.95)$$

where $\alpha_i(u, v, w)$ are given by Eq.(1.81), giving rise to the reciprocal unitary vectors

$\mathbf{a}^u$, $\mathbf{a}^v$, $\mathbf{a}^w$. The vector interpolation functions **are** obtained by the **scalar functions** multiplying the reciprocal unitary vectors. These **scalars are the polynomial terms of the** covariant projections. From Eqs.(1.94(a-c)) for the case $m=1$, $n=2$, there are 2 x 3 x 3 terms with a similar number of undetermined coefficients E^e , associated with each reciprocal unitary vector resulting in a total of 54 degrees of freedom. The Figure (l(i)) above shows schematically how the reciprocal unitary vectors $\mathbf{a}^u$, $\mathbf{a}^v$, $\mathbf{a}^w$ relate to the faces and edges of the curvilinear hexahedron, thereby facilitating the assembly of a collection of connected hexahedra, with each vector considered to point inwards. In the diagram, every vector is shown as if acting at the point on the edge or face where it becomes a maximum. These are continuous vector functions which **span the entire** finite element and the schematic points of action do not have the same **significance** as do the nodes in a scalar finite element interpolation.

BB. Quadrilateral vector elements: Equivalents of the hexahedral covariant projection elements are obtained by mapping quadrilateral elements in (x,y) space onto the normalized (u,v) square, with u and v ranging from -1 to 1. As in the three dimensional case, the electric field is represented in terms of its components

$E_u=\mathbf{E}$. $\mathbf{a_u}$, $E_v=\mathbf{E}$. $\mathbf{a_v}$.

The Vector E is reconstructed as

$$\mathbf{E}=E_u\left(\frac{\mathbf{a}_v\times\mathbf{a}_z}{\left|\mathbf{a}_u\times\mathbf{a}_v\right|}\right)+E_v\left(\frac{\mathbf{a}_z\times\mathbf{a}_u}{\left|\mathbf{a}_u\times\mathbf{a}_v\right|}\right) \qquad (1.96)$$

where $\mathbf{a_u}$ and $\mathbf{a_v}$ are the unitary vectors and $\mathbf{a}_w$ is the unit vector in the z-direction. Then it follows that,

$$E_u = \sum_{i=0}^{m} \sum_{j=0}^{n} E_{uij} h_i(u) h_j(v) \qquad (1.97)$$

$$E_v = \sum_{i=0}^{m} \sum_{j=0}^{n} E_{vij} h_i(u) h_j(v) \qquad (1.98)$$

where the h-functions are defined in Eq.(1.73). The orders m and n of the polynomials are not the same. The figure below shows the quadrilateral elements.

Q_{11} $\qquad\qquad$ Q_{12} $\qquad\qquad$ Q_{22}
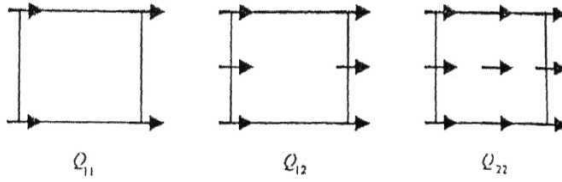
Fig.1(j). Three Quadrilateral edge Elements with each arrow representing one of the u vector interpolation functions making up the summation in Eq.(1.77).

CC. Spurious modes and covariant projection elements:

Dillon, Liu and Webb (1994) [33] tried out a number of different possibilities using up to 32 of the quadrilateral vector elements Q_{mn} to model a 1 meter square wave guide in comparison with the known eigen solutions. Testing up as far as m=5, n=5, they arrived at the following conclusions: **only** tangential and not normal continuity has to be maintained between the quadrilaterals, and $m<n$ to prevent spurious modes to appear in the vector finite element solutions.

To summarize the application of the finite element method in electromagnetics, it can be said that the tangentially continuous vector finite element method with covariant projection elements or edge elements provide a satisfactory tool for determining the eigen modes and eigen solutions of three dimensional or two dimensional structures where the fields considered are essentially vectorial in nature.

The following discussion orients towards a novel scaled boundary finite element method, the theory and its application being developed in the successive chapters.

DD. The Scaled boundary finite element method: In the discussion on the application of the tangentially continuous vector finite element method do deal with the electromagnetic fields which are basically vectorial in nature, the fact that is to be observed is that, in general, for structures in three dimensions devoid of any symmetry along a particular axis, the discretization is to be performed along all the 3 axes (volume discretization). In case of the finite element analysis of two dimensional structures, the discretization is to be performed on the 2-dimensional surface. This correspondingly leads to enormous storage and computation time requirements with increasing complexity in the numerical implementation.

As an alternative, the boundary element method has the advantage of only surface discretization for three dimensional geometries with analogous reduction in the dimension for discretization in the case of 2-D geometries. But this method requires the fundamental solution (Green's function) to be known in advance. Also, singularity appears in the integrals involving the fundamental solution and hence provisions are to be made to avoid the singularity during the evaluation of such integrals. Also, the

knowledge of the fundamental solution is extremely **difficult** if not impossible except for some simple structures. In the case of a general anisotropic medium, it is extremely difficult to find the greens function. Moreover, the matrix resulting from the boundary element method is full and non-symmetric unlike the finite element matrix, which is sparse and symmetric. In spite of these disadvantages, the boundary element method has the advantage that the radiation condition at infinity is exactly satisfied, whereas in the case of finite element method, it is only approximately satisfied. Hence this makes the boundary element method favorable while dealing with unbounded domains usually encountered in open boundary problems.

A novel semi-analytical method called **"The Scaled Boundary Finite Element Method"** based on finite elements was recently developed by Chongmin Song and John.P.Wolf [34-46] to successfully solve Elastodynamic and allied problems in Civil Engineering and soil-structure interaction. It retains the advantages of both the finite element and the boundary element methods. The key advantages of this method are as follows:

a) Reduction of the spatial dimension by one, reducing the discretization effort and the number of degrees of freedom.

b) No fundamental solution required which permits general anisotropic material to be addressed and eliminates singular integrals.

c) The method being analytical in the radial direction, permits the radiation condition at infinity is satisfied exactly for unbounded media.

d) No discretization on that part of the boundary and interfaces between different materials passing through the scaling center.

e) Converges to the exact solution in the finite-element sense in the circumferential directions.

f) Tangential continuity conditions at the interfaces of different elements are automatically satisfied.

The main theme of this thesis is to reformulate the scaled boundan' finite element method for analyzing problems in electromagnetics, which is described in detail in the successive chapters.

References

1) P.P.Silvester, Giuseppe Pelosi, *"Finite Elements for Wave Electromagnetics - Methods and Techniques"*, IEEE Press, Pp.1, 1994.

2) J.N.Reddy, *"An Introduction to the Finite Element Method"*, McGraw Hill, Pp.11, p.23-26, 1986.

3) Ibid, p.26.

4) Ibid, p.37-38.

5) Ibid, p.44-47.

6) Ibid, p.64.

7) Ibid, p.65.

8) Ibid, p.38.

9) J.E.Akin, *"Application and Implementation of Finite Element Methods"*, Academic Press Inc, p.4, 1982.

10) Ibid.

11) J.N.Reddy, *"An Introduction to the Finite Element Method"*, McGraw Hill, p.66-79, 1986.

12) Ibid.

13) Ibid, p.l33-138.

14) P.P.Silvester, Giuseppe Pelosi, "Finite Elements for Wave Electromagnetics - Methods and Techniques", IEEE Press, Pp.5, 1994.

15) Ibid.

16) Csendes Z.J, and P.Silvester, "Numerical Solution of dielectric loaded waveguides.-I finite-element analysis", *IEEE. Transactions on Microwave Theory and Techniques"*, Vol.MTT-19, pp.504-9, 1971.

17) P.P.Silvester, Giuseppe Pelosi, "Finite Elements for Wave Electromagnetics – Methods and Techniques", IEEE Press, Pp.5, 1994.

18) Benedek,P. and Silvester, "Capacitance of parallel rectangular plates separated by a dielectric sheet", *IEEE Transactions on Microwave Theory and Techniques*, Vol.MTT-20, pp.504-10, 1972.

19) Silvester,P. and K.K.Chan, "Bubnov-Galerkin solutions to wire-antenna problems", *Proceedings of IEE*,Vol.199, pp. 1095-99, 1972.

20) P.P.Silvester, Giuseppe Pelosi, "Finite Elements for Wave Electromagnetics - Methods and Techniques", p.5, IEEE Press, 1994.

21) Ibid, p-8.

22) P.P.Silvester and R.L.Ferrari, "Finite elements for Electrical Engineers", 3rd Ed, Cambridge University Press, p.390, 1996.

23) Ibid.p.312

24) Ibid, p.313.

25) Ibid, p.315.

26) P.P.Silvester and R.L.Ferrari, "Finite elements for Electrical Engineers", 3rd Ed, Cambridge University Press, pp.96-99, 1996.

27) J.C.Nedelec, "Mixed finite elements in R^{3}", *Numerische Mathematik*, 35, pp.315-41, 1980.

28) A.Bossavit, "Finite Elements for the electricity equation", *The mathematics of Finite Elements and Applications*, pp.85-91, ed.J.R.Whiteman, London:Academic Press, 1982.

29) J.S.Van Welij,"Calculation of eddy currents in terms of H on hexahedra", *IEEE Transactions on Magnetics*, 21, pp.2239-41, 1985.

30) C.W.Crowley,P.P.Silvester,and H.Hurwitz, "Covariant Projection Elements for 3D Vector field problems", *IEEE Transactions on Magnetics,* pp.397-400, January 1988.

31) P.P.Silvester and R.L.Ferrari, "Finite elements for Electrical Engineers", 3rd Ed, Cambridge University Press, p.304-311,315-316,1996.

32) Ibid.

33) B.M.Dillon,P.T.S.Liu,J.P.Webb, "Spurious modes in quadrilateral and triangular edge elements", COMPEL, 13,Supplement A, pp.311-16, 1994.

34) Chongmin Song and John P. Wolf, "The Scaled boundary finite-element method- alias Consistent infinitesimal finite-element cell method - for elastodynamics", *Computer Methods in applied mechanics and engineering*, No. 147, pp. 329-355, 1997.

35) Chongmin Song and John P. Wolf, "Consistent Infinitesimal Finite-Element Cell Method: Three-Dimensional Vector Wave Equation", *International Journal for Numerical Methods in Engg,* Vol.39, pp.2189-2208, 1996.

36) Chongmin Song and John P. Wolf, "Consistent Infinitesimal Finite Element Cell method for incompressible medium", *Communications in Numerical Methods in Engineering,* Vol.13 pp.21-32, 1997.

37) Chongmin Song and John P. Wolf, "Unit-impulse response of unbounded medium by scaled boundary finite-element method", *Comput. Methods Appl. Mech Engg,* 159, pp.355-367, 1998.

38) Chongmin Song and John P. Wolf, "The scaled boundary finite-element method: analytical solution in frequency domain", *Comput. Methods Appl. Mech. Engg,* 164, pp.249-264, 1998.

39) Chongmin Song and John P. Wolf, "Body loads in scaled boundary finite-element method", *Comput. Methods Appl. Mech. Engg,* 180, pp.117-135, 1999.

40) Chongmin Song and John P. Wolf, "The scaled boundary finite element method-alias Consistent infinitesimal finite element cell method -for diffusion", *International Journal for Numerical Methods in Engineering*, 45, pp. 1403-1431, 1999.

41) John. P. Wolf and Chongmin Song, "The scaled boundary finite element method - a primer : derivations", *Computers and Structures ,* 78, pp. 191-210, 2000.

42) Chongmin Song and John P. Wolf, "The scaled boundary finite-element method - a primer: solution procedures", *Computers and Structures ,* 78, pp.211-225, 2000.

43) J.P. Wolf and F.G.Huot, "On modelling unbounded saturated poro-elastic soil with the scaled boundary finite element method", *Proc. of the First Asian-Pacific Congress on Computational Mechanics,* Vol.2, pp.1047-1056, November 2001.

44) Chongmin Song and John P. Wolf, "Semi-analytical representation of stress singularities as occurring in cracks in anisotropic multi-materials with the scaled boundary finite element method", *Computers and Structures ,* 80, pp. 183-197, 2002.

45) Andrew J. Deeks and John. P. Wolf, "Stress recovery and error estimation for the scaled boundary finite element method", *Int.J.Numer.Meth.Engng,* 54, pp.557-583, 2002.

46) Andrew J. Deeks and John. P. Wolf, "An h-hierarchical adaptive procedure for the scaled boundary finite-element method", *Int.J.Numer.Meth.Engng,* 54, pp.585-605, 2002.   •   .

CHAPTER – II

THE SCALED BOUNDARY FINITE ELEMENT METHOD

CHAPTER – II

THE SCALED BOUNDARY FINITE ELEMENT METHOD

A. Introduction: The Scaled Boundary Finite Element method is a novel semi-analytical method which was initially developed by Chongmin Song and John.P.Wolf to successfully solve Elastodynamic and allied problems of Civil Engineering and Soil structure interaction.

The initial development of the novel method was based on an approach, using the concept of assemblage and similarity familiar to engineers, and the method was then **called as the** *Consistent Infinitesimal Finite Element Cell method* [1] **reflecting its** derivation. Successive developments of the method led to its reformulation based on the scaled boundary transformation, starting from the governing differential equations using a Galerkin weighted residual technique resulting in the scaled boundary finite-element equation of the problem [2], and the method is called the *Scaled Boundary Finite Element method.* This weighted residual formulation of the method is reformulated in \ this thesis, suitable for electromagnetics.

The Scaled Boundary finite element method, is based entirely on finite elements, but with a discretization only on the boundary. Unlike the boundary element method, this method doesn't require any fundamental solution to be known in advance. The scaled boundary finite element method combines the advantages of both the finite and boundary element methods. This novel method is analytical in its approach in the radial direction with respect to an origin, and implements the finite element method in the circumferential direction. In this sense, the method is semi-analytical.

As a prelude to the reformulation of the scaled boundary finite element method for electromagnetics, the concept of the scaled boundary transformation and the equations associated with such a transformation are explained in detail in this chapter.

B. Concept of the Scaled Boundary Transformation: In order to apply this novel method, a scaling center is first chosen in such a way that the total boundary under consideration is visible from it[3]. In case of geometries where it is not possible to find such a scaling center, the entire geometry can be sub-structured [4], and in each substructure, the scaling center can be chosen and the scaled boundary finite element method can be applied to each substructure independently and can be combined together so that in effect, the whole geometry is analyzed .

The concept of the scaled boundary transformation is that, by scaling the boundary in the radial direction with respect to a scaling center **O**, with a scaling factor smaller than 1, the whole domain is covered. Hence the upper and lower bounds of the scaling factor are 1 and 0 respectively for bounded domains. For the problems dealing with unbounded domains, the corresponding lower and upper bounds of the scaling factor are 1 and ∞ respectively. The Figures.(2a) and (2b) shown below, illustrate the concept of the scaled boundary transformation.
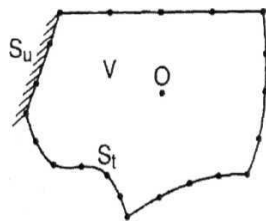
Fig.(2a) Unbounded Medium with Scaling center inside the medium (section).
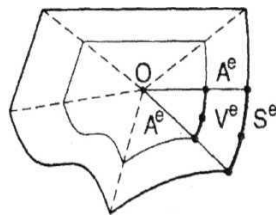
Fig.(2b) Scaled Boundary(Section).

The scaling applies to each surface finite element. Its discretized surface on the boundary is denoted as S^e (superscript e for element). Continuous scaling of the element yields a pyramid with volume V^e. The scaling center O is at its apex. The base of the pyramid is the surface finite element. The sides of the pyramid forming the boundary A^e follow from connecting the curved edge of the surface finite element to the scaling center by straight lines. **No discretization of A^e occurs.** Assembling all the pyramids by connecting their sides which corresponds to enforcing compatibility and equilibrium results in the total medium with volume V and the closed boundary S. No boundaries A^e passing through the scaling center remain. Mathematically, the scaling corresponds to a transformation of the coordinates for each finite element, resulting in the two curvilinear local coordinates in the circumferential directions on the surface and the dimensionless radial coordinate representing the scaling factor. This transformation is unique due to the choice of the scaling center from which the total boundary of the geometry is visible.

A typical case in which the scaling center not located on the boundary for a bounded medium, is shown in Fig.(2c) below.
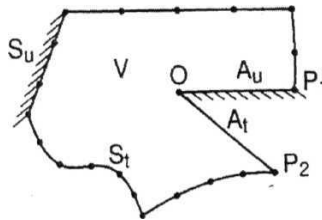
Fig.(2c) Modeling of bounded medium with surface finite elements with scaling center on boundary.(Section)

When during the assemblage process, some sides **of** the pyramids **are** not connected or some pyramids are missing, then an additional boundary A passing through the scaling center is created and this is shown in Fig.(2c). This is the case of a missing pyramid with the boundary conditions prescribed on A_u and A_t respectively. Thus, the boundary conditions on A_u and A_t can be modeled without spatial discretization by formulating them only on the finite-element edges P_1 and P_2 located on the boundary. The bases of all pyramids form the boundary S, which is not a closed surface. The total boundary of the medium consists of S and A. Such applications occur in Fracture Mechanics, where adjacent sides of pyramids forming the crack faces are not connected. In that situation, the scaling center is chosen at the crack tip, whereby the crack faces are not discretized.

The scaled boundary finite-element method also applies to unbounded media. This is shown below in Fig.(2d).
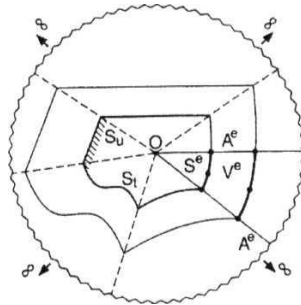
Fig.(2d) Modeling of unbounded medium with surface finite elements (section) with the scaling center outside the medium.

In the case of unbounded media, the scaling center 0 is chosen outside the unbounded medium, from which the total boundary is visible. Scaling the surface finite elements with a scaling factor larger than 1 results in truncated semi-infinite pyramids.

When the extension of the boundary passes through the scaling center, that part of the boundary A_u and A_t (corresponding to non-connected sides of the pyramids) is again not discretized. This is shown **below** in **Fig.(2d.a).**
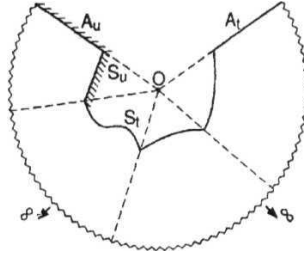
Fig.(2d.a) Extension of boundary passing through scaling center for an unbounded medium.

The key advantages of the novel method is already mentioned towards the end of the first chapter. In the forthcoming paragraphs, the scaled boundary **transformation** of the geometry is discussed.

C. **Scaled boundary transformation of the geometry: Three Dimensional Case:**

The transformation of the geometry corresponding to the scaled boundary illustrated in Fig.(2a) is addressed. The scaled boundary transformation of the geometry corresponding to Fig.(2a) is shown in Fig.(2e) in the following page.[5] The transformation of the geometry corresponding to the scaled boundary in Fig.1 is addressed and the scaled boundary transformation equations between the derivatives in the cartesian space and the derivatives in terms of scaled boundary variables is derived .
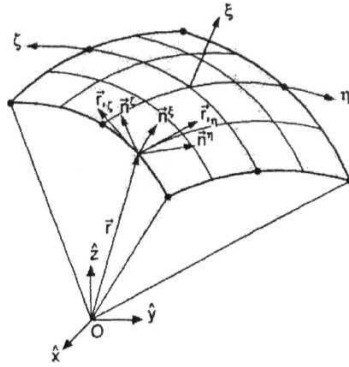
Fig.(2e). The Scaled boundary transformation of the geometry of surface finite element.

In Fig.(2e) given above, a specific finite element is addressed. The coordinates on the doubly-curved boundary are denoted as x, y, z. A point on the boundary is described by its position vector

$$\mathbf{r} = x\,\mathbf{i} + y\,\mathbf{j} + z\,\mathbf{k} \tag{2.1}$$

The cartesian coordinates x, y, z are transformed to the curvilinear coordinates ξ, η, ζ which is shown in (Fig.2e). The scaling center is chosen in the interior of the domain. It coincides with the origin of the coordinate system x, y, z.

The dimensionless radial coordinate ξ is measured from the scaling center along the position vector

$$\hat{\mathbf{r}} = \hat{x}\,\mathbf{i} + \hat{y}\,\mathbf{j} + \hat{z}\,\mathbf{k} \tag{2.2}$$

where i, **j,** k are unit normal vectors, and ξ is constant (equal to 1) on the boundary. In a practical application, the geometry of the boundary is so general that only a piecewise description is feasible. Accordingly, doubly-curved surface finite elements are used.

A specific finite element is addressed. The geometry of this finite element on the boundary is represented by interpolating its nodal coordinates $\{x\},\{y\},\{z\}$ using the local coordinates η,ζ.

$$x(\eta,\zeta)=[N(\eta,\zeta)]\,\{x\} \tag{2.3a}$$

$$y(\eta,\zeta)=[N(\eta,\zeta)]\,\{y\} \tag{2.3b}$$

$$z(\eta,\zeta)=[N(\eta,\zeta)]\,\{z\} \tag{2.3c}$$

with the mapping functions

$$[N(\eta,\zeta)]=[N_1(\eta,\zeta) \quad N_2(\eta,\zeta)\ldots\ldots] \tag{2.4}$$

where $-1\leq(\eta,\zeta)\leq1$

A point in the domain is obtained by scaling that on the boundary.

$$\hat{r}=\xi\,r \tag{2.5}$$

Expressed in coordinates

$$\hat{x}(\xi,\eta,\zeta)=\xi\,x(\eta,\zeta) \tag{2.6a}$$

$$\hat{y}(\xi,\eta,\zeta)=\xi\,y(\eta,\zeta) \tag{2.6b}$$

$$\hat{z}(\xi,\eta,\zeta)=\xi\,z(\eta,\zeta) \tag{2.6c}$$

applies with $\xi=1$ on the boundary and $\xi=0$ in the scaling center.

The uniqueness of the transformation is guaranteed by the choice of the scaling center, from which the total boundary must be visible.

To transform the differential operator **[L]** in the $\hat{x}, \hat{y}, \hat{z}$ coordinate system to that in

the ξ ,r| ,ζcoordinate system, the Jacobian matrix is required.

$$\left[\hat{J}(\xi,\eta,\zeta)\right] = \begin{bmatrix} \hat{x}_{,\xi} & \hat{y}_{,\xi} & \hat{z}_{,\xi} \\ \hat{x}_{,\eta} & \hat{y}_{,\eta} & \hat{z}_{,\eta} \\ \hat{x}_{,\zeta} & \hat{y}_{,\zeta} & \hat{z}_{,\zeta} \end{bmatrix} \qquad (2.7)$$

The partial derivatives are calculated using Eqs.(2.3 and 2.6) leading to

$$\hat{x}_{,\xi} = x \quad = [N]\{x\} \qquad (2.8a)$$

$$\hat{x}_{,\eta} = \xi\, x_{,\eta} = \xi\, [N_{,\eta}]\{x\} \qquad \textbf{(2.8b)}$$

$$\hat{x}_{,\zeta} = \xi\, x_{,\zeta} = \xi\, [N_{,\zeta}]\{x\} \qquad \textbf{(2.8c)}$$

and similar relations involving other two circumferential scaled boundary co-ordinates.

Substituting Eq.(2.8) in Eq.(2.7),

$$\left[\hat{J}(\xi,\eta,\zeta)\right] = \begin{bmatrix} 1 & \xi & \xi \end{bmatrix} \left[J(\eta,\zeta)\right] \qquad (2.9)$$

with the abbreviation

$$\left[J(\eta,\zeta)\right] = \begin{bmatrix} x & y & z \\ x_{,\eta} & y_{,\eta} & z_{,\eta} \\ x_{,\zeta} & y_{,\zeta} & z_{,\zeta} \end{bmatrix} \qquad \textbf{(2.10)}$$

The argument η and ζ are omitted for conciseness.

[J 1 depends only on the **geometry** of the boundary.

Its determinant is equal to

$$|J| = x\left(y_{,\eta}z_{,\zeta} - z_{,\eta}y_{,\zeta}\right) + y\left(z_{,\eta}x_{,\zeta} - x_{,\eta}z_{,\zeta}\right) + z\left(x_{,\eta}y_{,\zeta} - y_{,\eta}x_{,\zeta}\right) \tag{2.11}$$

[J] and | J | can be non-dimensionalized with a characteristic length r_o with respect to the boundary as

$$[J] = r_o[\bar{J}] \tag{2.12a}$$

$$|J| = r_o^3 |\bar{J}| \tag{2.12b}$$

where [J] and | J | are dimensionless.

The inverse of the matrix [J] is written as

$$[J]^{-1} = \frac{1}{|J|} \begin{bmatrix} y_{,\eta}z_{,\zeta} - y_{,\zeta}z_{,\eta} & y_{,\zeta}z - yz_{,\zeta} & yz_{,\eta} - y_{,\eta}z \\ x_{,\zeta}z_{,\eta} - x_{,\eta}z_{,\zeta} & xz_{,\zeta} - x_{,\zeta}z & x_{,\eta}z - xz_{,\eta} \\ x_{,\eta}y_{,\zeta} - x_{,\zeta}y_{,\eta} & x_{,\zeta}y - xy_{,\zeta} & xy_{,\eta} - x_{,\eta}y \end{bmatrix} \tag{2.13}$$

The coefficients in Eq.(2.13) satisfy the identities

$$\left(y_{,\zeta}z - yz_{,\zeta}\right)_{,\eta} + \left(yz_{,\eta} - y_{,\eta}z\right)_{,\zeta} = -2\left(y_{,\eta}z_{,\zeta} - y_{,\zeta}z_{,\eta}\right) \tag{2.14a}$$

$$\left(xz_{,\zeta} - x_{,\zeta}z\right)_{,\eta} + \left(x_{,\eta}z - xz_{,\eta}\right)_{,\zeta} = -2\left(x_{,\zeta}z_{,\eta} - x_{,\eta}z_{,\zeta}\right) \tag{2.14b}$$

$$\left(x_{,\zeta}y - xy_{,\zeta}\right)_{,\eta} + \left(xy_{,\eta} - x_{,\eta}y\right)_{,\zeta} = -2\left(x_{,\eta}y_{,\zeta} - x_{,\zeta}y_{,\eta}\right) \tag{2.14c}$$

The derivatives with respect to x, y and z are transformed to those with respect to ξ, η, ζ using Eq.(2.9) giving

$$\begin{pmatrix} \dfrac{\partial}{\partial x} \\ \dfrac{\partial}{\partial y} \\ \dfrac{\partial}{\partial z} \end{pmatrix} = [\hat{J}]^{-1} \begin{pmatrix} \dfrac{\partial}{\partial \xi} \\ \dfrac{\partial}{\partial \eta} \\ \dfrac{\partial}{\partial \zeta} \end{pmatrix} = [J]^{-1} \begin{pmatrix} \dfrac{\partial}{\partial \xi} \\ \dfrac{1}{\xi}\dfrac{\partial}{\partial \eta} \\ \dfrac{1}{\xi}\dfrac{\partial}{\partial \zeta} \end{pmatrix} \tag{2.15}$$

The geometrical interpretation of the coordinate transformation is discussed in the following paragraphs. For this purpose the diagrammatic representation of Fig.(2e) is considered.

The derivatives of the position vector of a point on the boundary (Eq.2.1) with respect to r| and q represent two tangential vectors

$$\mathbf{r}_{,\eta} = x_{,\eta}\mathbf{i} + y_{,\eta}\mathbf{j} + z_{,\eta}\mathbf{k} \tag{2.16a}$$

$$\mathbf{r}_{,\varsigma} = x_{,\varsigma}\mathbf{i} + y_{,\varsigma}\mathbf{j} + z_{,\varsigma}\mathbf{k} \tag{2.16b}$$

with q and η respectively being constant. The three vectors $\mathbf{r}$, r_{η}, $\mathbf{r}_{,\varsigma}$ form the base of the transformed coordinate system of the finite element. Eq.(2.11) is equivalent to

$$|J| = \mathbf{r} \cdot \left(\mathbf{r}_{,\eta} \times \mathbf{r}_{,\varsigma} \right) \tag{2.17}$$

$$dv = \hat{\mathbf{r}}_{\varepsilon} \cdot \left(\hat{\mathbf{r}}_{\eta} \times \hat{\mathbf{r}}_{\varsigma} \right) d\xi\, d\eta\, d\varsigma \tag{2.18}$$

Using Eq.(2.5) and Eq.(2.17),

$$dv = \xi^{2}\,|J|\,d\xi\, d\eta\, d\varsigma \tag{2.19}$$

The outward normal vectors to the surfaces (η,ς), (ς,ξ), (ξ,η), where the coordinates ξ, η, ς, respectively are constant, are equal on the boundary $(\xi=1)$ to

$$\mathbf{g}^{\xi} = \mathbf{r}_{,\eta} \times \mathbf{r}_{,\varsigma} = \left(y_{,\eta}z_{,\varsigma} - y_{,\varsigma}z_{,\eta} \right)\mathbf{i} + \left(x_{,\varsigma}z_{,\eta} - x_{,\eta}z_{,\varsigma} \right)\mathbf{j} + \left(x_{,\eta}y_{,\varsigma} - x_{,\varsigma}y_{,\eta} \right)\mathbf{k} \tag{2.19a}$$

$$\mathbf{g}^{\eta} = \mathbf{r}_{,\varsigma} \times \mathbf{r} = \left(y_{,\varsigma}z - yz_{,\varsigma} \right)\mathbf{i} + \left(xz_{,\varsigma} - x_{,\varsigma}z \right)\mathbf{j} + \left(x_{,\varsigma}y - xy_{,\varsigma} \right)\mathbf{k} \tag{2.19b}$$

$$\mathbf{g}^{\varsigma} = \mathbf{r} \times \mathbf{r}_{,\eta} = \left(yz_{,\eta} - y_{,\eta}z \right)\mathbf{i} + \left(x_{,\eta}z - xz_{,\eta} \right)\mathbf{j} + \left(xy_{,\eta} - x_{,\eta}y \right)\mathbf{k} \tag{2.19c}$$

The magnitude of a vector is denoted with the same symbol omitting the arrow sign.

The transformation of infinitesimal surfaces for any ξ between the two coordinate systems is specified using Eqs.(2.5) and (2.19) as

$$dS^\xi = |\hat{\mathbf{r}}_{,\eta} \times \hat{\mathbf{r}}_\zeta| \, d\eta \, d\zeta = |\xi \mathbf{r}_{,\eta} \times \xi \mathbf{r}_\zeta| \, d\eta \, d\zeta = \xi^2 g^\xi d\eta \, d\zeta \tag{2.20a}$$

$$dS^\eta = |\hat{\mathbf{r}}_\zeta \times \hat{\mathbf{r}}_\zeta| \, d\xi \, d\zeta = |\xi \mathbf{r}_\zeta \times \mathbf{r}| \, d\xi \, d\zeta = \xi g^\eta d\zeta \, d\xi \tag{2.20b}$$

$$dS^\zeta = |\hat{\mathbf{r}}_\zeta \times \hat{\mathbf{r}}_{,\eta}| \, d\xi \, d\eta = |\mathbf{r} \times \xi \mathbf{r}_{,\eta}| \, d\xi \, d\eta = \xi g^\zeta d\eta \, d\xi \tag{2.20c}$$

The unit normal vectors of the three surfaces shown in Fig.(2e) follow from Eqs.(2.19a (2.19b), and (2.19c) as

$$\mathbf{n}^\xi = n_x^\xi \mathbf{i} + n_y^\xi \mathbf{j} + n_z^\xi \mathbf{k} = \frac{\mathbf{g}^\xi}{g^\xi} \tag{2.21a}$$

$$\mathbf{n}^\eta = n_x^\eta \mathbf{i} + n_y^\eta \mathbf{j} + n_z^\eta \mathbf{k} = \frac{\mathbf{g}^\eta}{g^\eta} \tag{2.21b}$$

$$\mathbf{n}^\zeta = n_x^\zeta \mathbf{i} + n_y^\zeta \mathbf{j} + n_z^\zeta \mathbf{k} = \frac{\mathbf{g}^\zeta}{g^\zeta} \tag{2.21c}$$

Equations (2.13, 2.19a, 2.19b, 2.19c and 2.21) yield

$$[J]^{-1} = \frac{1}{|J|} \begin{bmatrix} g^\xi n_x^\xi & g^\eta n_x^\eta & g^\zeta n_x^\zeta \\ g^\xi n_y^\xi & g^\eta n_y^\eta & g^\zeta n_y^\zeta \\ g^\xi n_z^\xi & g^\eta n_z^\eta & g^\zeta n_z^\zeta \end{bmatrix} \tag{2.22}$$

Substituting Eq.(2.22) in (2.15) results in,

$$\begin{pmatrix} \dfrac{\partial}{\partial \hat{x}} \\ \dfrac{\partial}{\partial \hat{y}} \\ \dfrac{\partial}{\partial \hat{z}} \end{pmatrix} = \frac{g^\xi}{|J|} \{n^\xi\} \frac{\partial}{\partial \xi} + \frac{1}{\xi} \left(\frac{g^\eta}{|J|} \{n^\eta\} \frac{\partial}{\partial \eta} + \frac{g^\zeta}{|J|} \{n^\zeta\} \frac{\partial}{\partial \zeta} \right) \tag{2.23}$$

70

The partial derivatives with respect to x, y, z are expressed as a function of those with respect to ξ, η, ζ and the Eq.(2.23) is the differential form of the scaled boundary transformation of the geometry shown in Fig.(2e).

D. Two Dimensional Case: In the case of 2-D, a single line finite element, with two nodes (Fig.2f) and its corresponding triangle (Fig.2g), is addressed as an illustrative example.

A typical two node line element is shown below in Fig.(2f). [6]
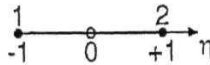
Fig.(2f). A parent two node line finite element.

In the Fig.(2f) , the two nodes of the line element are represented as 1 and 2 respectively with the scaled boundary variable r| with values ranging from a minimum of -1 to a maximum of +1.

The corresponding scaled boundary transformation of the two node line finite element shown in Fig.(2f) is shown below in Fig.(2g).
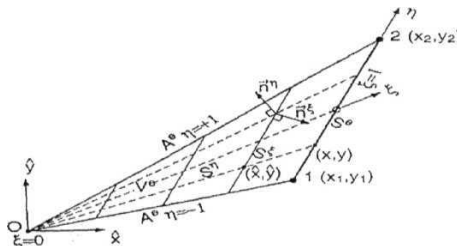
Fig.(2g). The scaled boundary transformation of the two node line finite element shown in Fig.(2f). The triangle corresponding to the line element is represented as O-1-2.

In Fig.(2g), the numbers 1,2 correspond to the two nodes of the line element and the radial vector normal to the element is denoted by ξ. The value of $\xi=1$ corresponds to the points on the boundary. The scaled boundary coordinates ξ,η forms a right-handed system. Lines with S^ξ with a constant ξ are parallel to the line finite element S^e. Lines S^η with a constant r| pass through the scaling center O and the point on the line finite element with the same η.

For the bounded and unbounded cases, the sides 1-2 corresponding to the line elements are positive and negative respectively. The sides $\eta=+1$ and r|= -1 are positive and negative respectively, for both the bounded and unbounded cases. This is shown below in Fig(2h) and Fig.(2i).
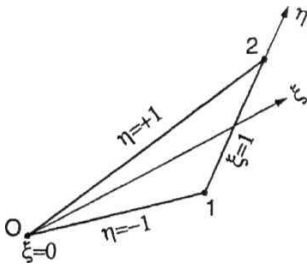
Fig.(2h) Bounded medium with positive side 1-2 ($\xi=1$), positive side-face O-2 ($\eta=+1$) and negative side-face O-1 ($\eta=-1$).
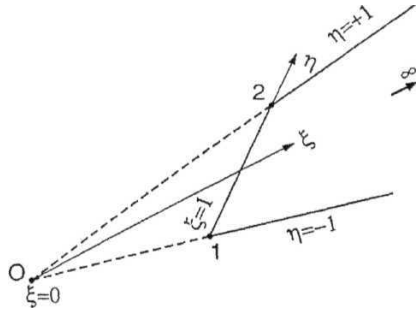
Fig.(2i). Unbounded medium with negative side 1-2 ($\xi=1$), positive side-face 2- ∞ ($\eta=+1$) and negative side-face 1- oo ($\eta=-1$).

In the discussion that follows, the scaled boundary transformation of the geometry, for the two-dimensional case is derived.

For deriving the scaled boundary transformation equations, the figures (2f and 2g) are considered. [7]

Considering Fig.(2g), the scaling center O coincides with the origin of the cartesian coordinate system. Moving from 1 to 2, O must be on the left. The coordinates of a point on the line element are denoted as x, y. Two nodes with the coordinates (x_1, y_1) and (x_2, y_2) are arranged as

$$\{x\} = \begin{pmatrix} x_1 \\ x_2 \end{pmatrix} \qquad (2.24a)$$

$$\{y\} = \begin{pmatrix} y_1 \\ y_2 \end{pmatrix} \qquad (2.24b)$$

The line element is generated from its parent element (Fig.2f) with the mapping functions

$$[N] = \left[\frac{1}{2}(1-\eta) \quad \frac{1}{2}(1+\eta) \right] \qquad (2.25)$$

as

$$x = [N]\{x\} = \bar{x} + \frac{1}{2}\Delta_x \eta \qquad (2.26a)$$

$$y = [N]\{y\} = \bar{y} + \frac{1}{2}\Delta_y \eta \qquad (2.26b)$$

with the abbreviations

$$\Delta_x = x_2 - x_1 \qquad (2.27a)$$

$$\Delta_y = y_2 - y_1 \qquad (2.27b)$$

$$\bar{x} = \frac{1}{2}(x_1 + x_2) \qquad (2.28a)$$

$$\bar{y} = \frac{1}{2}(y_1 + y_2) \qquad (2.28b)$$

The scaled boundary transformation relates any point in the domain with the coordinates denoted as $\hat{x}\ \hat{y}\ \hat{z}$ to the corresponding point on the line element as (Fig.2g)

$$\hat{x} = \xi\, x = \xi\left(\bar{x} + \frac{1}{2}\Delta_x \eta\right)$$

$$\hat{y} = \xi\, y = \xi\left(\bar{y} + \frac{1}{2}\Delta_y \eta\right) \tag{2.28d}$$

The dimensionless radial coordinate ξ points from **O** to a point on the boundary (with $\xi{=}1$).

This equations (2.28a, b, c and d) define the transformation from the Cartesian coordinates $\hat{x}$, $\hat{y}$ to the scaled boundary coordinates ξ, η which forms a right - handed system.

The spatial derivatives in the two coordinate systems are related as

$$\begin{pmatrix} \dfrac{\partial}{\partial \xi} \\[2mm] \dfrac{\partial}{\partial \eta} \end{pmatrix} = \left[\hat{J}(\xi, \eta)\right] \begin{pmatrix} \dfrac{\partial}{\partial \hat{x}} \\[2mm] \dfrac{\partial}{\partial \hat{y}} \end{pmatrix} \tag{2.29}$$

with the Jacobian matrix defined as

$$\left[\hat{J}(\xi, \eta)\right] = \begin{bmatrix} \hat{x}_{,\xi} & \hat{y}_{,\xi} \\ \hat{x}_{,\eta} & \hat{y}_{,\eta} \end{bmatrix} \tag{2.30}$$

The partial derivatives of $\hat{x}$, $\hat{y}$ with respect to ξ, η are determined using Eqs.(2.28a) and (2.28b) as,

$$\hat{x}_{,\xi} = x = \bar{x} + \frac{1}{2}\Delta_x \eta \tag{2.31a}$$

$$\hat{y}_{,\xi} = y = \bar{y} + \frac{1}{2}\Delta_y \eta \tag{2.31b}$$

74

$$\hat{x}_{,\eta} = \xi\, x_{,\eta} = \frac{1}{2}\Delta_x\,\xi \tag{2.31c}$$

$$\hat{y}_{,\eta} = \xi\, y_{,\eta} = \frac{1}{2}\Delta_y\,\xi \tag{2.31d}$$

$\left[\hat{J}(\xi,\eta)\right]$ can be written as

$$[\hat{J}(\xi,\eta)] = \begin{bmatrix} 1 \\ & \xi \end{bmatrix}[J(\eta)] \tag{2.32}$$

where

$$[J(\eta)] = \begin{bmatrix} x & y \\ x_{,\eta} & y_{,\eta} \end{bmatrix} \tag{2.33}$$

Using Eqs.(2.26a and 2.26b),

$$x_{,\eta} = [N]_{,\eta}\{x\} = \frac{1}{2}\Delta_x$$

$$y_{,\eta} = [N]_{,\eta}\{y\} = \frac{1}{2}\Delta_y$$

$[J(\eta)]$ is a function of the geometry of the line element only. The argument η is omitted for conciseness.

The derivatives with respect to x, y follow from Eq.(2.29).

$$\begin{Bmatrix} \dfrac{\partial}{\partial \hat{x}} \\[2mm] \dfrac{\partial}{\partial \hat{y}} \end{Bmatrix} = \left[\hat{J}(\xi,\eta)\right]^{-1} \begin{Bmatrix} \dfrac{\partial}{\partial \xi} \\[2mm] \dfrac{\partial}{\partial \eta} \end{Bmatrix} \tag{2.35}$$

Substituting Eq.(2.32 and 2.33) in Eq.(2.35),

$$\begin{pmatrix} \dfrac{\partial}{\partial \hat{x}} \\ \dfrac{\partial}{\partial \hat{y}} \end{pmatrix} = \{b^1\}\dfrac{\partial}{\partial \xi} + \{b^2\}\dfrac{1}{\xi}\dfrac{\partial}{\partial \eta} \qquad (2.36)$$

where

$$\{b^1\} = \dfrac{1}{|J|}\begin{pmatrix} y_{,\eta} \\ -x_{,\eta} \end{pmatrix} \qquad (2.37a)$$

$$= \dfrac{1}{x_1 y_2 - x_2 y_1}\begin{pmatrix} \Delta_y \\ -\Delta_x \end{pmatrix} \quad \text{(in this example)}$$

$$\{b^2\} = \dfrac{1}{|J|}\begin{pmatrix} -y \\ x \end{pmatrix} \qquad (2.37b)$$

$$= \dfrac{1}{x_1 y_2 - x_2 y_1}\begin{pmatrix} -2\bar{y} - \Delta_y \eta \\ 2\bar{x} + \Delta_x \eta \end{pmatrix} \quad \text{(in this example)}$$

with the determinant

$$|J| = \dfrac{1}{2}\left(x_1 y_2 - x_2 y_1\right) \qquad (2.38)$$

The Equations (2.36, 2.37) constitute the general Scaled boundary transformation equations in two **dimensions** with the determinant given by Eq.(2.38).

The relationship between $\{b^1\}$ and $\{b^2\}$ is given by

$$\left(\{b^2\}|J|\right)_{,\eta} = -\{b^1\}|J| \qquad (2.39)$$

The infinitesimal area dV^e of the domain is calculated as

$$dV^e = |\hat{J}(\xi,\eta)| \, d\xi \, d\eta = \xi |J| \, d\xi \, d\eta \qquad (2.40)$$

The infinitesimal length of a line S^ξ with constant ξ (Fig.2g) equals

$$dS^\xi = \sqrt{\left(\left(\hat{x}_{,\eta}\right)^2 + \left(\hat{y}_{,\eta}\right)^2\right)} \, d\eta = \frac{1}{2}\xi\sqrt{\Delta_x^2 + \Delta_y^2} \, d\eta \quad (2.41)$$

The unit normal vectors $\{ n^\xi \}$ and $\{ n^\eta \}$ of the lines S^ξ and S^η with constant ξ and η respectively, are

$$\{n^\xi\} = \frac{1}{\sqrt{\Delta_x^2 + \Delta_y^2}} \begin{pmatrix} \Delta_y \\ -\Delta_x \end{pmatrix} \qquad (2.42a)$$

$$\{n^\eta\} = \frac{1}{\sqrt{x^2 + y^2}} \begin{pmatrix} -y \\ x \end{pmatrix} \qquad (2.42b)$$

The corresponding expressions for $\{b^1\}$ and $\{b^2\}$ are given by,

$$\{b^1\} = \frac{\sqrt{\Delta_x^2 + \Delta_y^2}}{x_1 y_2 - x_2 y_1} \{n^\xi\} = \frac{\sqrt{\Delta_x^2 + \Delta_y^2}}{2|J|} \{n^\xi\}$$

$$\{b^2\} = \frac{2\sqrt{x^2 + y^2}}{x_1 y_2 - x_2 y_1} \{n^\eta\} = \frac{\sqrt{x^2 + y^2}}{2|J|} \{n^\eta\} \qquad (2.43b)$$

E. Physical picture of the scaled boundary transformation equations:

The physical process underlying the scaled boundary transformation equations can be easily explained for the bounded case[8] of the illustrative example shown in Fig.(2g). The Figs.(2j) (a) and (2j) (b) shown in the next page, are considered for the purpose of illustration.
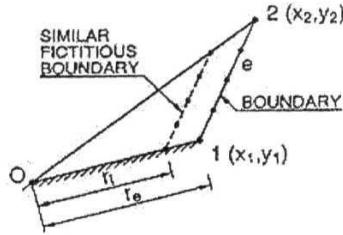
Fig.(2j) (a) Representation of the Actual Boundary and a Similar fictitious Boundary.

Referring to Fig.(2g), the side 1-2 represents the boundary (interface) which is discretized. This is shown below in Fig.(2j) (a). **O** denotes the similarity center and 1-2 corresponds to $\xi=1$ with the characteristic length r_e (e for exterior). A similar fictitious boundary with the scaling factor $\xi_i<1$ and the characteristic length r_i ($=\xi_i\ r_e$) is constructed (i for interior). The discretization of the similar fictitious boundary is selected to be similar to that of the boundary. The wedge (referred to r_e) is divided by the fictitious boundary into two parts. The wedge with a similar boundary (referred to r_i) (Fig.(2j) (b)) and a trapezoid with its exterior boundary coinciding with the boundary and its interior boundary with the fictitious boundary (Fig.(2j) (c)).
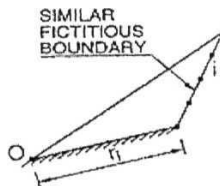
Fig.(2j). (b) Wedge with a Similar boundary
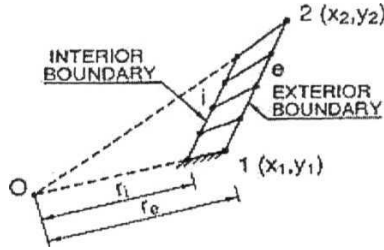
Fig.(2j). (c) Interior and Exterior boundary of the trapezoid.

The discretizations of the exterior and interior boundaries are identical to those of the boundary and the fictitious boundary of the wedge. The finite-element discretization of the trapezoid is defined by connecting the corresponding nodes on its exterior and interior boundaries. The discretized trapezoid is called the finite-element cell. Adding the finite-element cell (Fig.(2j) (c)) to the wedge referred to as r_i (Fig.(2j) (b)) results in the wedge referred to r_e . This process is equivalent to the enforcement of compatibility and equilibrium conditions and leads to a relationship linking the matrices at the two similar boundaries of the wedge via that of the finite element cell along with a relationship at the boundaries of the wedge. Thus, the matrices at the two boundaries of the wedge can be expressed as a function of that of the finite-element cell. After performing the limit of the cell width r_e-r_i tending to zero, analytically, an equation for the matrix of the wedge is obtained. The same concept also applies to the truncated semi-infinite wedge shown in Fig.(2k) in the following page.
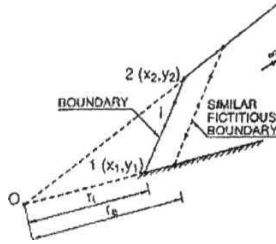
Fig.(2k) (a) Boundary and the Similar Fictitious boundary for the unbounded medium.
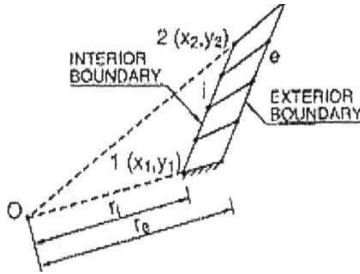
Fig.(2k) (b) Interior boundary and the Exterior boundary for theunbounded medium.

In the case of unbounded medium, the boundary and the similar fictitious boundary corresponds to r_i and r_e respectively. The scaling factor ξ_e is larger than 1.

The finite element equations derived from the concept of similarity and assembly described above [9]are the same equations obtained by following the purely mathematical approach of applying the scaled boundary transformation equations to the differential equations and arriving at the finite element equation via the weighted residual method [10]. This observation shows the equivalence between the purely mathematical approach followed in the Scaled boundary finite element method and the practical engineering

approach to arrive at the finite element equations as done in the infinitesimal finite element cell method.

In the forthcoming paragraphs, the reformulation of the scaled boundary finite element method, suitable for application in electromagnetics is discussed.

F. The scaled boundary finite element method in electromagnetics:

The scaled boundary transformation equations derived for the case of 3-D and 2-D structures, are quite general, and they can be applied to differential equations governing the dynamic phenomena in any discipline. However, it is important to note that, the actual formulation of the scaled boundary finite element equation depends upon the additional constraints that are specific to the discipline, which are to be satisfied. This approach ensures that, the scaled boundary finite element equation thus framed taking into account the specific features of that discipline is indeed a closest possible representation of the system represented by the original differential equations along with the constraints in the form of boundary conditions.

In this context, it is to be pointed out that when the scaled boundary is reformulated in electromagnetics in H **formulation,** it is necessary that apart from satisfying the essential boundary conditions, the fields should satisfy the condition that the divergence of the magnetic field should be zero.

This condition should be necessarily incorporated while formulating the scaled boundary finite element equation in electromagnetics, for problems dealing with wave guides, multi-conductor transmission lines, and cavity structures. This is achieved by noting that the scaled boundary finite element method, being analytical in the radial

direction, the radial part of the field is expanded as a power series in the radial coordinate for all the components of the field.

A relationship between the unknown coefficients in the radial expansion for all the components of the field is obtained by rewriting the equation for the zero divergence of the magnetic field, in terms of the scaled boundary transformation.

This relationship is substituted back in the radial expansion of the fields for the unknown coefficients, so that the physical requirement of the zero divergence of the magnetic field is satisfied exactly.

Then the functional corresponding to the boundary value problem is formulated, and the process rendering the functional stationary, results in the solution of the boundary value problem.

The distinct feature of the scaled boundary finite element method when formulated in electromagnetics is that, the accuracy of the eigen solutions also depend upon the number of terms included in the radial expansion of the field, apart from depending on the conventional factors like the choice of the interpolation functions, size of the element, accuracy of the Jacobian transformation, etc, as encountered in the traditional vector finite element method.

G. Conclusion: The basic concepts of the scaled boundary finite element has been explained and the scaled boundary transformations for two and three dimensional structures were derived. Also the crucial aspects regarding the reformulation of the scaled boundary finite element method in electromagnetics is explained.

The procedure outlined in this chapter for the implementation of the zero divergence condition of the magnetic field will be followed so that the fields that arise as the solution of the scaled boundary finite element equation satisfies the condition exactly.

In the successive chapters dealing with cavities and waveguides, the H formulation will be used as the functional associated with the helmholtz differential equation, and the functional will be recast in terms of the scaled boundary coordinates.

The next chapter deals with the scaled boundary finite element formulation for cavity structures, which are bounded by metallic surfaces.

References

1) Chongmin Song and John P.Wolf, "Consistent Infinitesimal Finite-Element Cell Method: Three-Dimensional Vector Wave Equation", *International Journal for Numerical Methods in Engg,* Vol.39, pp.2189-2208, 1996.

2) Chongmin Song and John P. Wolf, "The Scaled boundary finite-element method- alias Consistent infinitesimal finite-element cell method - for elastodynamics", *Computer Methods in applied mechanics and engineering,* No. 147 , pp. 329-355, 1997.

3) Ibid, pp.330-332.

4) Andrew J. Deeks and John.P. Wolf,"An h-hierarchical adaptive procedure for the scaled boundary finite-element method", *Int.J.Numer.Meth.Engng,* 54, pp.585-605, 2002.

5) Chongmin Song and John P.Wolf, "The Scaled boundary finite-element method- alias Consistent infinitesimal finite-element cell method - for elastodynamics", *Computer Methods in applied mechanics and engineering,* No.147,pp. 334-337, 1997.

6) John.P. Wolf and Chongmin Song, "The scaled boundary finite element method - a primer : derivations", *Computers and Structures* , 78, pp. 196-197,2000.

7) Ibid.

8) Ibid, pp.201-202.

9) Chongmin Song and John P. Wolf, "The Scaled boundary finite-element method- alias Consistent infinitesimal finite-element cell method - for elastodynamics", *Computer Methods in applied mechanics and engineering,* No.l47,pp. 334-337, 1997.

10) Chongmin Song and John P. Wolf, "The Scaled boundary finite-element method- alias Consistent infinitesimal finite-element cell method - for elastodynamics", *Computer Methods in applied mechanics and engineering,* No. 147 , pp. 332-333, 1997.

CHAPTER-III

THE SCALED BOUNDARY FINITE ELEMENT FORMULATION FOR CAVITY STRUCTURES

CHAPTER – III

THE SCALED BOUNDARY FINITE ELEMENT FORMULATION FOR CAVITY STRUCTURES

A. Introduction: The boundary value problem representing the cavity structures form a separate class, in the sense that the ideal metallic cavity structures represent the total confinement of the electromagnetic field in a volume of space bounded externally by metallic surfaces. The eigen-modes of the cavity structures are in fact the standing wave field patterns corresponding to various eigen values, with the tangential component of the electric field and the normal component of the magnetic field vanishing at the boundary comprising the metallic surfaces, under the assumption that the metallic surface is a perfect conductor.

In this chapter, the scaled boundary finite element equation is developed for a general metallic cavity structure, and a numerical implementation is illustrated for the case of a spherical metallic cavity.

B. Theory: The vector helmholtz equation in **H formulation**[1] is given by

$$\nabla \times \varepsilon_r^{-1} \nabla \times \mathbf{H} - k^2 \mu_r \mathbf{H} = 0 \qquad \text{(3.1a)}$$

where ε_r and μ_r are the local material properties corresponding to the relative permittivity and relative permeability of the medium respectively. The associated **natural boundary** condition is given by

$$\mathbf{1}_n \cdot \nabla \times \mathbf{H} = 0 \qquad \text{(3.1b)}$$

The natural boundary condition implies that the magnetic field is purely tangential to the bounding metallic surface.

The associated functional for Eq.(3.1a) can be developed by taking the dot product of Eq.(3.1a) by an arbitrary test vector W, and integrating over the whole domain Ω,

$$\int_{\Omega} \mathbf{W} \cdot \left(\nabla \times \varepsilon_r^{-1} \nabla \times \mathbf{H} - k^2 \mu_r \mathbf{H} \right) d\Omega = 0 \qquad (3.2)$$

Using the following identity

$$\int_{\Omega} \mathbf{P} \cdot (\nabla \times \nabla \times \mathbf{Q}) d\Omega = \int_{\Omega} (\nabla \times \mathbf{P}) \cdot (\nabla \times \mathbf{Q}) d\Omega - \oint_{S} (\mathbf{P} \times \nabla \times \mathbf{Q}) \cdot \mathbf{1}_n \, dS \qquad (3.3)$$

the equation (3.2) can be written as,

$$\int_{\Omega} (\nabla \times \mathbf{W}) \cdot \varepsilon_r^{-1} (\nabla \times \mathbf{H}) d\Omega - \oint_{S} \left(\mathbf{W} \times \varepsilon_r^{-1} \nabla \times \mathbf{H} \right) \cdot \mathbf{1}_n \, dS - k^2 \mu_r \int_{\Omega} \mathbf{W} \cdot \mathbf{H} \, d\Omega = 0 \quad (3.4)$$

The boundary integral can be re-arranged as

$$\int_{S} \mathbf{W} \cdot (\varepsilon_r^{-1} \nabla \times \mathbf{H} \times \mathbf{1}_n) \, dS$$

Also,

$$\nabla \times \mathbf{H} = j\omega\varepsilon \mathbf{E} \qquad (3.5)$$

for time harmonic variation of the magnetic field.

Hence, the rearranged boundary integral vanishes over a perfect metallic surface since the tangential electric field over the metallic surface is zero and the cross product of the normal to the surface $\mathbf{1}_n$ with the normal component of the electric field will be zero. Hence, Eq.(3.4) can then be written as,

$$\int_{\Omega} (\nabla \times \mathbf{W}) \cdot \varepsilon_r^{-1} (\nabla \times \mathbf{H}) d\Omega - k^2 \int_{\Omega} \mathbf{W} \cdot \mu_r \mathbf{H} \, d\Omega = 0 \qquad (3.6)$$

The Eq. (3.6) represents the weighted residual form of the vector helmholtz equation in H formulation.

The associated variational form of Eq.(3.6) is obtained by substituting $W = H$ in Eq.(3.6) and introducing a numerical factor of ½ before the integral expression. This gives,

$$F = \frac{1}{2}\int_{\Omega}\left((\nabla \times H) \cdot \varepsilon_r^{-1}(\nabla \times H) - k^2 H \cdot \mu_r H\right)d\Omega \qquad \text{(3.7)}$$

The expression for F given in (3.7) is the variational functional associated with the vector helmholtz equation (3.1a) subject to the natural boundary condition given in (3.1b).

The variational functional given in (3.7) is made stationary, with respect to the unknown coefficients in the expansion of H, which corresponds to the solution of the vector helmholtz equation.

C. Implementation of the stationary functional in the scaled boundary finite element formulation:

Expanding the components of H in terms of the variables (ξ,η,ς) as

$$H_i(\xi,\eta,\zeta) = f_1(\xi)\sum_{i=0}^{m}\sum_{j=0}^{n}h_{i(i,j)}\, h_{ii}(\eta)h_{ij}(\zeta) \qquad \text{(3.7a)}$$

$$H_j(\xi,\eta,\zeta) = f_2(\xi)\sum_{i=0}^{m}\sum_{j=0}^{n}h_{j(i,j)}\, h_{ji}(\eta)h_{jj}(\zeta) \qquad \text{(3.7b)}$$

$$H_k(\xi,\eta,\zeta) = f_3(\xi)\sum_{i=0}^{m}\sum_{j=0}^{n}h_{k(i,j)}\, h_{ki}(\eta)h_{kj}(\zeta) \qquad \text{(3.7c)}$$

where the functions f_1, f_2, f_3 are unknown radial functions depending on the radial

coordinate ξ, and $h_{x(ij)}\, h_{y(i\,j)}\, h_{z(ij)}$ are unknown coefficients, and $h_i(\eta), h_i(\zeta)$ are the

single variable functions of η, ζ representing the variations in η and ζ respectively

and $m < n$, $m \neq 0$ and $n \neq 0$.

The form of the functions $h_i(\eta)$ and $h_i(\zeta)$ are given as [2]

$$h_0(r) = 1 - r \tag{3.8a}$$

$$h_1(r) = 1 + r \tag{3.8b}$$

$$h_i(r) = \left(1 - r^2\right)r^{i-2} \quad \text{for } i \geq 2 \tag{3.8a}$$

Hence, the vector form for H is given as,

$$\mathbf{H}(\xi,\eta,\zeta) = H_i(\xi,\eta,\zeta)\,\mathbf{i} + H_j(\xi,\eta,\zeta)\,\mathbf{j} + H_k(\xi,\eta,\zeta)\,\mathbf{k} \tag{3.9}$$

It is shown in detail in [3] that for two dimensional surface finite elements employing the functions of the form given in Eq.(3.8), the condition m<n is necessary in the double summation series expansion and only the tangential continuity between adjacent elements need to be imposed in order to avoid spurious modes.

The functions $f_1(\xi), f_2(\xi)$ and $f_3(\xi)$ in the form of the power series expansion in ξ as

$$f_1(\xi) = \sum_{k=0}^{N} a_k \xi^k \tag{3.10a}$$

$$f_2(\xi) = \sum_{k=0}^{N} b_k \xi^k \tag{3.10b}$$

$$f_3(\xi) = \sum_{k=0}^{N} c_k \xi^k \tag{3.10c}$$

D. Implementation of the Divergence condition:

The divergence condition for the magnetic field is given by,

$$\nabla \cdot (\mu \mathbf{H}) = 0 \tag{3.11}$$

When μ is a scalar constant,

$$\mu \nabla . \mathbf{H} = 0 \tag{3.12}$$

$$\mu \left(\frac{\partial \mathbf{H}_{\hat{i}}}{\partial x} + \frac{\partial \mathbf{H}_{\hat{j}}}{\partial y} + \frac{\partial \mathbf{H}_{\hat{j}}}{\partial y} \right) = 0 \tag{3.13}$$

Expanding Eq.(3.12),

Since $\mu \neq 0$, this gives,

$$\left(\frac{\partial \mathbf{H}_{\hat{i}}}{\partial x} + \frac{\partial \mathbf{H}_{\hat{j}}}{\partial y} + \frac{\partial \mathbf{H}_{\hat{j}}}{\partial y} \right) = 0 \tag{3.14}$$

Rewriting the Eq.(3.14) in terms of scaled boundary coordinates[4] and using Eq.(3.7),

$$\frac{g^{\xi}}{|J|} n_x^{\xi} \frac{\partial \mathbf{H}_{\hat{i}}}{\partial \xi} + \frac{1}{\xi}\left(\frac{g^{\eta}}{|J|} n_x^{\eta} \frac{\partial \mathbf{H}_{\hat{i}}}{\partial \eta} + \frac{g^{\zeta}}{|J|} n_x^{\zeta} \frac{\partial \mathbf{H}_{\hat{i}}}{\partial \zeta} \right) + \frac{g^{\xi}}{|J|} n_y^{\xi} \frac{\partial \mathbf{H}_{\hat{j}}}{\partial \xi} + \frac{1}{\xi}\left(\frac{g^{\eta}}{|J|} n_y^{\eta} \frac{\partial \mathbf{H}_{\hat{j}}}{\partial \eta} + \frac{g^{\zeta}}{|J|} n_y^{\zeta} \frac{\partial \mathbf{H}_{\hat{j}}}{\partial \zeta} \right)$$

$$+ \frac{g^{\xi}}{|J|} n_z^{\xi} \frac{\partial \mathbf{H}_{\hat{k}}}{\partial \xi} + \frac{1}{\xi}\left(\frac{g^{\eta}}{|J|} n_z^{\eta} \frac{\partial \mathbf{H}_{\hat{k}}}{\partial \eta} + \frac{g^{\zeta}}{|J|} n_z^{\zeta} \frac{\partial \mathbf{H}_{\hat{k}}}{\partial \zeta} \right) = 0 \tag{3.15}$$

Multiplying both sides of Eq.(3.15) by ξ,

$$\frac{\xi g^{\xi}}{|J|} n_x^{\xi} \frac{\partial \mathbf{H}_{\hat{i}}}{\partial \xi} + \left(\frac{g^{\eta}}{|J|} n_x^{\eta} \frac{\partial \mathbf{H}_{\hat{i}}}{\partial \eta} + \frac{g^{\zeta}}{|J|} n_x^{\zeta} \frac{\partial \mathbf{H}_{\hat{i}}}{\partial \zeta} \right) + \frac{\xi g^{\xi}}{|J|} n_y^{\xi} \frac{\partial \mathbf{H}_{\hat{j}}}{\partial \xi} + \left(\frac{g^{\eta}}{|J|} n_y^{\eta} \frac{\partial \mathbf{H}_{\hat{j}}}{\partial \eta} + \frac{g^{\zeta}}{|J|} n_y^{\zeta} \frac{\partial \mathbf{H}_{\hat{j}}}{\partial \zeta} \right)$$

$$+ \frac{\xi g^{\xi}}{|J|} n_z^{\xi} \frac{\partial \mathbf{H}_{\hat{k}}}{\partial \xi} + \left(\frac{g^{\eta}}{|J|} n_z^{\eta} \frac{\partial \mathbf{H}_{\hat{k}}}{\partial \eta} + \frac{g^{\zeta}}{|J|} n_z^{\zeta} \frac{\partial \mathbf{H}_{\hat{k}}}{\partial \zeta} \right) = 0 \tag{3.16}$$

Rewriting Eq.(3.16) using Eq.(3.10) and grouping the terms of ξ^{k},

$$\sum_{k=0}^{m}\left[\left(\frac{g^{\eta}}{|J|}\right)\left[n_x^{\eta}a_k\frac{dN_1}{d\eta}+n_y^{\eta}b_k\frac{dN_2}{d\eta}+n_z^{\eta}c_k\frac{dN_3}{d\eta}\right]+\left(\frac{g^{\eta}}{|J|}\right)\left[n_x^{\zeta}a_k\frac{dN_1}{d\zeta}+n_y^{\zeta}b_k\frac{dN_2}{d\zeta}+n_z^{\zeta}c_k\frac{dN_3}{d\zeta}\right]\right]\xi^{k}$$
$$+\sum_{k=1}^{m}\left(\frac{g^{\xi}}{|J|}\right)k\left[a_k n_x^{\xi}N_1(\eta,\zeta)+b_k n_y^{\xi}N_2(\eta,\zeta)+c_k n_z^{\xi}N_3(\eta,\zeta)\right]\xi^{k}=0 \tag{3.17}$$

The relationship between the unknown coefficients of the power series of the radial

variable ξ is given from Eq.(3.17) as

$$c_k=\frac{-\left[a_k\left(\frac{g^{\xi}}{|J|}n_x^{\xi}kN_1+\frac{g^{\eta}}{|J|}n_x^{\eta}\frac{dN_1}{d\eta}+\frac{g^{\zeta}}{|J|}n_x^{\zeta}\frac{dN_1}{d\zeta}\right)+b_k\left(\frac{g^{\xi}}{|J|}n_y^{\xi}kN_2+\frac{g^{\eta}}{|J|}n_y^{\eta}\frac{dN_2}{d\eta}+\frac{g^{\zeta}}{|J|}n_y^{\zeta}\frac{dN_2}{d\zeta}\right)\right]}{\left(\frac{g^{\xi}}{|J|}n_z^{\xi}kN_3+\frac{g^{\eta}}{|J|}n_z^{\eta}\frac{dN_3}{d\eta}+\frac{g^{\zeta}}{|J|}n_z^{\zeta}\frac{dN_3}{d\zeta}\right)}$$

$$\tag{3.18}$$

valid for $k>0$ and N_1, N_2 and N_3 correspond to

$$N_1=\sum_{i=0}^{m}\sum_{j=0}^{n}h._{i(i,j)}\ h._{ii}(\eta)h._{j\ j}(\zeta) \tag{3.19a}$$

$$N_2=\sum_{i=0}^{m}\sum_{j=0}^{n}h._{j(i,j)}\ h._{ji}(\eta)h._{j\ j}(\zeta) \tag{3.19b}$$

$$N_3=\sum_{i=0}^{m}\sum_{j=0}^{n}h._{k(i,j)}\ h._{ki}(\eta)h._{kj}(\zeta) \tag{3.19c}$$

The following section, discusses, the variational form of the functional in terms of

the scaled boundary variables. Also, the mathematical form of the individual terms in the

functional is given.

E. The variational form of the functional in the scaled boundary coordinates:

The variational form of the functional given in Eq.(3.7) written in terms of the variables of the scaled boundary coordinates is given by,

$$\frac{1}{2}\int_0^1\int_{(\eta,\zeta)}\left[\frac{\varepsilon_r^{-1}}{|J|}\right]\left[\left(\xi g^\xi\right)^2(A+B+C)+\left(g^\eta\right)^2(D+E+F)+\left(g^\zeta\right)^2(G+H+I)\right]$$

$$+\frac{2\varepsilon_r^{-1}}{|J|}\left[\left(g^\eta g^\zeta\right)(J+K+L)+\left(g^\eta g^\xi\right)(M+N+P)+\left(g^\xi g^\zeta\right)(Q+R+S)\right]$$

$$-k_0^2\mu_r\left[\left(f_1(\xi)N_1(\eta,\zeta)\right)^2+\left(f_2(\xi)N_2(\eta,\zeta)\right)^2+\left(f_3(\xi)N_3(\eta,\zeta)\right)^2\right]d\xi\,d\eta\,d\zeta=0$$

...(3.20)

The expressions for the terms from A to S are given as follows:

$$A=\left[n_y^\xi\frac{\partial H_i}{\partial\xi}-n_z^\xi\frac{\partial H_i}{\partial\xi}\right]^2 \tag{3.21a}$$

$$B=\left[n_z^\xi\frac{\partial H_i}{\partial\xi}-n_x^\xi\frac{\partial H_k}{\partial\xi}\right]^2 \tag{3.21b}$$

$$C=\left[n_x^\xi\frac{\partial H_j}{\partial\xi}-n_y^\xi\frac{\partial H_i}{\partial\xi}\right]^2 \tag{3.21c}$$

$$D=\left[n_y^\eta\frac{\partial H_k}{\partial\eta}-n_z^\eta\frac{\partial H_j}{\partial\eta}\right]^2 \tag{3.21d}$$

$$E=\left[n_z^\eta\frac{\partial H_i}{\partial\eta}-n_x^\eta\frac{\partial H_k}{\partial\eta}\right]^2 \tag{3.21e}$$

$$F=\left[n_x^\eta\frac{\partial H_j}{\partial\eta}-n_y^\eta\frac{\partial H_k}{\partial\eta}\right]^2 \tag{3.21f}$$

$$G = \left[n_y^\zeta \frac{\partial H_{\hat{k}}}{\partial \zeta} - n_z^\zeta \frac{\partial H_{\hat{j}}}{\partial \zeta} \right]^2$$

$$H = \left[n_z^\zeta \frac{\partial H_{\hat{i}}}{\partial \zeta} - n_x^\zeta \frac{\partial H_{\hat{k}}}{\partial \zeta} \right]^2$$

$$I = \left[n_x^\zeta \frac{\partial H_{\hat{j}}}{\partial \zeta} - n_y^\zeta \frac{\partial H_{\hat{k}}}{\partial \zeta} \right]^2$$

$$J = \left[n_y^\eta \frac{\partial H_{\hat{k}}}{\partial \eta} - n_z^\eta \frac{\partial H_{\hat{j}}}{\partial \eta} \right]\left[n_y^\zeta \frac{\partial H_{\hat{k}}}{\partial \zeta} - n_z^\zeta \frac{\partial H_{\hat{j}}}{\partial \zeta} \right]$$

$$K = \left[n_z^\eta \frac{\partial H_{\hat{i}}}{\partial \eta} - n_x^\eta \frac{\partial H_{\hat{k}}}{\partial \eta} \right]\left[n_z^\zeta \frac{\partial H_{\hat{i}}}{\partial \zeta} - n_x^\zeta \frac{\partial H_{\hat{i}}}{\partial \zeta} \right]$$

$$L = \left[n_x^\eta \frac{\partial H_{\hat{j}}}{\partial \eta} - n_y^\eta \frac{\partial H_{\hat{i}}}{\partial \eta} \right]\left[n_x^\zeta \frac{\partial H_{\hat{j}}}{\partial \zeta} - n_y^\zeta \frac{\partial H_{\hat{i}}}{\partial \zeta} \right]$$

$$M = \left[n_y^\xi \frac{\partial H_{\hat{k}}}{\partial \xi} - n_z^\xi \frac{\partial H_{\hat{j}}}{\partial \xi} \right]\left[n_y^\eta \frac{\partial H_{\hat{k}}}{\partial \eta} - n_z^\eta \frac{\partial H_{\hat{j}}}{\partial \eta} \right]$$

$$N = \left[n_z^\xi \frac{\partial H_{\hat{i}}}{\partial \xi} - n_x^\xi \frac{\partial H_{\hat{k}}}{\partial \xi} \right]\left[n_z^\eta \frac{\partial H_{\hat{i}}}{\partial \eta} - n_x^\eta \frac{\partial H_{\hat{k}}}{\partial \eta} \right]$$

$$P = \left[n_x^\xi \frac{\partial H_{\hat{j}}}{\partial \xi} - n_y^\xi \frac{\partial H_{\hat{i}}}{\partial \xi} \right]\left[n_x^\eta \frac{\partial H_{\hat{j}}}{\partial \eta} - n_y^\eta \frac{\partial H_{\hat{i}}}{\partial \eta} \right]$$

$$Q = \left[n_y^\zeta \frac{\partial H_{\hat{k}}}{\partial \zeta} - n_z^\zeta \frac{\partial H_{\hat{j}}}{\partial \zeta} \right]\left[n_y^\xi \frac{\partial H_{\hat{k}}}{\partial \xi} - n_z^\xi \frac{\partial H_{\hat{j}}}{\partial \eta} \right]$$

$$R = \left[n_z^\zeta \frac{\partial H_{\hat{i}}}{\partial \zeta} - n_x^\zeta \frac{\partial H_{\hat{k}}}{\partial \zeta} \right]\left[n_z^\xi \frac{\partial H_{\hat{i}}}{\partial \xi} - n_x^\xi \frac{\partial H_{\hat{k}}}{\partial \xi} \right]$$

$$\text{(3.21r)}$$

$$S = \left[n_x^\zeta \frac{\partial H_{\hat{j}}}{\partial \xi} - n_y^\xi \frac{\partial H_{\hat{i}}}{\partial \xi} \right]\left[n_x^\xi \frac{\partial H_{\hat{j}}}{\partial \zeta} - n_y^\zeta \frac{\partial H_{\hat{i}}}{\partial \zeta} \right]$$

$$\text{(3.21s)}$$

The expression for c_k is substituted in Eq.(3.10c) so that f_3 is also expressed entirely in terms of the radial variable ξ and the unknown h-coefficients. The resulting expressions of f_1, f_2 and f_3 are substituted in Eq.(3.20) and Eq.(3.21).

As the radial coordinate ξ is independent of the two circumferential coordinates η and ς, integrating Eq.(3.20) with respect to ξ with its lower and upper limits being 0 and 1, makes Eq.(3.20) entirely in terms of the circumferential variables η and q. The functional entirely expressed in terms of the surface integrals will be of the form

$$\frac{1}{2} \int_{(\eta,\zeta)} A' + B' + C' + D' + E' + F' + G' + H' + I' + J' + K' + L' + M' + N' + P' +$$
$$Q' + R' + S' - k_0^2 \mu_r \left[T' + U' + V' \right] d\eta \, d\zeta$$

$$\text{...(3.22)}$$

where the letters with a prime denote the terms after the integration with the radial variable ξ. An important observation that is to be noted is that, the terms in Eq.(3.22) contains only the surface integral terms in the finite-element integrals even for the general 3-D structures, unlike the conventional finite element method where for analyzing 3-D structures devoid of any symmetry, involves integration in three dimension during the evaluation of the finite-element integrals .

The Eq.(3.22) is evaluated for every surface element characterized by the circumferential variables η and q. Then the variation with respect to each undetermined coefficient is set to zero. This process leads to a set of linear equations. Imposing only tangential continuity of the field component between the adjacent elements, the final system equation is of the form

$$A\,\mathbf{h} + k_0^2 B\,\mathbf{h} = 0 \qquad\qquad\qquad\qquad (3.24)$$

The Eq.(3.24) is a standard form of the matrix eigen value equation which can be solved numerically.

F. Numerical Implementation:

The theoretical formulation thus developed, is implemented numerically for the case of a spherical metallic cavity, with air being the dielectric medium. The spherical metallic cavity considered for the numerical implementation is shown below in Fig.(3a)
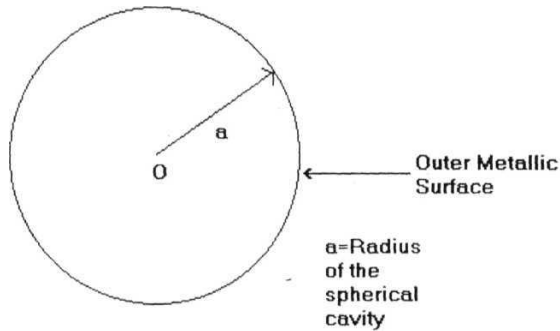
Fig.(3a) Spherical metallic Cavity

For the finite element discretization of the surface, an eight node curvilinear quadrilateral elements were used with the mesh of one octant consisting of three finite elements.

The discretized boundary of the solid sphere of one octant is shown below in Fig.(3b).
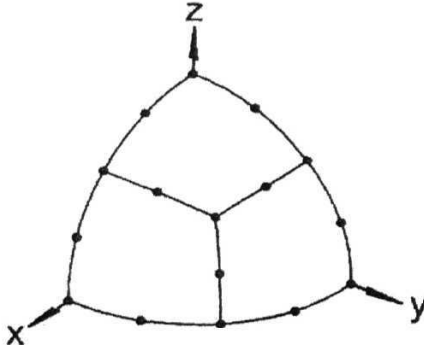
Fig.(3b) Finite Element mesh of one octant of boundary of solid sphere.

The integration which is performed involving the circumferential variables are done numerically using 5 point gaussian quadrature. The eigen value equation resulting from the assembling the element matrices were solved by using the standard LAPACK[5] collection of Fortran subroutines. The number of terms were used in the radial expansion of the fields were five. The resonant frequencies of TM on mode for the spherical cavity were computed by varying the radius of the spherical cavity, and the numerically obtained results show close agreement to the values obtained by a full theoretical analysis[6], and is shown in Table .(3.1) in the following page.

Table (3.1) showing the close agreement between the theoretical and the numerical values of the resonant frequency of TM (011) mode.

S.No	Radius of the spherical metallic cavity. a (in cms)	Resonant frequency computed for the TM_{011} mode by theory. f_r (10^9 Hz)	Resonant frequency computed by scaled boundary Finite element method. F_r (10^9 Hz)
1	3	4.369	4.3684
2	4	3.277	3.278
3	5	2.622	2.6215
4	6	2.185	2.1848

By theoretical modal field analysis, the resonant frequency f_r for a spherical cavity of radius 3 cms for $TM^{(even)}(011) = TM^{(even)}(111) = TM^{(odd)}(111)$ and it is equal to 4.367 x 10^9 Hz . [6] Accordingly, the resonant frequency obtained through the scaled boundary formulation for the spherical cavity of radius 3cms for the above mentioned modes were also constant with a value of 4.3668 x 10^9 Hz, further confirming the validity of the new method.

   Another important feature of the scaled boundary finite element formulation, is the effect of the number of terms in the radial expansion of the field variable on the accuracy of the eigen values. Table (3.2) in the following page, shows the effect of increase in the number of terms in the radial expansion of the field variable, on the accuracy of the resonant frequency.

Table (3.2) showing the effect of increase in the number of terms in the radial expansion of the field variable, on the resonant frequency of TM (011) mode.

No. of terms in the radial expansion of the field variable	Radius of the spherical metallic cavity. a (in cms)	Resonant frequency computed for the TM_{011} mode by theory. f_r $(10^9\,Hz)$	Resonant frequency computed by scaled boundary Finite element method. F_r $(10^9\,Hz)$
5	3	4.369	4.3684
6	3	4.369	4.3687
7	3	4.369	4.3689
8	3	4.369	4.3690

From Table (3.2), it can be inferred that, the number of terms in the radial expansion of the field variable, has a marked influence on the accuracy of the resonant frequency. It is observed from the above table that, the increase in the number of terms in the radial expansion of the field variable, is accompanied by the corresponding increase in the accuracy of the eigen values.

G. Conclusion: The close agreement between the theoretical and numerically computed values of the resonant frequency, proves the validity of the scaled boundary finite element method for cavity structures. Also, this method involves only the surface discretization unlike the finite element method which involves discretization in three dimensions, increasing the storage and computational requirements. The next chapter presents the scaled boundary finite element formulation for shielded microstrip transmission line structures and Very Large Scale Integrated Circuit Interconnects.

References

1) P.P.Silvester and R.L.Ferrari, "Finite elements for Electrical Engineers", 3rd Ed, Cambridge University Press, pp.97-99,1996.

2) Ibid, pp.308.

3) Ibid, pp.315.

4) Chongmin Song and John P. Wolf, "The Scaled boundary finite-element method- alias Consistent infinitesimal finite-element cell method - for elastodynamics", *Computer Methods in applied mechanics and engineering,* No. 147, pp. 334-337, 1997.

5) LAPACK users guide, 3rd Ed, SIAM, Philadelphia.

6) C.A.Balanis, "Advanced Engineering Electromagnetics", pp.560-562.

CHAPTER-IV

THE SCALED BOUNDARY FINITE ELEMENT FORMULATION FOR SHIELDED MICROSTRIP TRANSMISSION LINE STRUCTURES AND VERY LARGE SCALE INTEGRATED CIRCUIT (VLSI) INTERCONNECTS

CHAPTER – IV

THE SCALED BOUNDARY FINITE ELEMENT FORMULATION FOR SHIELDED MICROSTRIP TRANSMISSION LINE STRUCTURES AND VERY LARGE SCALE INTEGRATED CIRCUIT (VLSI) INTERCONNECTS

A. Introduction: A shielded transmission line structure represents a transverse confinement of the electromagnetic field with respect to the direction of propagation. The structure usually consists of an outer metallic shield, with one or more metallic conductors embedded in the intervening dielectric medium. The geometry representing a shielded transmission line, is an open structure along the direction of propagation of the field. For the transmission line having a geometrical invariance along the direction of propagation of the field, the field variation along the direction of propagation can always be represented as $e^{-\gamma z}$, where y is a complex number called the propagation constant, and the variable z denotes the coordinate along the direction of propagation. This feature is quite distinct from the cavity structure, where the cavity structure represents a total confinement of the electromagnetic field.

A shielded microstrip transmission line structure consists of a metallic ground plane, on top of which there exists a single or multiple layers of higher dielectric constant substrate. The multiple substrate layers may be of the same material or of different dielectric materials. The metallic conductors are etched on the substrate layers, and the whole structure is enclosed in an outer metallic shield. A typical planar microstrip structure shown in Fig.4(a), in the following page.
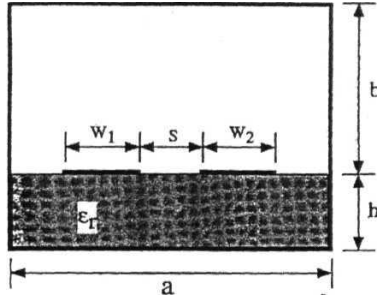
Fig.4(a). A shielded and coupled microstrip planar transmission line structure.

In the figure shown above, the width of the ground plane is denoted by a. w_1 and w_2 denotes the width of the conducting metallic strips. The thickness of the dielectric layer on the top of the ground plane is h, and its dielectric constant is denoted by ε_r. The separation between the conducting strips is denoted by s. The thickness of the air layer is denoted as b.

Another category of the planar microstrip transmission line structure is the open microstrip structure, which is very much similar to the closed microstrip structure, the only difference is that there is no external metallic shield for the open microstrip structure.

An important feature of the microstrip structure is that, the structure, being inhomogenous, cannot support a pure TEM mode, and the modes that are supported by such a structure are called hybrid modes. They are the superposition of all possible Transverse Electric and Transverse Magnetic modes. As a consequence of this, the device parameters of the microstrip structure, namely, the characteristic impedance and the effective dielectric constant, become frequency dependent.

This frequency dependence of the device **parameters** of the microstrip structure becomes more pronounced after the X-band of the microwave spectrum [1]. The characteristic impedance of the microstrip structure is of crucial importance while designing the microwave integrated circuits at higher frequencies, for determining the **characteristic** terminations and also to couple the structure with proper impedance matching with other devices. [2]

Under these conditions, it is necessary to perform a full-wave analysis. This takes care of the hybrid mode propagation as well as the frequency dependence of the device parameters of the microstrip structure . [3]

The microstrip transmission line structures are extensively used in the miniaturized microwave circuits leading to their application in directional radio, satellites, direction - location equipment, and industrial test and measurement systems. [4]

In the case of the VLSI interconnects, they physically resemble a typical multilayered multi conductor open microstrip structure, and are encountered in very high speed digital circuits and microprocessors. The continuous advances in integrated circuit technology makes it possible to build microprocessors to operate at clock rates in the range of GHz.[5] Under these conditions, the dimensions of the interconnections between chips become comparable to the wavelength of the signal through them, and the transmission line properties of the interconnects will have to be taken into consideration. Under these conditions, the transmission line properties of the interconnects influence by introducing signal delay, clock-skew, and cross-talk, which degrade the quality of the signal.[6]

The traditional lumped RC representation underestimates both cross-talk and signal delay as the frequency dependence of the parameters R and C themselves are not taken into account.[7]

The frequency dependence of characteristic impedance plays a crucial role in the reliable performance of the interconnect structures when used in high-speed digital circuits. Hence, it is necessary to perform a full-wave analysis of the VLSI interconnect structure.

In this chapter, the theory of the scaled boundary finite element formulation suitable for analyzing a multi-layered and multi-conductor microstrip transmission line structure and VLSI interconnects will be developed, along with the expressions for determining the characteristic impedance. The numerical implementation will be illustrated by taking two practical structures.

B. Theory:

The vector helmholtz equation in **H-variable** is given as, [8]

$$\nabla \times \varepsilon_r^{-1} \nabla \times \mathbf{H} - k_0^2 \mu_r \mathbf{H} = \mathbf{0} \text{ where } k_0^2 = \mu_0 \varepsilon_0 \tag{4.1}$$

Taking the axis of the transmission line to lie along the z-direction and propagation to be characterized by a complex wave number $y = \alpha + j\beta$, corresponding to the general lossy case, the vector operator ∇ appearing in Eq.(4.1) may be divided into its transverse and longitudinal parts as,

$$\nabla = \nabla_t^{'} - \mathbf{1}_z \gamma \tag{4.2a}$$

$$\nabla_t = \mathbf{1}_x \frac{\partial}{\partial x} + \mathbf{1}_y \frac{\partial}{\partial y} \tag{4.2b}$$

Omitting the common factor $\exp(j\omega t - \gamma z)$ throughout, the phasor vector magnetic field can be split up similarly as,

$$H = H_t(x, y) + 1_z H_z(x, y) \tag{4.3}$$

Using the expression given in (4.3) the Eq.(4.1) is separated into its transverse and longitudinal parts as, [9]

$$\nabla_t \times \varepsilon_r^{-1} \nabla_t \times H_t - \gamma \varepsilon_r^{-1} \nabla_t H_z - \left(k_0^2 \mu_r + \gamma^2 \varepsilon_r^{-1}\right) H_t = 0 \tag{4.4}$$

$$\nabla_t \cdot \varepsilon_r^{-1} \nabla_t H_z + \gamma \nabla_t \cdot \varepsilon_r^{-1} H_t + k_0^2 \mu_r H_z = 0 \tag{4.5}$$

Multiplying Eq.(4.4) by an arbitrary transverse weight function W_t and Eq.(4.5) by an arbitrary axial weight function W_z and integrating over the wave guide cross-section gives,

$$R_t = \int_\Omega W_t \cdot \left(\nabla_t \times_r^{-1} \nabla \times H_t - \gamma \varepsilon_r^{-1} \nabla_t H_z\right) d\Omega - \int_\Omega \left(k_0^2 \mu_r + \gamma^2 \varepsilon_r^{-1}\right) W_t \cdot H_t \, d\Omega \tag{4.6a}$$

$$R_z = \int W_z \left(\nabla_t \cdot \varepsilon_r^{-1} \nabla_t H_z + \gamma \nabla_t \cdot \varepsilon_r^{-1} H_t + k_0^2 \mu_r H_z\right) d\Omega \tag{4.6b}$$

Using the vector integration by parts formula given by

$$\int_\Omega u\nabla \cdot F \, d\Omega = \oint_S uF.1_n \, dS - \int_\Omega \nabla u \cdot F \, d\Omega \tag{4.7}$$

$$\int_\Omega P \cdot \left(\nabla \times \nabla \times Q\right) d\Omega = \int_\Omega \left(\nabla \times P\right) \cdot \left(\nabla \times Q\right) d\Omega - \oint_S \left(P \times \nabla \times Q\right) \cdot 1_n \, dS \tag{4.8}$$

The expressions for the transverse and longitudinal residuals can be written as,

$$R_t = \int_\Omega \left((\nabla_t \times W_t) \cdot \varepsilon_r^{-1} (\nabla_t \times H_t) - (k_0^2 \mu_r + \gamma^2 \varepsilon_r^{-1}) W_t \cdot H_t \right) d\Omega - \int_\Omega \gamma \varepsilon_r^{-1} W_t \cdot \nabla_t H_z d\Omega$$

$$- \int_C (1_n \times W_t) \cdot 1_z \, j\omega\varepsilon_0 E_z dC \tag{4.9}$$

$$R_z = \int_\Omega \left(\nabla_t W_z \cdot \varepsilon_r^{-1} \nabla_t H_z + \gamma \nabla_t W_z \cdot \varepsilon_r^{-1} H_t \right) d\Omega - \int_\Omega k_0^2 \mu_r W_z H_z \, d\Omega$$

$$- \int_C \left(W_z \varepsilon_r^{-1} \nabla_t H_z + \gamma W_z \varepsilon_r^{-1} H_t \right) \cdot 1_n dC \tag{4.10}$$

The third term in (4.9) and (4.10) represent the contour integral with C representing the boundary of the finite element.

Considering the contour integral term in (4.9), it corresponds to the natural continuity of E_z across all internal boundaries between elements even when ε_r is discontinuous. The vectors 1_n on the common boundary of any adjacent pair of elements are equal and opposite, while W_t is continuous across the boundary. Hence, omitting the contour integral in the finite element construction is equivalent to allowing such integrals to cancel at inter- element boundaries, implying the correct continuity for E_z. Therefore, the required continuity in E_z occurs as a natural condition; provided H_t and W_t are tangential ly continuous vectors and both are constrained to have zero tangential components at magnetic walls.

Similarly considering the contour integral term in (4.10), it can be rearranged using the Maxwell's magnetic curl equation, as

$$- \int_C \left(W_z \varepsilon_r^{-1} \nabla_t H_z + \gamma W_z \varepsilon_r^{-1} H_t \right) \cdot 1_n dC = - \int_C W_z (E_t \times 1_z) \cdot 1_n dC = -j\omega\varepsilon_0 \int_C W_z (E_t \cdot 1_t) dC \qquad \textbf{(4.11)}$$

where $\mathbf{1_t}$ is the unit tangential **vector** on C. To simulate continuous tangential E across inter element boundaries, and vanishing tangential electric field at an electric wall, as natural **interface and boundary** conditions, the contour integral should be ignored. Also, considering the case that if there is a magnetic wall, $\mathbf{W_z}$ is set to zero to correspond with the essential constraint of tangential magnetic field being zero. This necessitates to ignore this contour integral term in the finite element analysis.

The required transverse and axial functionals corresponding to the transverse and longitudinal field components respectively are given by,

$$F_t = \frac{1}{2}\int_\Omega \left((\nabla_t \times \mathbf{H_t})\cdot\varepsilon_r^{-1}(\nabla_t \times \mathbf{H_t}) - (k_0^2\mu_r + \gamma^2\varepsilon_r^{-1})\mathbf{H_t}\cdot\mathbf{H_t}\right)d\Omega - \int_\Omega \gamma\varepsilon_r^{-1}\mathbf{H_t}\cdot\nabla_t H_z d\Omega \qquad (4.12)$$

$$F_z = \frac{1}{2}\int_\Omega \left(\nabla_t H_z\cdot\varepsilon_r^{-1}\nabla_t H_z - k_0^2\mu_r H_z^2\right)d\Omega + \int_\Omega \gamma\nabla_t H_z\cdot\varepsilon_r^{-1}\mathbf{H_t}\, d\Omega \qquad (4.13)$$

where Ω denotes the transverse cross sectional area.

The divergence condition for the magnetic field is represented as,

$$\nabla\cdot\mathbf{B} = 0 \qquad (4.14)$$

In terms of H, the above equation can be written as,

$$\nabla\cdot\mu\mathbf{H} = 0 \qquad (4.15)$$

For the case of wave propagation in the z-direction,

$$\frac{\partial}{\partial z} \equiv -\gamma, \quad \text{permitting Eq.(4.15) to be re - written as}$$

$$\left(\frac{\partial H_x}{\partial x} + \frac{\partial H_y}{\partial y}\right)\mu = \gamma H_z, \text{ where } \mathbf{u} \text{ is a scalar constant.} \tag{4.16}$$

Using the Equations (2.36, 2.37, and 2.38) of Chapter-II, representing the scaled boundary transformation in two dimensions [10], Eq.(4.16) can be written as,

$$\frac{\partial y}{\partial \eta}\frac{df_1}{d\xi}N_1 - \frac{y}{\xi}f_1\frac{dN_1}{d\eta} - \frac{\partial x}{\partial \eta}\frac{df_2}{d\xi}N_2 + \frac{x}{\xi}f_2\frac{dN_2}{d\eta} = \frac{\gamma|J|}{\mu}f_3 N_3(\eta) \tag{4.17}$$

where,

$$H_x(\xi,\eta) = f_1(\xi)N_1(\eta) \tag{4.18a}$$
$$H_y(\xi,\eta) = f_2(\xi)N_2(\eta) \tag{4.18b}$$
$$H_z(\xi,\eta) = f_3(\xi)\sum_{l=1}^{m}H_{zl}N_{3l}(\eta) \tag{4.18c}$$

Let

$$f_1(\xi) = \sum_{k=1}^{m}a_k\xi^k \tag{4.19a}$$

$$f_2(\xi) = \sum_{k=1}^{m}b_k\xi^k \tag{4.19b}$$

$$f_3(\xi) = \sum_{k=1}^{m}c_k\xi^k \tag{4.19c}$$

Multiplying (4.17) on both sides by 'ξ' and substituting the expansions given in (4.18) and (4.19), and regrouping the terms of ξ^k and ξ^{k+1}, the following relations between the unknown coefficients in the radial expansions in H are obtained.

$$b_1 = \frac{a_1\left[y\dfrac{dN_1}{d\eta} - N_1\dfrac{\partial y}{\partial \eta}\right]}{\left[x\dfrac{dN_2}{d\eta} - N_2\dfrac{\partial x}{\partial \eta}\right]} \tag{4.20a}$$

$$a_{k+1}\left[(k+1)N_1\frac{\partial y}{\partial \eta}-y\frac{dN_1}{d\eta}\right]+b_{k+1}\left[x\frac{dN_2}{d\eta}-(k+1)N_2\frac{\partial x}{\partial \eta}\right]=c_k\left[\frac{\gamma|J|}{\mu}\sum_{l=1}^{m}H_{zl}N_{3l}(\eta)\right]$$

for $1\le k\le m-1$.   **(4.20b)**

From (4.20b) the expression for b_{k+1} can be written as,

$$b_{k+1}=\frac{c_k\left[\dfrac{\gamma|J|}{\mu}\displaystyle\sum_{l=1}^{m}H_{zl}N_{3l}(\eta)\right]-a_{k+1}\left[(k+1)N_1\dfrac{\partial y}{\partial \eta}-y\dfrac{dN_1}{d\eta}\right]}{\left[x\dfrac{dN_2}{d\eta}-(k+1)N_2\dfrac{\partial x}{\partial \eta}\right]}$$ **(4.20c)**

for $1<k<m-1$.

The terms $f(\xi)$ and $N(\eta)$ in (4.18a) and (4.18b) represent the radial function and the scalar component of the tangentially continuous vector interpolation functions respectively. The form of the expression in (4.18c) represents the nodal expansion of the z-component of the field variable **on the boundary of the domain** with the variation of the nodal interpolation function of the surface finite element, along the radial direction given by $f_3(\xi)$.

The summation on the right hand side of (4.18c) indicates the general nodal expansion with 'm' nodes and the function N_{3l} (η) indicates the nodal interpolation in terms of the variable r] at the node T on the boundary, and the subscript T varying from 1 to m. The notation H_{zl} indicates the unknown value of the z-component of H at the node T, to be determined by the variational process.

The form of the function $N(r|)$ occurring in the x and y components of H are

$$N_1(\eta) = \sum_{i=0}^{m} n_{1i} g_i(\eta) \qquad \text{(4.21a)}$$

$$N_2(\eta) = \sum_{i=0}^{m} n_{2i} g_i(\eta) \qquad \text{(4.21b)}$$

where n_{1i} and n_{2i} are unknown coefficients and

$$g_0(\eta) = 1 - \eta \qquad \text{(4.21c)}$$
$$g_1(\eta) = 1 + \eta \qquad \text{(4.21d)}$$
$$g_i(\eta) = (1 - \eta^2) \eta^{(i-2)} \quad \text{for } i \geq 2. \qquad \text{(4.21e)}$$

The nodal interpolation function N_{3z} occurring in the z-component of **H** can be chosen from the interpolation functions used for the isoparametric elements.

The expansions given in (4.18 and 4.19) and the expression for b_1 given in (4.20a), and b_{k+1} given in (4.20c) are substituted in the transverse and axial functionals given in (4.12) and (4.13).

The individual terms in the transverse and axial functionals take the following forms:

$$d\Omega = \xi \, |J| \, d\xi \, d\eta \qquad \text{(4.22a)}$$

$$H_z^2 = \left(f_3 \sum_{l=1}^{m} H_{zl} N_{3l}(\eta) \right)^2 \qquad \text{(4.22b)}$$

$$\gamma \varepsilon_r^{-1} \left(\mathbf{H}_t \cdot \nabla_t \mathbf{H}_z \right) = \frac{\gamma \varepsilon_r^{-1}}{|J|} \left[\begin{array}{l} \left(\dfrac{df_3}{d\xi} \right) \left(\displaystyle\sum_{l=1}^{m} H_{zl} N_{3l}(\eta) \right) \left[f_1 N_1 \dfrac{\partial y}{\partial \eta} - f_2 N_2 \dfrac{\partial x}{\partial \eta} \right] + \\ \left(\dfrac{f_3}{\xi} \displaystyle\sum_{l=1}^{m} H_{zl} \dfrac{dN_{3l}\eta}{d\eta} \right)(x - y) \end{array} \right]$$

$$\text{...(4.22c)}$$

$$(\nabla\times\mathbf{H}_t)\cdot\varepsilon_r^{-1}(\nabla\times\mathbf{H}_t)=\varepsilon_r^{-1}\left(\frac{1}{|J|}\right)^2\left[\begin{array}{l}\left(\dfrac{\partial y}{\partial\eta}\dfrac{df_2}{d\xi}N_2\right)^2+\left(\dfrac{y}{\xi}\dfrac{dN_2}{d\eta}f_2\right)^2+\left(-\dfrac{\partial x}{\partial\eta}\dfrac{df_1}{d\xi}N_1\right)^2\\[3mm]+\left(\dfrac{x}{\xi}\dfrac{dN_1}{d\eta}f_1\right)^2\\[3mm]-2\left[\begin{array}{l}\left(f_2N_2\dfrac{y}{\xi}\dfrac{df_2}{d\xi}\dfrac{dN_2}{d\eta}\dfrac{\partial y}{\partial\eta}\right)+\left(f_1N_1\dfrac{\partial x}{\partial\eta}\dfrac{x}{\xi}\dfrac{df_1}{d\xi}\dfrac{dN_1}{d\eta}\right)\\[3mm]-\left(N_1N_2\dfrac{df_1}{d\xi}\dfrac{df_2}{d\xi}\dfrac{\partial x}{\partial\eta}\dfrac{\partial y}{\partial\eta}\right)+\left(f_1N_2\dfrac{x}{\xi}\dfrac{\partial y}{\partial\eta}\dfrac{df_2}{d\xi}\dfrac{dN_1}{d\eta}\right)\\[3mm]+\left(f_2N_1\dfrac{y}{\xi}\dfrac{\partial x}{\partial\eta}\dfrac{df_1}{d\xi}\dfrac{dN_2}{d\eta}\right)-\left(\dfrac{xy}{\xi^2}\right)\left(f_1f_2\dfrac{dN_1}{d\eta}\dfrac{dN_2}{d\eta}\right)\end{array}\right]\end{array}\right]$$

$$...(4.22d)$$

$$\varepsilon_r^{-1}\left(\nabla_t\mathbf{H}_z\cdot\nabla_t\mathbf{H}_z\right)=\varepsilon_r^{-1}\left(\frac{1}{|J|}\right)^2\left[\begin{array}{l}\left(\displaystyle\sum_{l=1}^{m}\mathbf{H}_{zl}N_{3l}(\eta)\dfrac{df_3}{d\xi}\right)^2\left[\left(\dfrac{\partial y}{\partial\eta}\right)^2+\left(\dfrac{\partial x}{\partial\eta}\right)^2\right]+\left(\dfrac{f_3}{\xi}\displaystyle\sum_{l=1}^{m}\mathbf{H}_{zl}\dfrac{dN_{3l}(\eta)}{d\eta}\right)^2\\[4mm]\left(x^2+y^2\right)-2\left[\begin{array}{l}\left(\displaystyle\sum_{l=1}^{m}\mathbf{H}_{zl}N_{3l}(\eta)\right)\dfrac{df_3}{d\xi}\left[\dfrac{\partial y}{\partial\eta}+\dfrac{\partial x}{\partial\eta}\right]+(xy)\left(\dfrac{f_3}{\xi}\right)\\[3mm]\left(\displaystyle\sum_{l=1}^{m}\mathbf{H}_{zl}\dfrac{dN_{3l}(\eta)}{d\eta}\right)\end{array}\right]\end{array}\right]$$

$$...(4.22e)$$

The expressions given in (4.22) are substituted in the transverse and axial functionals so as to render the functionals entirely in terms of the scaled boundary variables. Integrating the transverse and axial functionals with respect to 'ξ' from 0 to 1 renders the functionals independent of 'ξ'. The transverse and axial functionals are evaluated for every surface element with η^c being the contour for every curved finite element on the boundary. In order to satisfy the essential boundary constraints, the corresponding unknown coefficients occurring in the circumferential term in the expansion of the fields,

111

are set to zero. According to the principle of superposition, the functional for the whole domain is the sum of the functional for every surface finite element.

The functional for the whole domain is made stationary by taking the partial derivatives of the unknown coefficients and setting them to zero. This process yields a set of sparse matrix eigen value equations for the transverse and longitudinal components of the form

$$\mathbf{Ah_t} - k_0^2 \mathbf{Bh_t} - \gamma \mathbf{Ch_z} - \gamma^2 \mathbf{Dh_t} = 0 \tag{4.23a}$$
$$\mathbf{Eh_z} - k_0^2 \mathbf{Fh_z} + \gamma \mathbf{C^T h_t} = 0 \tag{4.23b}$$

where $\mathbf{h_t}$ and $\mathbf{h_z}$ are column vectors representing the unknown coefficients.

From (4.23b), $\mathbf{h_z}$ is given by,

$$\mathbf{h_z} = -\gamma \mathbf{E} - k_0^2 \mathbf{F^{-1} C^T h_t} \tag{4.24a}$$

Substituting (4.24a) in (4.23a), gives the standard eigen equation of the form

$$\mathbf{A} - k_0^2 \mathbf{Bh_t} + \gamma^2 \left(\mathbf{CE} - k_0^2 \mathbf{F^{-1} C^T} - \mathbf{D} \right) \mathbf{h_t} = 0 \tag{4.24b}$$

The solution of the eigen equation (4.24b) for y, can be achieved numerically by using standard linear algebra routines.

C. Expression for characteristic **impedance:**

In multi-conductor systems with n conductors (except the ground conductor), n fundamental modes which are orthogonal to each other can propagate along the longitudinal direction. Each fundamental mode is specified by its phase constant and the overall power transported along the total conductor configuration. For such a configuration there can be two types of characteristic impedance- the total characteristic impedance and the modal characteristic impedance. Through the finite element field

solutions, the current matrix **[I]** can be constructed, each element of which is the axial current I_{ik} on /th line for a given mode k. [10]

Thus, for an n conductor system, a complete set of currents will be defined by an n x n matrix **[I].** An $n \times n$ voltage matrix **[V]** can also be constructed with components V_{ik}, if modal characteristic impedance Z^m_{ik} is assumed to exist, such that [10]

$$V_{ik} = Z^{ik}_m I_{ik} \qquad \qquad (4.25a)$$

Thus, the modal characteristic impedance is defined by the ratio of voltage to current on a line for a given mode. The total characteristic impedance is determined in the matrix form, [Z^t], given by,

$$\{V^t\} = [Z^t]\{I^t\} \qquad \qquad (4.25b)$$

where $\{V^{\ t}\}$ and $\{I^{\ t}\}$ are arbitrary total voltage vector and total current vector, respectively, due to a superposition of all modes on each of the n lines. They are obtained from [V] and [I], such that $\{I^t\} = [I]\{A\}$ and $\{V^t\} = [V]\{A\}$.

The components I^t_i and V^t_i of $\{I^t\}$ and $\{V^t\}$, respectively, are the total arbitrary current and voltage on /th line. The components A_k of $\{A\}$ are the coefficients for mode k in the modal expansion. Therefore, the total characteristic impedance matrix is given by,

$$[Z^t] = [V] [I]^{-1} \qquad \qquad (4.25c)$$

where $[I]^{-1}$ is the inverse matrix of [I]. Using the relation

$$[I]^T[V] = [P] \qquad \qquad (4.25d)$$

the total characteristic impedance matrix becomes

$$[Z^t] = ([I]^T)^{-1} [P][I]^{-1} \qquad \qquad (4.25e)$$

where [P] is a diagonal matrix and each diagonal element, P_{kk} is the propagating power for the k mode, and T denotes a transpose.

Thus, the total characteristic impedance relating the voltage of /th line to the current on jth line Z ' $_{ij}$ can be calculated from (4.25e), by manipulating the matrices [I] and **[P].** The modal characteristic impedance of the /th line for the kth mode, Z $^m_{ik}$ can also be calculated.

The modal characteristic impedance is useful for studying the nature of hybrid mode propagation on multi-conductor transmission line systems. The total characteristic impedance is useful for the circuit designers, where the emphasis is on the equivalent circuits and the characteristic terminations.

D. Calculation of Current and Power: The axial current and the propagating power can be calculated using the FEM field solutions. For evaluating the axial current in /th conductor

for a given mode k, the Ampere's law gives, [10]

$$I_{ik} = \oint_{C_i} \mathbf{H}_k \cdot d\mathbf{l} \tag{4.26}$$

The integration contour C_i is taken to be a path around the surface of the /th strip. To evaluate the integral, only the tangential fields on the strip surface are required. The propagating power for the orthogonal modes is described by the Poynting vector as

$$P_{kk'} \delta_{kk'} = \iint_{\Omega} \left[\mathbf{E}_k \times (\mathbf{H}_{k'})^* \right] \cdot \mathbf{z} \, dx \, dy \tag{4.27}$$

where $\mathbf{E}_k$ is the electric field, the asterisk denotes complex conjugate, and the Kronecke delta $\delta_{kk'} = 0$ if $k \neq k'$ and $\delta_{kk'} = 1$ if $k = k'$.

Using Maxwell's equation , the expression for power is,

$$P_{kk} = \frac{\gamma_k}{\omega\varepsilon_0} \{H_{tk}\}^{*T}\left(CE - k_0^2 F^{-1}C^T - D\right)\{H_{tk}\} \qquad (4.28)$$

where ε_0 is the permittivity of free space and the '$*^T$' denotes the complex conjugate **and** transpose.

Thus, the modal power can be easily calculated using the finite element method.

E. **Numerical Implementation:** The theory developed above for computing the eigen modes and the device parameters of the microstrip structures and VLSI interconnects is numerically implemented by taking the Fig.(4a) as a representative structure of a typical planar shielded microstrip transmission line. By using the domain sub-structuring, the domain is divided into sub-domains, where, in each sub-domain, the scaled boundary finite element method can be implemented independently with the continuity imposed at the common boundary. This approach greatly reduces the number of elements required for the numerical implementation as well as the time required for the computation. The typical dimensions used in the numerical calculation for Fig.(4a) were, a=10 mm, h=1.0 mm, and b= 4.0 mm. The transmission line structure is assumed to be loss free.

The strips were assumed to have zero thickness and strip widths were taken as $W_1 = W_2 = 2.0$ mm, and the separation between the strips denoted by S to be 1.0 mm. The relative permittivity of the substrate, $\varepsilon_r = 4.0$. For the numerical implementation, 350 boundary line elements were used for discretizing the structure theoretically. The number of terms used in the radial expansion was five. The nodal interpolation functions used in the numerical implementation, was the one-dimensional equivalent of the two-

dimensional interpolation functions for an eight noded isoparametric quadrilaterals [11]. The numerical integration of the element matrices was done by using a 5-point gaussian quadrature. The matrix eigen equation was solved by using LAPACK [12].

For the structure given in Fig.(4a), the normalized propagation constant was calculated for various frequencies, where the frequency was normalized with respect to the thickness 'h' of the dielectric layer. The variation of the propagation is shown below in Fig.(4b).
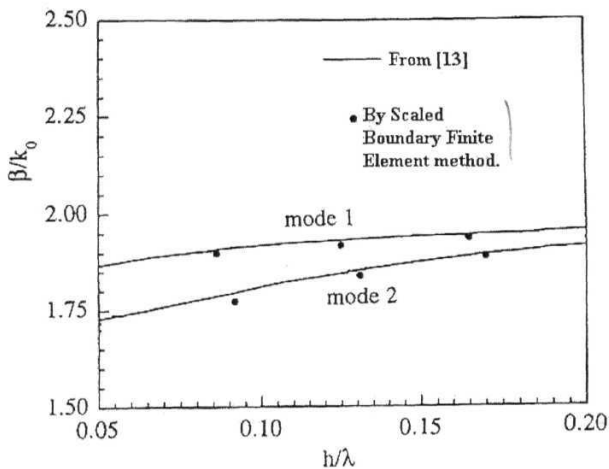
Fig.(4b). Normalized propagation constant versus frequency for the coupled microstrip line shown in Fig.(4a).

The variation of the total characteristic impedance with respect to frequency is shown below in Fig.(4c) and that of modal characteristic impedance in Fig.(4d).

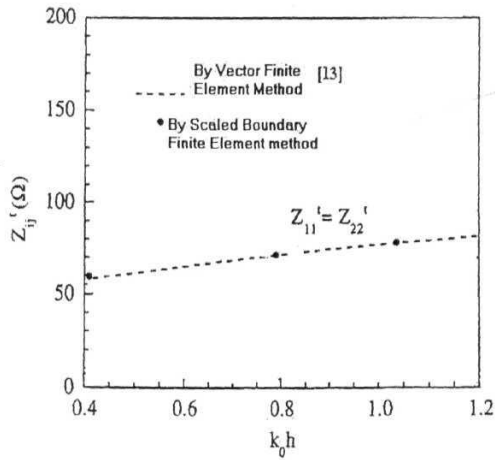Fig.(4c). Variation of the Total characteristic impedance with respect to frequency for the coupled microstrip line shown in Fig.(4a).
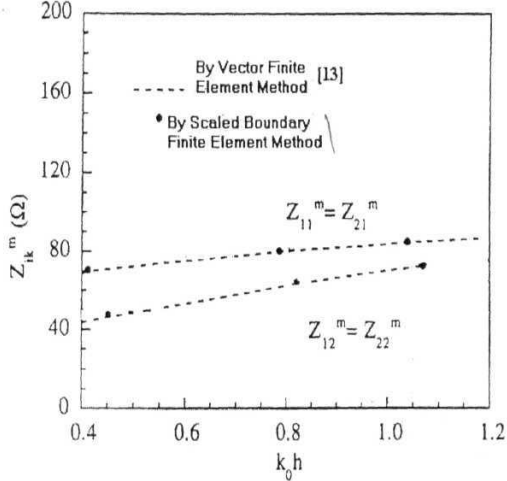

Fig.(4d). Variation of the modal characteristic impedance with respect to frequency for the coupled microstrip structure shown in Fig.(4a).

For the case of the analysis of VLSI interconnects, an unbounded microstrip like structure with two conducting metallic strips of widths W_1 and W_2 embedded in layer 1 and layer 2 with the thickness of the dielectric layers being h_1 and n_2, is taken as a representative structure. This is shown below in Fig.(4e).
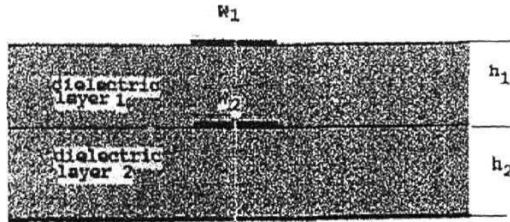
Fig.(4e). A typical VLSI interconnect structure.

Fig.(4e). A typical VLSI interconnect structure.

The substrate dielectric constant is taken to be $\varepsilon_r = 4.0$ and the widths W_1 and W_2 of the metallic strips were taken to be equal to 1.0 mm. The thickness h_1 and h_2 of the dielectric layers were taken to be equal to 1.0 mm. To analyze the open structure of Fig.(4e) with the finite element method, the geometry was truncated on both sides by a metallic shield separated horizontally and vertically by a distance equal to 10 times the thickness of a single substrate layer. The structure is assumed to be loss free.

The geometry shown in Fig.(4e) is discretized theoretically, by using 1300 boundary line elements. The number *of* terms used in the radial expansion was seven. The impedance curves for the two microstrip modes obtained by the scaled boundary finite element method is compared with those obtained by a vector finite element method. This is shown graphically in Fig.(4f) and Fig.(4g).

Total **Characteristic** Impedance
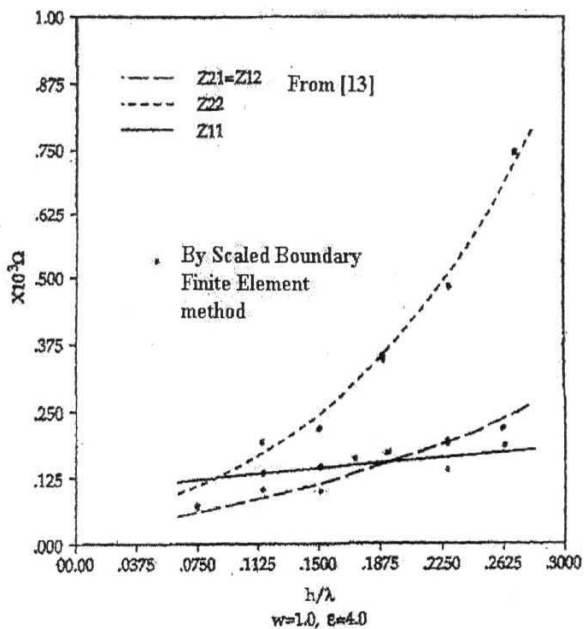
Normalized Frequency

Fig.(4f). Variation of the total characteristic impedance with respect to frequency, of the VLSI interconnect structure shown in Fig.(4e).
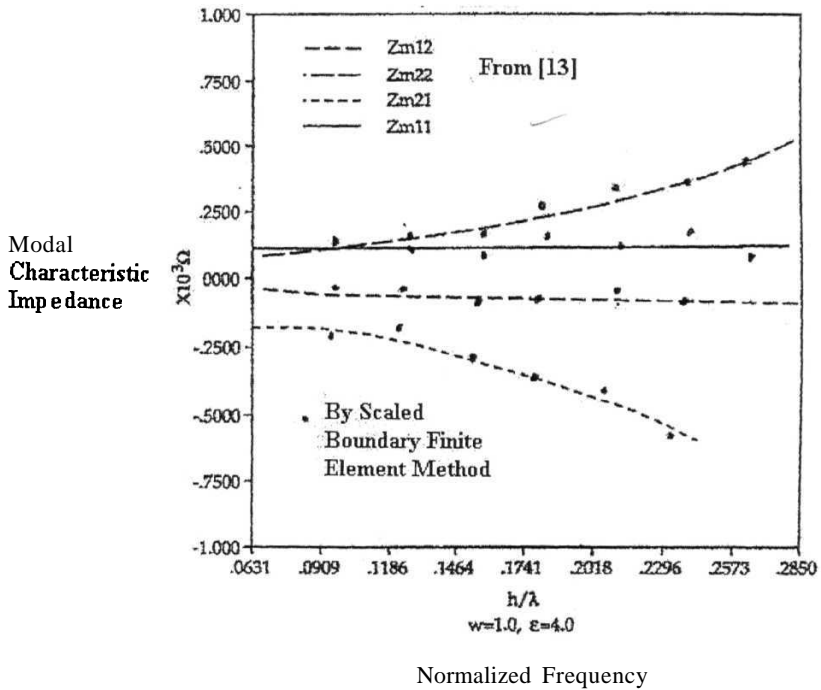
Fig.(4g). Variation of Modal Characteristic impedance with respect to frequency, of the VLSI interconnect structure shown in Fig.(4e).

The dispersion curves for various modes corresponding to the VLSI interconnect structure of Fig.(4e) is shown below in Fig.(4h).

Modal Dispersion

Normalized Frequency
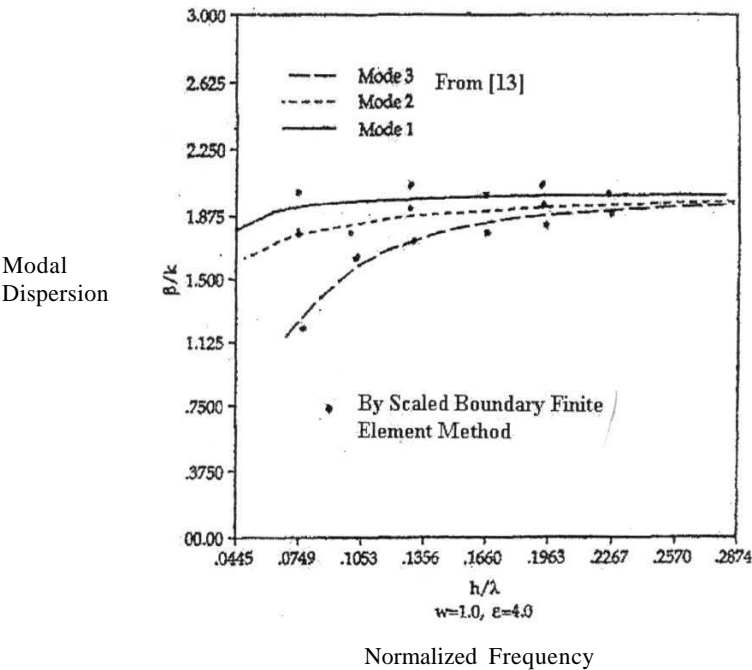
Fig.(4h). The dispersion curves for various modes corresponding to the VLSI interconnect structure shown in Fig.(4e).

F. Conclusion: The close agreement between the values determined from the Vector finite element method and the scaled boundary finite element method validates the theory of the scaled boundary finite element method developed for the analysis of transmission line structures and VLSI interconnects.

Moreover, the approach developed here can solve problems with any number of conduction wires of any shape. Inhomogenous and anisotropic dielectric materials can also be dealt with the theoretical approach developed in this chapter. The notable feature of the methodology is that, a finite element field solution is used to compute circuit quantities for transmission lines.

The next chapter deals with the theory of the scaled boundary finite element method suitable for analyzing periodic structures.

References

1. V.S.Prasanna Rajan, K.C.James Raju, "*Role of the full-wave analysis of Microstrip transmission line in the design and fabrication of MIC structures at higher microwave frequencies*", Proc. of APSYM- 1998, pp.280-285, held during Dec. 15-16 1998, at the Dept of Electronics, Cochin University of Science and Technology, Cochin.

2. R.K.Hoffmann, *Handbook of Microwave Integrated circuits*, pp. 162-167, 1992. Artech House.

3. Ibid, pp.245.

4. Ibid, pp.11-12.

5. Alina Deutsch, Gerard V.Kopcsay, "When are Transmission-Line Effects Important for on-chip interconnections ?", *IEEE Trans. On Microwave Theory and Tech.*, Vol.45, No. 10, pp. 1836-1846, Oct. 1997.

6. Jin Zhao and Zheng-Fan Li, "A Time-Domain Full-Wave Extraction Method of Frequency-Dependent Circuit Parameters of Multiconductor Interconnection Lines", IEEE Trans. On Microwave Theory and Tech., Vol.45, No.1, pp.23-31, Jan. 1997.

7. Zhenhai Zhu and Wei Hong, "An Efficient Algorithm for the Parameter Extraction of 3-D Interconnect Structures in the VLSI Circuits : Domain Decomposition Method", *IEEE Trans. On Microwave Theory and Tech,* Vol.45, No.8, pp.1179-1184, August 1997.

8. P.P.Silvester and R.L.Ferrari, "Finite Elements for Electrical Engineers", pp.379, 3rd Ed, Cambridge University Press, 1996.

9. John.P. Wolf and Chongmin Song, "The scaled boundary finite element method - a primer : derivations", *Computers and Structures ,* 78, pp. 196-197, 2000.

10. M.Shah Alam, Masanori Koshina, Koichi Hirayama, and Yoshio Hayashi, "Hybrid-mode Analysis of Multilayered and Multiconductor Transmission Lines", *IEEE Trans. On Microwave Theory and Tech*, Vol.45, No.2, pp.205-211, February 1997.

11. P.P.Silvester and R.L.Ferrari, "Finite Elements for Electrical Engineers", pp.286, 3rd Ed, Cambridge University Press, 1996.

12. LAPACK users guide, 3rd Ed, SIAM, Philadelphia.

13. G.W.Slade and K.J.Webb, "Computation of characteristic impedance for multiple microstrip transmission lines using a vector finite element method", *IEEE. Trans. Microwave Theory and Tech*., Vol.40, pp.34-40, Jan. 1992.

CHAPTER-V

THE SCALED BOUNDARY FINITE ELEMENT FORMULATION FOR PERIODIC STRUCTURES

CHAPTER – V

THE SCALED BOUNDARY FINITE ELEMENT FORMULATION FOR PERIODIC STRUCTURES

A. Introduction: The various class of **structures, that have been** considered so far, were either bounded on all sides or **bounded only** on **the transverse plane and unbounded along** the direction of wave propagation. The metallic cavity structures belong to the former class and the multi conductor and multi-layered microstrip like structures belong to the latter class. However, none of these structures considered, did not exhibit any geometric periodicity along the axial coordinate.

Those structures, which exhibit periodicity in the geometric and/or material properties along the axial coordinate are classified as periodic structures. These periodic structures find a number of practical applications, both as filters and delay lines.[1,2]

In this chapter, the scaled boundary finite element formulation is developed for the periodic structures, and it is illustrated with a numerical example.

B. Theory:

Consider a waveguide, with its axis aligned in the z-direction, defined by material characterized by ε (x, y, z) and μ (x, y, z) varying with spatial periodicity L such that [3]

$$\varepsilon\,(x, y, z+L) = \varepsilon\,(x, y, z) \tag{5.1a}$$

$$\mu\,(x, y, z+L) = \mu\,(x, y, z) \tag{5.1b}$$

while the electric and/or magnetic boundary walls, if any, exhibit a similar geometric periodicity. Electromagnetic wave propagation in such an arrangement is governed by Floquet's theorem, which states that the field vectors in complex phasor form at frequency ω , must vary (for H) as [4]

$$H(x, y, z) = \mathbf{H_p}(x, y, z) \exp(-j\ \beta z) \tag{5.2}$$

where **the** complex wave amplitude has the same spatial periodicity as that of the wave guide. The expression in (5.2) is for the loss free case. This can be expressed as,

$$\mathbf{H_p}(x, y, z+L) = \mathbf{H_p}(x, y, z) \tag{5.3}$$

The figure given below, shows the general representation of a spatially periodic wave guide unit cell. [5]
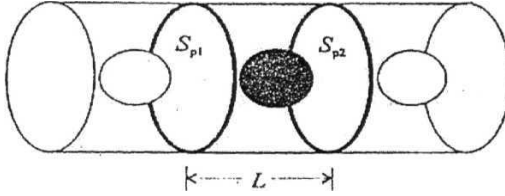
Fig.(5a). A spatially periodic wave guide unit cell. The arbitrary surfaces S_{p1} and S_{p2} are identical and spaced apart by the periodic length L.

The vector Helmholtz complex phasor equation in the **H-variable** is given by,

$$\nabla \times \varepsilon_r^{-1} \nabla \times \mathbf{H} - k^2 \mu_r \mathbf{H} = 0 \tag{5.4}$$

where ε_r and μ_r are the permittivity and permeability of the medium respectively. This equation is to be solved subject to the wall constraints. Additionally, the constraint corresponding to the periodicity from one end of the unit cell to the other is to be imposed. [6]

The weighted residual form of Eq.(5.4) got by following the procedure described in Chapter-Ill, and by using the vector integration by parts formula

$$\int_\Omega \mathbf{P} \cdot \left(\nabla \times \nabla \times \mathbf{Q} \right) d\Omega = \int_\Omega \left(\nabla \times \mathbf{P} \right) \cdot \left(\nabla \times \mathbf{Q} \right) d\Omega - \oint_S \left(\mathbf{P} \times \nabla \times \mathbf{Q} \right) \cdot \mathbf{1}_n \, dS \tag{5.5}$$

is given by,

$$R = \int_\Omega (\nabla \times W) \cdot \varepsilon_r^{-1}(\nabla \times H)\, d\Omega - \oint_S \left(W \times \varepsilon_r^{-1}\nabla \times H\right) \cdot 1_n\, dS - k^2\mu_r \int_\Omega W \cdot H\, d\Omega \qquad (5.6)$$

The variational expression for Eq.(5.4) can be obtained from the weighted residual expression (5.6) is given by,

$$F = \frac{1}{2}\int_\Omega \left((\nabla \times H) \cdot \varepsilon_r^{-1}(\nabla \times H) - k^2\mu_r H \cdot H\right) d\Omega + \oint_S \left(H \times \varepsilon_r^{-1}\nabla \times H\right) \cdot 1_n\, dS \qquad \textbf{(5.7)}$$

The surface integral in (5.7) vanishes over the wave guide walls either naturally at any electric wall or as a result of an essential boundary constraint,

$$H \times 1_n = 0 \qquad (5.8)$$

at any magnetic walls. If any part of the wave guide wall is at infinity and there arc no transverse radiative modes, the associated surface integral may similarly be neglected.[7] Also, the surface integral over the ends of the unit cell S_{p1} and S_{p2} is to be accounted as follows.

The surface integral term in the variational functional becomes,

$$I_s = \oint_{S_{p1}+S_{p2}} \left(H \times \left(\varepsilon_r^{-1}\nabla^- \times H\right) \cdot 1_n\right) dS \qquad (5.9)$$

This integral also vanishes, since the integrand is periodic (as observed from the expressions (5.2) and (5.3)) and exactly the same at one end of the unit cell as at the other, except for the unit normals 1_n, which are equal and opposite. [8]

The notation adopted in Eq.(5.9) is defined as,

$$\nabla^- = \left(\frac{\partial}{\partial x}, \frac{\partial}{\partial y}, \frac{\partial}{\partial z} - j\beta \right)$$

The variational expression is thus given by,

$$F = \frac{1}{2} \int_\Omega \left(\left(\nabla^- \times \mathbf{H}_p \right) \cdot \varepsilon_r^{-1} \left(\nabla^- \times \mathbf{H}_p \right) - k_0^2 \mu_r \mathbf{H}_p \cdot \mathbf{H}_p \right) d\Omega \qquad \textbf{(5.10)}$$

It is important to note that, the spatial periodicity is such that, only a single unit cell, say from $z=0$ to $z = L$, needs to be employed as the computational working space. Also, it is necessary to investigate pL only over a range of *2n,* as it is obvious from the form of the expression given in (5.2).

The range of βL is usually taken as,

$$-\pi \le \beta L \le \pi \qquad (5.11)$$

since the Floquet periodicity is such that all results outside that range are simply related to those within.

The scaled boundary finite element formulation can be developed from the variational expression given in (5.10), by expanding $\mathbf{H_p}$ in terms of the scaled boundary variables ξ, η, and ζ of the form given in Eqs.(3.7, 3.8, 3.9 and 3.10), and by incorporating the condition that the divergence of the magnetic field is zero, in the variational expression. The implementation of the condition is essential in order to avoid the spurious solutions in the resulting matrix eigen equation, and it is derived in the following section.

C. Implementation of the divergence condition of the magnetic field:

The divergence condition is given by

$$\nabla.(\mu \mathbf{H}) = 0 \qquad\qquad (5.12)$$

where μ is the permeability of the medium and H is the magnetic field strength.

Rewriting (5.12) by using (5.2),

$$\frac{\partial}{\partial x}\left(\mu H_{px}\right) + \frac{\partial}{\partial y}\left(\mu H_{py}\right) + \frac{\partial}{\partial z}\left(\mu H_{pz}\right) = j\beta\mu H_{pz} \qquad\qquad (5.13)$$

where H_{px}, H_{py} and H_{pz} denote the x , y and z components of $\mathbf{H_p}$.

Using the scaled boundary transformation equation for 3-D case [9], the equation (5.13) can be written as,

$$\frac{g^{\xi}}{|J|}n_x^{\xi}\frac{\partial\left(\mu H_{px}\right)}{\partial\xi} + \frac{1}{\xi}\left(\frac{g^{\eta}}{|J|}n_x^{\eta}\frac{\partial\left(\mu H_{px}\right)}{\partial\eta} + \frac{g^{\xi}}{|J|}n_x^{\xi}\frac{\partial\left(\mu H_{px}\right)}{\partial\zeta}\right) + \frac{g^{\xi}}{|J|}n_y^{\xi}\frac{\partial\left(\mu H_{py}\right)}{\partial\xi}$$

$$+ \frac{1}{\xi}\left(\frac{g^{\eta}}{|J|}n_y^{\eta}\frac{\partial\left(\mu H_{py}\right)}{\partial\eta} + \frac{g^{\xi}}{|J|}n_y^{\xi}\frac{\partial\left(\mu H_{py}\right)}{\partial\zeta}\right)$$

$$+ \frac{g^{\xi}}{|J|}n_z^{\xi}\frac{\partial\left(\mu H_{pz}\right)}{\partial\xi} + \frac{1}{\xi}\left(\frac{g^{\eta}}{|J|}n_z^{\eta}\frac{\partial\left(\mu H_{pz}\right)}{\partial\eta} + \frac{g^{\xi}}{|J|}n_z^{\xi}\frac{\partial\left(\mu H_{pz}\right)}{\partial\zeta}\right) = (j\beta\mu)\,H_{pz}$$

$$...(5.14)$$

Multiplying both sides by ξ and expanding the x, y and z components of H_p, as given in Eq.(3.7) of Chapter-3, and using the following finite partial Taylor series expansions for the permeability and its derivatives,

$$\mu(\xi,\eta,\zeta) = \sum_{k=0}^{m}\left(\frac{\partial^k\mu(0,\eta,\zeta)}{\partial\xi^k}\right)\frac{\xi^k}{k!}$$

$$\frac{\partial\mu}{\partial\xi} = \sum_{k=0}^{m}\left(\frac{\partial^{k+1}}{\partial\xi^{k+1}}\mu(0,\eta,\zeta)\right)\frac{\xi^k}{k!}$$

$$\frac{\partial\mu}{\partial\eta} = \sum_{k=0}^{m}\left(\frac{\partial^{k+1}}{\partial\eta\partial\xi^k}\mu(0,\eta,\zeta)\right)\frac{\xi^k}{k!}$$

129

$$\frac{\partial \mu}{\partial \zeta} = \sum_{k=0}^{m} \left(\frac{\partial^{k+1}}{\partial \zeta \partial \xi^{k}} \mu(0,\eta,\zeta) \right) \frac{\xi^{k}}{k!} \qquad \textbf{(5.15d)}$$

and grouping the terms of ξ^{k}, the following relations relating the unknown coefficients a_k, b_k, and c_k in the radial power series expansion, are obtained.

$$c_m = \frac{-\left(a_m N_1(\eta,\zeta) + b_m N_2(\eta,\zeta)\right)\left(\frac{\partial^{m+1}}{\partial \xi^{m+1}} \mu(0,\eta,\zeta)\right)\left(\begin{array}{l} \left(\frac{\partial^{m+1}}{\partial \xi^{m+1}} \mu(0,\eta,\zeta)\right) + \\ \left(|J|(j\beta)\frac{\partial^{m}}{\partial \xi^{m}} \mu(0,\eta,\zeta)\right) \end{array} \right)}{N_3(\eta,\zeta)\left[\left(\frac{\partial^{m+1}}{\partial \xi^{m+1}} \mu(0,\eta,\zeta)\right)^2 + \left(|J|\beta \frac{\partial^{m}}{\partial \xi^{m}} \mu(0,\eta,\zeta)\right)^2\right]}$$

$$...\text{(5.15e)}$$

$$c_k T_1 + c_{k-1} T_2 = a_k T_3 + a_{k-1} T_4 + b_k T_5 + b_{k-1} T_6 \qquad \text{for } 1 \le k < m \qquad \text{(5.15f)}$$

where, the terms T_1 to T_6 are given by

$$T_1 = \left(\frac{N_3(\eta,\zeta)}{(k-1)!}\right)\left[(j\beta|J|)\left(\frac{\partial^{k-1}\mu(0,\eta,\zeta)}{\partial \xi^{k-1}}\right) - \left(\frac{\partial^{k}\mu(0,\eta,\zeta)}{\partial \xi^{k}}\right)\right] -$$
$$\left(\frac{1}{k!}\right)\left(\begin{array}{l} \frac{\partial^{k}\mu(0,\eta,\zeta)}{\partial \xi^{k}}\left(kg^{\xi}n_z^{\xi}N_3(\eta,\zeta)\right) + \left(g^{\eta}n_z^{\eta}\frac{\partial N_3(\eta,\zeta)}{\partial \eta}\right) + \\ \left(g^{\zeta}n_z^{\zeta}\frac{\partial N_3(\eta,\zeta)}{\partial \zeta}\right) + N_3(\eta,\zeta)\left(\begin{array}{l}\left(\frac{\partial^{k+1}\mu(0,\eta,\zeta)}{\partial \xi^{k}\partial \eta}\right)\left(g^{\eta}n_z^{\eta}\right) + \\ \left(\frac{\partial^{k+1}\mu(0,\eta,\zeta)}{\partial \xi^{k}\partial \zeta}\right)\left(g^{\zeta}n_z^{\zeta}\right)\end{array}\right)\end{array}\right) \qquad \textbf{(5.15g)}$$

$$T_2 = \left(\frac{N_3(\eta,\zeta)}{k!}\right)\left[(j\beta|J|)\left(\frac{\partial^{k}\mu(0,\eta,\zeta)}{\partial \xi^{k}}\right) - \left(\frac{\partial^{k+1}\mu(0,\eta,\zeta)}{\partial \xi^{k+1}}\right)\right] \qquad \text{(5.15h)}$$

130

$$T_3 = \left[\left(\frac{\partial^k \mu(0,\eta,\zeta)}{\partial \xi^k} \right) \left(\begin{array}{c} N_1(\eta,\zeta)\left(\dfrac{1}{(k-1)!} + \dfrac{kg^\xi n_x^\xi}{k!} \right) \\ + g^\eta n_x^\eta \dfrac{\partial N_1(\eta,\zeta)}{\partial \eta} + g^\zeta n_x^\zeta \dfrac{\partial N_1(\eta,\zeta)}{\partial \zeta} \end{array} \right) + N_1 \left[\begin{array}{c} \left(\dfrac{\partial^{k+1}\mu(0,\eta,\zeta)}{\partial \xi^k \partial \eta} g^\eta n_x^\eta \right) \\ + \left(\dfrac{\partial^{k+1}\mu(0,\eta,\zeta)}{\partial \xi^k \partial \zeta} g^\zeta n_x^\zeta \right) \end{array} \right] \right]$$

...(5.15i)

$$T_4 = \left(\frac{1}{k!} \right) \left(N_1(\eta,\zeta) \frac{\partial^{k+1}\mu(0,\eta,\zeta)}{\partial \xi^{k+1}} \right) \tag{5.15j}$$

$$T_5 = \left(\frac{\partial^k \mu(0,\eta,\zeta)}{\partial \xi^k} \right) \left[N_2(\eta,\zeta) \left[\frac{1}{(k-1)!}\left(1 + g^\xi n_y^\xi\right) \right] + g^\eta n_y^\eta \frac{\partial N_2(\eta,\zeta)}{\partial \eta} + g^\zeta n_y^\zeta \frac{\partial N_2(\eta,\zeta)}{\partial \zeta} \right] +$$
$$N_2(\eta,\zeta) \left[\left(\frac{\partial^{k+1}\mu(0,\eta,\zeta)}{\partial \xi^k \partial \eta} g^\eta n_y^\eta \right) + \left(\frac{\partial^{k+1}\mu(0,\eta,\zeta)}{\partial \xi^k \partial \zeta} g^\zeta n_y^\zeta \right) \right] \tag{5.15k}$$

$$T_6 = \left(\frac{1}{k!} \right) \left(N_2(\eta,\zeta) \frac{\partial^{k+1}\mu(0,\eta,\zeta)}{\partial \xi^{k+1}} \right) \tag{5.15l}$$

The relation (5.15e) gives the last coefficient in the radial expansion c_m, in terms of a_m and b_m. The remaining coefficients c_k are evaluated recursively using the relations from (5.15 f) to (5.15 l).

These resulting expressions for c_k are substituted in the variational functional, while expressing the functional in terms of the scaled boundary transformation variables, so that the fields exactly satisfy the zero divergence requirement of the magnetic field. The functional is then integrated with respect to ξ from 0 to 1, so that the resulting functional is purely in terms of the circumferential variables η and ζ. The resulting functional is evaluated numerically for every surface finite element. Then the derivative with respect to every unknown coefficient is taken and set to zero. This process is repeated for every surface finite element. Imposing only tangential continuity between the adjacent

131

elements, the process of assembling results in a system of matrix eigen equation of the form

$$\mathbf{P}\,(j\beta)\,\mathbf{h_p} + k_0{}^2\,\mathbf{h_p} = 0 \qquad\qquad\qquad (5.16)$$

The equation (5.16) results in a countably infinite set of eigen vectors $\mathbf{h_{pn}}$ and eigen values k_{0n} , $n= 1,2,\ldots$ for a given p, and may be obtained using standard linear algebra routines.

D. Numerical implementation: The theory developed above is applied to a three dimensional periodic wave guide shown below in Fig.(5b). [10]
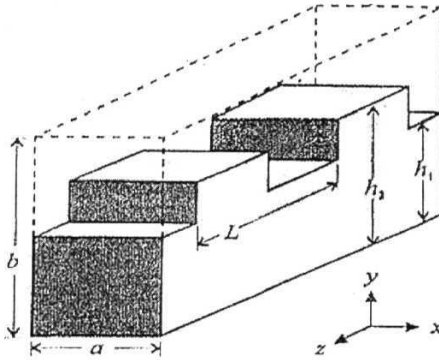

Fig.(5b). The geometry of the three dimensional periodic wave guide.

To apply the scaled boundary finite element method, to the geometry shown in Fig.(5b), the whole geometry was sub-structured so that in each individual sub-structure a scaling center can be found and the method is applied for every sub-structure individually, and the continuity of the fields at the interface between sub-structures were imposed. The relative permittivity of the dielectric material shown as shaded region is 2.28. For the analysis, covariant projection quadrilateral elements of mixed order m=1, and n=2 were

used. Seven terms were used **in the analytical expression for the fields in the radial** direction. The geometry shown in Fig.(5b) **is divided theoretically into** 10 **substructures.** A total of 500 quadrilateral elements with **eight node** per element were used in **each** substructure. The **numerical integration was performed using gaussian quadrature. The** eigen values of **the resulting** matrix **eigen equation were obtained** using LAPACK.[11]

A plot of β_z versus k_o L over a range of 0 to 2π for the three lowest propagating modes is shown below in Fig.(5c).
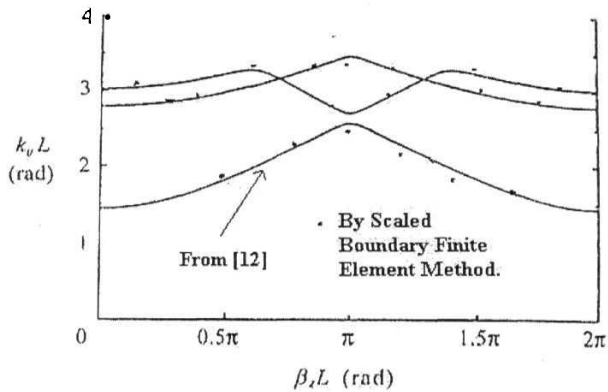

Fig.(5c) A plot of β_z versus k_o L over a range of 0 to *2n* for the structure shown in Fig.(5b).

The results obtained from a conventional three dimensional vector finite element method are shown as thick curves. The results obtained from that of the scaled boundary finite element method are shown as dots. The ratios of the dimensions of the structure considered for numerical implementation were b/a = 2, L/a = 1.26, h_1 /a=1, and h_2 /a=1 .4. The graphical representation of the variation of k_0 versus β_z shown in Fig.(5c) for the three lowest propagating modes, shows good agreement between the values determined by the scaled boundary finite element method and the values determined by the

conventional three dimensional vector finite element method. This validates the theory of the scaled boundary finite element method developed for the analysis of the periodic structures,

E. Conclusion: The theory of the scaled boundary finite element formulation for the analysis of periodic structures is proposed, and its numerical validation is illustrated by taking an example of a known three dimensional periodic wave guide. As a further extension, the theory can also be generalized to cover the case of lossy media.

References

1. P.P.Silvester and R.L.Ferrari, "*Finite elements for Electrical Engineers",* 3 rd Ed, Cambridge University Press, p.396, 1996.

2. Shyh-Jjong and Jiunn-Lang Chen, "A Modified Finite Element Method for Analysis of Finite Periodic Structures", *IEEE. Trans. on Microwave Theory and Tech.,* Vol.42, No.7,p.1561, July 1994.

3. P.P.Silvester and R.L.Ferrari, "*Finite elements for Electrical Engineers",* 3rd Ed, Cambridge University Press, p.396, 1996.

4. Ibid.

5. Ibid.

6. Ibid, p.397.

7. Ibid.

8. Ibid.

9. Chongmin Song and John P. Wolf, "The Scaled boundary finite-element method- alias Consistent infinitesimal finite-element cell method - for elastodynamics", *Computer Methods in applied mechanics and engineering,* No.147, pp. 334-337, 1997.

10. P.P.Silvester and R.L.Ferrari, "*Finite elements for Electrical Engineers*", 3rd Ed, Cambridge University Press, p.399, 1996.

11. LAPACK users guide, 3rd Ed, SIAM, Philadelphia.

12. P.P.Silvester and R.L.Ferrari, *"Finite elements for Electrical Engineers",* 3rd Ed, Cambridge University Press, p.399, 1996.

CHAPTER - VI

CONCLUSION

CHAPTER - VI

CONCLUSION

The scaled boundary finite element method is a novel semi analytical method based on finite elements. It was originally developed in the field of civil engineering to study problems pertaining to elastodynamics and Soil structure interaction. This novel method has the advantages of both the finite and boundary element method. The notable feature of this method is that it involves only surface discretization on the boundary of the three dimensional geometry. For two dimensional structures, the novel method involves only the discretization of the contour on the periphery of the region. This reduction of dimension of discretization is an enormous advantage in terms of computing time, and storage requirements. The novel method, being analytical in the radial direction, permits the radiation condition to be satisfied exactly for the problems dealing with unbounded media.

This novel method, based on the weighted residual approach, is reformulated to suite problems in electromagnetics. The crucial aspect in the reformulation of the novel method is the implementation of the solenoidality requirement of the magnetic field. This is necessary so that no spurious solutions occur as eigen solutions of the boundary value problem.

The scaled boundary finite element method is formulated to analyze cavity structures, multi-layered and multi-conductor microstrip transmission line structures, VLSI interconnects, and periodic structures. The implementation of the solenoidality requirement of the magnetic field depends on whether the structure is bounded completely on all sides or unbounded along a particular direction.

It also depends whether the structure is periodic or **non-periodic**. This is clearly illustrated in various physical structures considered in the thesis. The closeness of the numerical results obtained from the scaled boundary finite element method to those obtained from analytical or the conventional finite element method, proves the validity of the novel method.

An important consequence of the method being semi-analytical is that, the accuracy of the numerical values depend not only on the element size as in the conventional finite element method, but also on the number of terms that are used in the radial series expansion of the fields. This enables to get accurate numerical results even by increasing the number of terms in the radial expansion of the fields without tampering with the element size.

The success of the scaled boundary finite element method in dealing with unbounded media, as demonstrated by Wolf and Chongmin Song can be taken as a motivation for the corresponding reformulation of the method in dealing with the unbounded media in electromagnetics. The class of problems in electromagnetics, dealing with unbounded media are the radiation and scattering problems.

For problems involving radiation, the reformulation necessitates the implementation of the Lorentz gauge and the equation of continuity, in the scaled boundary finite element equations. This involves computational complexity, and can be taken up for further study.

This novel method can also handle the anisotropy in the material properties of the medium, without much computational effort. Hence problems involving anisotropy in material properties can also be taken up for solution by this method.

List of Publications

(a) **V.S.Prasanna Rajan,** K.C.James Raju, "Sensitivity Analysis of the cross-talk in micro-strip transmission lines", Proc. of the International Conference on Electromagnetic Interference and Compatibility, pp. 129-132, organized by the Society of EMC Engineers (India), held during Dec-6-8, 1999, New-Delhi.

(b) P.K.Banmeru,**V.S.Prasanna Rajan,** P.B.Patil, "E Field Finite Element Method with Covariant Projection Elements for Waveguide Analysis", Proceedings of the National Seminar on Recent Trends in Communication Technology", Pp. 125-128, organized by School of Studies in Physics and Electronics, Jiwaji University, Gwalior, during April- 13-14,2002.

(c) **V.S.Prasanna Rajan,** K.C.James Raju, "Transient field analysis of a open microstrip line like structure fed by a pulsed voltage source", National Conference on Emerging Trends and Advances in Microwave measurements and Techniques, pp.37-38, held during March 2nd - 3rd 2001, Babasaheb Ambedkar Marathwada Unversity, Aurangabad.

(d) **V.S.Prasanna Rajan,** K.C.James Raju, "Periodic pulse propagation in microstrip line like VLSI interconnects", Proc. of APSYM - 2000, pp. 170-172, held during Dec. 6-8, 2000, at the Dept of Electronics, Cochin University of Science and Technology, Cochin.

(e) **V.S.Prasanna Rajan,** K.C.James Raju, "Role of the full-wave analysis of a Microstrip transmission line in the design and fabrication of MIC structures at higher microwave frequencies", Proc. of APSYM- 1998, pp.280-285, held during Dec.15-16 1998, at the Dept of Electronics, Cochin University of Science and Technology, Cochin.

List of Journal Papers communicated

(a) **V.S.Prasanna Rajan,** K.C.James Raju, "Theoretical aspects of a Novel Scaled Boundary Finite Element formulation in Computational Electromagnetics", communicated to the Journal of Applied Computational Electromagnetics Society.

(b) **V.S.Prasanna Rajan,** K.C.James Raju, "Constraint relations between the unknown coefficients in the scaled boundary finite element formulation in Electromagnetics", communicated to the Journal of Applied Electromagnetics Society.

(c) **V.S.Prasanna Rajan,** K.C.James Raju, "Application of the Covariant Projection finite elements in the E field formulation for wave guide analysis", Communicated to the Journal of Applied Computational Electromagnetics Society.